US Army Corps of Engineers

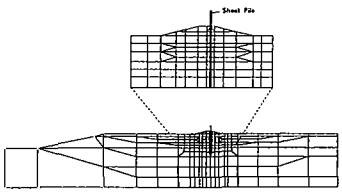

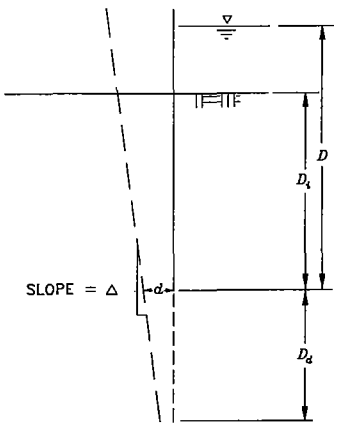

GEOTECHNICAL LABORATORY

TECHNICAL REPORT GL-89-14

DEVELOPMENT OF FINITE-ELEMENT-BASED DESIGN PROCEDURE FOR SHEET-PILE WALLS

by

D. A. Leavell, J. F. Peters, E. V. Edris, T. L. Holmes

Geotechnical Laboratory

DEPARTMENT OF THE ARMY
Waterways Experiment Station, Corps of Engineers
3909 Halls Ferry Road, Vicksburg, Mississippi 39180-6199

September 1989
Final Report

Prepared for US Army Engineer District, New Orleans
New Orleans, Louisiana 70160-0267

Destroy this report when no longer needed. Do not return it to the originator.

The findings in this report are not to be construed as an official Department of the Army position unless so designated by other authorized documents.

The contents of this report are not to be used for advertising, publication, or promotional purposes. Citation of trade names does not constitute an official endorsement or approval of the use of such commercial products.

Unclassified

SECURITY CLASSIFICATION OF THIS PAGE

REPORT DOCUMENTATION PAGE

Form Approved OMB No. 0704-0188

1a. REPORT SECURITY CLASSIFICATION Unclassified	1b. RESTRICTIVE MARKINGS
2a. SECURITY CLASSIFICATION AUTHORITY	3. DISTRIBUTION/AVAILABILITY OF REPORT Approved for public release; distribution unlimited.
2b. DECLASSIFICATION/DOWNGRADING SCHEDULE	
4. PERFORMING ORGANIZATION REPORT NUMBER(S) Technical Report GL-89-14	5. MONITORING ORGANIZATION REPORT NUMBER(S)
6a. NAME OF PERFORMING ORGANIZATION USAEWES Geotechnical Laboratory 6b. OFFICE SYMBOL (If applicable)	7a. NAME OF MONITORING ORGANIZATION
6c. ADDRESS (City, State, and ZIP Code) 3909 Halls Ferry Road Vicksburg, MS 39180-6199	7b. ADDRESS (City, State, and ZIP Code)
8a. NAME OF FUNDING/SPONSORING ORGANIZATION US Army Engineer District, New Orleans 8b. OFFICE SYMBOL (If applicable)	9. PROCUREMENT INSTRUMENT IDENTIFICATION NUMBER
8c. ADDRESS (City, State, and ZIP Code) New Orleans, LA 70160-0267	10. SOURCE OF FUNDING NUMBERS PROGRAM ELEMENT NO. / PROJECT NO. / TASK NO. / WORK UNIT ACCESSION NO.
11. TITLE (Include Security Classification) Development of Finite-Element-Based Design Procedure for Sheet-Pile Walls	
12. PERSONAL AUTHOR(S) Leavell, D. A., Peters, J. F., Edris, E. V., Holmes, T. L.	
13a. TYPE OF REPORT Final report 13b. TIME COVERED FROM _____ TO _____	14. DATE OF REPORT (Year, Month, Day) September 1989 15. PAGE COUNT 123
16. SUPPLEMENTARY NOTATION Available from National Technical Information Service, 5285 Port Royal Road, Springfield, VA 22161.	

17. COSATI CODES			18. SUBJECT TERMS (Continue on reverse if necessary and identify by block number)	
FIELD	GROUP	SUB-GROUP		
			Finite elements	Sheet pile
			Floodwall	Soft clay
			Limit-equilibrium	Soil-structure interaction

19. ABSTRACT (Continue on reverse if necessary and identify by block number)

The performance of sheet-pile I walls is evaluated using the SOILSTRUCT computer program, which is based on the finite element method. The analysis models the levee-pile system as a two-dimensional plane-strain problem. The analysis includes computations for a field test case and a parametric study of a proposed I-wall section. The principal finding was that traditional limit-equilibrium methods provide a reasonable conservative estimate of pile stability but one-dimensional beam analysis greatly underestimates movements caused by flood and wave loads. One-dimensional analyses do not account for the deep-seated movement caused by the surcharge load of floodwater. The finite element analysis showed that surcharge loading is the major cause of movement in soft clay foundations. It is recommended that conventional stability analyses should be used for design of the sheet pile-levee system; the foundation stability can be addressed by standard slope stability analysis and pile stability can be analyzed using the traditional limit-equilibrium method. The sheet pile

(Continued)

20. DISTRIBUTION/AVAILABILITY OF ABSTRACT ☒ UNCLASSIFIED/UNLIMITED ☐ SAME AS RPT. ☐ DTIC USERS	21. ABSTRACT SECURITY CLASSIFICATION Unclassified
22a. NAME OF RESPONSIBLE INDIVIDUAL	22b. TELEPHONE (Include Area Code) / 22c. OFFICE SYMBOL

19. ABSTRACT (Continued).

should be designed to resist moments computed from the limit-equilibrium pressure diagram for a pile penetration corresponding to a factor of safety equal to 1.0. Charts are provided to estimate "additional" movements caused by surcharge loading although it is recommended that new finite element analyses be performed when subsurface conditions deviate significantly from those assumed for the parametric study.

PREFACE

This study was sponsored by the New Orleans District, US Army Engineer Division, Lower Mississippi Valley (LMVD), under IAO No. CELMNED-87-38 dated 10 Feb 87 and IAO No. CELMNED-88-50 dated 11 Apr 88. The investigation was conducted during FY 1987 to FY 1989.

The study was conducted under the direction of Dr. W. F. Marcuson III, Chief, Geotechnical Laboratory (GL), and under the general supervision of Mr. C. L. McAnear (ret), Chief, Soils Mechanics Division (SMD), Dr. D. C. Banks, Chief, Soil and Rock Mechanics Division (SRMD), and Mr. G. P. Hale, Chief, Soils Research Center (SRC). The principal investigator for the study was Mr. D. A. Leavell, SRC, SRMD. This report was prepared by Mr. D. A. Leavell, Dr. J. F. Peters, Mr. E. V. Edris, and Mrs. T. L. Holmes. Laboratory testing was performed by Mr. R. L. Coffing.

Commander and Director of WES was COL Larry B.Fulton, EN. Dr. Robert W. Whalin was the Technical Director.

CONTENTS

LIST OF FIGURES

CONVERSION FACTORS, NON-SI TO SI (METRIC) UNITS OF MEASUREMENT

Non-SI units of measurement used in this report can be converted to SI (metric) units as follows:

Multiply	By	To Obtain
degrees (angle)	0.01745329	radians
feet	0.3048	metres
inches	25.4	millimetres
pounds (force)	4.448222	newtons
pounds (force) per foot	14.5939	newtons per metre
pounds (force) per square foot	47.88026	pascals
pounds (force) per square inch	6894.757	pascals
pounds (mass) per cubic foot	16.01846	kilograms per cubic metre
tons (force) per square foot	95.76052	kilopascals

DEVELOPMENT OF FINITE-ELEMENT-BASED DESIGN PROCEDURE FOR SHEET-PILE WALLS

PART I: INTRODUCTION

Background

1. The US Army Engineer (USAE) New Orleans District (NOD) uses cantilever sheet-pile walls (I walls) to provide: (a) flood protection along the Mississippi and Atchafalaya Rivers, and (b) hurricane protection along the Gulf of Mexico shoreline. It has been proposed that over the next few years many miles of these floodwalls be constructed at a cost of over $100 million. The actual cost of these walls, however, is dependent on both the sheet-pile section and the penetration needed to achieve the required stability. The current design procedure is based on the limit-equilibrium method using the computer code CANWAL (Manson 1978). Displacements are also estimated by CANWAL based on the limit-equilibrium pressure distribution. The stability of the levee foundation is assessed through conventional slope stability analysis.

2. In 1985 a field load test was performed by The Lower Mississippi Valley Division (LMVD) on a 200-ft-long [1] floodwall test section on the landside berm of the Item E-99 East Atchafalaya Basin Protection Levee (EABPL), located on Avoca Island just south of Morgan City, Louisiana. The field test was initially analyzed using the USAE Waterways Experiment Station (WES) computer code CSHTSSI (Dawkins 1983) which uses beams and springs to model the interaction between the sheet pile and soil. It was concluded from the analysis that the Corps' current design procedure for sheet-pile penetration, which is based on the drained (S) case and a safety factor of 1.5, was too conservative and required further investigation.

3. To supplement the one-dimensional analysis provided by the CSHTSSI code it was proposed to perform a detailed two-dimensional analysis using the computer code SOILSTRUCT (Clough 1984), which is based on the finite element method. The advantages of the SOILSTRUCT code are:

a. The soil is modeled realistically as a continuous mass rather than as discrete springs. Thus the soil's stress-strain response can be modeled accurately using data from laboratory tests without need of further approximation to determine an equivalent spring response.

b. A better representation of displacements can be achieved that includes deep-seated movements caused by surcharge loading of the floodwater. This is particularly important for soft soil foundations because lateral movements caused by surcharge loadings can be quite significant but are ignored by CSHTSSI.

[1] A table of factors for converting non-SI units of measurements to SI (metric) units is presented on page viii.

An analysis based on the SOILSTRUCT code could therefore provide an estimate of the overall performance of the combined levee-floodwall system as would be needed before a less conservative design could be proposed. The field load test further provided validation data for the analysis that reduces the total reliance on a relatively sophisticated analysis.

Purpose

4. The purpose of this work is to analyze the field load test on the E-99 sheet-pile wall using the finite element method and to develop recommendations for a sheet-pile I-wall design procedure. This investigation was divided into three tasks. The first task was to revise SOILSTRUCT for computation of moments in sheet-pile floodwalls without the use of specially formulated bending elements. The second task was to analyze the E-99 test section using the soil-structure interaction finite element computer code SOILSTRUCT and assess the applicability of the code in analyzing sheet-pile walls in soft clay. As part of this task it was found necessary to revise the solution algorithm to obtain better numerical performance as large areas of soil mobilized their full strength. Task three consisted of a detailed parametric study involving variations in soil properties, loadings, sheet-pile type, and depth of penetration. These results are presented as a design procedure detailing the parameters needed and limitations of the procedure.

Scope

5. The report is presented in five parts. After the introductory remarks of Part I, a brief description of the finite element analysis is presented in Part II. This Part is included for completeness and to document items used in this study that are not part of the original SOILSTRUCT code; a detailed understanding of Part II is not required for the remainder of the report. Part III presents the analysis of the load test on the E-99 sheet-pile wall. In this Part, the applicability of the SOILSTRUCT program for analysis of cantilever sheet piles in soft clay is established. Also, from comparisons between predicted and observed performance, values of soil parameters are recommended for design purposes. In Part IV parametric studies of I-wall designs are presented using the EABPL E-105 section as the basis for analysis. *The principal results of the parametric study are that limit-equilibrium analyses provide an adequate basis for selecting maximum permissible water loading and minimum pile embedment but that deflections computed by the CANWAL program are not accurate because deep-seated foundation movements are not included.* Design recommendations are presented in Part V.

6. The results of all analyses of the E-105 section are tabulated in Appendix A. However,

only the analyses that used the PZ-27 sheet pile are presented graphically in Appendix A. Included in the results are analyses of pile response to wave loading. These analyses were requested by LMVD and are beyond the scope of the study, but have been presented for completeness.

7. When the study was initiated detailed laboratory tests were not available and calibration of the soil model was based solely on comparison to field observations from the E-99 sheet-pile load test. Soil samples have since been obtained for determination of soil properties needed for the analysis. The results of the laboratory testing program were used in a more detailed analysis of the E-99 section and have replaced the original findings. The more detailed analyses revealed that the soil stiffness was underestimated in the original computations resulting in an overestimation of displacements. The revised analysis thus offers a more optimistic picture of the sheet-pile performance relative to the magnitude of movement. Conclusions regarding the relationships of movement versus embedment and movement versus pile stiffness were not affected by the soil stiffness.

PART II: DESCRIPTION OF FINITE ELEMENT ANALYSIS

Introduction

8. SOILSTRUCT is a plane-strain finite element code designed to model both soil masses and structural elements that are partially buried in soil. In addition, SOILSTRUCT simulates incremental loading conditions for which stresses and deformations are calculated. SOILSTRUCT provides a model that best represents geometry, structural details, soil behavior, and loading history.

9. The analyses presented in this report involved three major components:

   a. The soil elements, represented by quadrilateral and triangular elements.

   b. The sheet pile, represented by rectangular elements.

   c. The contact between the soil and sheet pile, represented by special interface elements.

In addition, the complete loading and construction history must be modeled, including the initial consolidation stress in the levee and foundation, insertion of the sheet pile, and water loading caused by flooding and wave action. A description of how each of the above details is addressed in the finite element analysis is presented in the following sections.

Soil Properties

10. The principal difficulty in determining the soil properties was the lack of data to determine the stress-strain properties of the soils. The only information available for the analyses presented in this report was the undrained strength of the soil. Therefore, much of the following description is guided by the need to estimate stress-strain parameters from comparisons between theoretical and observed performance of the E-99 test section.

11. The soil is modeled as a nonlinear "elastic" material whereby the stress-strain response is defined by a uniaxial compression loading stiffness modulus and Poisson's ratio. The uniaxial compression stress-strain response is represented as a hyperbolic curve, defined by the initial tangent modulus (E_i) [1] , the hyperbolic strength (S_f), and the failure stress of the soil (S_u). [2] As discussed in the section below on hyperbolic strength, S_f is specified by the ratio $R_f = S_u/S_f$.

[1] For convenience, symbols and abbreviations are listed in the Notation (Appendix C).

[2] Throughout this study the loading has been considered to be undrained; therefore the strength used is, in all cases, the undrained shear strength.

Initial soil modulus and Poisson's ratio

12. The soil stiffness is controlled by the initial tangent modulus. The initial tangent modulus is determined by:

$$E_i = p_a K_m \left(\frac{\sigma_3'}{p_a}\right)^n \tag{1}$$

where p_a is atmospheric pressure, K_m and n are material-dependent parameters, and σ_3' is the minimum principal effective stress. In the case of undrained conditions the stress-strain response is expressed in terms of total stresses. To avoid the complications associated with attempting to estimate induced pore pressure (to compute σ_3') n is set to zero and K_m is expressed as a function of the initial consolidation stress; this is an approach similar to that described below for soil strength whereby the strength is based on the initial consolidation state and the friction angle is set to zero. It has been found through experience that the initial modulus, $p_a\ K_m$, can be expressed as a ratio of the undrained shear strength (Clough and Tsui 1977 and Mana 1978) whereby $E_i = KS_u$. Thus, assuming K is known, the undrained shear strength becomes the fundamental parameter controlling the response of the soil.

13. Poisson's ratio is defined by its value at initial loading (ν_i); its value at subsequent loading steps is determined such that ν approaches 0.5 as the stiffness approaches its failure value. This idealization is used to model the relative incompressibility of the soil as its shear stiffness becomes small. Because undrained conditions have been assumed, $\nu_i \approx 0.5$.

Soil strength

14. Soil strength is typically defined in SOILSTRUCT by cohesion c and friction angle ϕ, which are chosen to be appropriate for the drainage condition of each element based on its permeability and the loading rate. For undrained conditions this approach is not suitable because to model the increase in strength produced by higher consolidation stress it is necessary to either assign a different cohesion (with $\phi = 0$) to each element, which is not practical, or to assign a total stress friction angle to each material, which is physically inconsistent for saturated materials. The correct result can only be obtained by selecting the undrained strength from the pre-loading consolidation conditions and setting $\phi = 0$ for all subsequent undrained loadings. Therefore, the program was modified to allow the strength to be input as a ratio of strength to effective consolidation pressure (S_u/p_c'). The procedure consists of the following:

a. The consolidation stress is computed for each element based on the geometry and boundary conditions prior to loading. For the present problem, it was assumed that the foundation had fully consolidated under the weight of the levee. Elements above the water table are assigned the total unit weight of the soil and elements below the water table are assigned the buoyant unit weight. The stresses created by this configuration are computed from an elastic analysis of the levee-foundation system.

b. The effective consolidation stress p'_c is computed for each element as:

$$p'_c = \tfrac{1}{2}(\sigma'_h + \sigma'_v) \tag{2}$$

where σ'_h and σ'_v are, respectively, the horizontal and vertical effective stresses. This value is stored for each element for use in all subsequent calculations.

c. Each material type is assigned a value of S_u/p'_c and K. These values are then combined with p'_c computed from the initial stress computations to determine S_u and E_i for each element. The property values assigned to each element therefore depend on material type and section geometry. For example, shear strengths were moderately higher under the levee centerline than at the toe as a result of the higher consolidation stress imposed by the levee.

Hyperbolic strength

15. The ultimate hyperbolic strength is the shear stress that would be obtained if the strain were increased without limit. However, it is often found that the hyperbolic shape does not fit the shape of stress-strain curves of many soils because the gradation into failure depicted by the hyperbolic shape is too gradual. To better model the break in the stress-strain curve that occurs near failure the true strength is introduced as an additional parameter. The stiffness of the soil is computed from the hyperbolic stress-strain curve up to the point that the strength is reached. For loading beyond the failure stress a low modulus is assigned to be consistent with failure of the element. Because of the limited data available for determining stress-strain properties, it was assumed that the strength of the soil S_u was 70.0 percent of the ultimate hyperbolic strength S_f (i.e. $R_f = 0.70$). This relatively low value of R_f gives a sharp break in the stress-strain curve at failure as compared to the relatively smooth hyperbolic shape. It was found by trial computations that the shape of the stress-strain curve for the individual soil elements did not influence the *shape* of the load-deflection curve for the sheet pile-levee system as a whole. This lack of correspondence between the soil's stress-strain response and the structural response is discussed in more detail in Part III.

Calibration to field observations

16. Based on the above considerations, the stress-strain response of the soil requires determination of two parameters, the undrained shear strength S_u and the modulus ratio K. The undrained shear strength was determined from data provided by NOD and from laboratory tests performed specifically for this study. Therefore, the principal task in analysis of the E-99 section was to determine the value of K that gave the best agreement between computed and observed performance.

Sheet-Pile Element

17. Representation of bending stiffness in soil-structure interaction analyses has always presented a difficulty. If an element is formulated for bending using the approach found in most structural analysis codes an incompatibility is created between the bending and solid (soil) elements. This incompatibility results from the technical requirement that displacement *gradients* (slope) must be continuous across beam elements whereas the solid elements generally only provide for continuous displacements. The incompatibility problem is avoided in SOILSTRUCT by using slender solid elements to model bending. These elements are similar to the soil elements, rather than true beam elements. In fact, the particular choice of element formulation selected for the SOILSTRUCT code was made to ensure that the solid elements would correctly model strain patterns associated with bending. Experience by Mana (1978) on a number of soil-structure interaction problems has shown this approach to work well.

Pile section properties

18. The properties of the solid elements used to model the sheet pile are the elastic properties, E and ν, and would be, respectively, 29×10^6 psi and 0.25 for steel. However, the solid element is rectangular-shaped and thus behaves differently in a bending mode of deformation than a sheet pile. To achieve the correct response to bending, the modulus of the element must be chosen to obtain the equivalent flexural stiffness as specified by the product EI, where I is the moment of inertia per foot of the sheet pile. Therefore, the properties of the sheet-pile elements are determined such that the section stiffness of the element $E_e I_e$ matches the EI of the sheet pile. To maintain reasonable aspect ratios for the sheet-pile elements in the finite element analyses, it was assumed that the finite elements representing the sheet piles were 1 ft wide and 1 ft thick, which implies $I_e = 1/12\,\text{ft}^4$. Therefore, the pile elements obtain proper bending stiffness when assigned the modulus given by:

$$E_e = 12EI \tag{3}$$

The I used for the PZ-27 sheet pile was 276.3 in^4 and 805.4 in^4 for the PZ-40 which have respective widths of 18.0 and 19.69 in. This relates to an I per foot of 184.2 in^4 for the PZ-27 and 490.8 in^4 for the PZ-40 sheet piles.

19. Another consideration is the three-dimensional aspect of the bending problem. In the plane-strain idealization of the bending process the finite element behaves as a 1-ft-wide plate and not as an idealized beam. In the bending mode the strains are distributed about the neutral axis such that half of the element is in tension and half is in compression, thus creating a bending moment along the beam to maintain a plane-strain condition. As a result of this three-dimensional effect the stiffness of the finite element is the equivalent plate bending stiffness of the element, $E/12(1-\nu^2)$. The bending stiffness of an elemental strip of a plate is given by Timoshenko and Woinowsky-Krieger (1959). Therefore, to obtain the proper bending stiffness, the element must be assigned $\nu = 0$. As a practical matter, a major finding of the parametric study described in Part IV is that bending stiffness had a relatively small effect on the performance of the pile-levee system. However, the stiffness is also used for moment computations and, as discussed in the next section, the value of ν had a significant effect on the computed moment.

Moment computations

20. While use of solid elements for bending members works well to represent the stiffness provided by bending, the problem remains as to how to compute moments. The solid element representation naturally provides statically equivalent stress values at the center of the element; these values cannot be related to a bending moment. An alternative sometimes attempted is to estimate moments from displacements using the formula

$$M = EI\frac{d^2u}{dx^2} \tag{4}$$

where E is Young's modulus, I the moment of inertia, u the lateral displacement, and x the distance along the beam. The second derivative is estimated numerically using a finite difference formula. In most cases the approximation is crude, at best, because of large node spacing, producing erratic moment distribution. Another approach is to impose the displacement computed

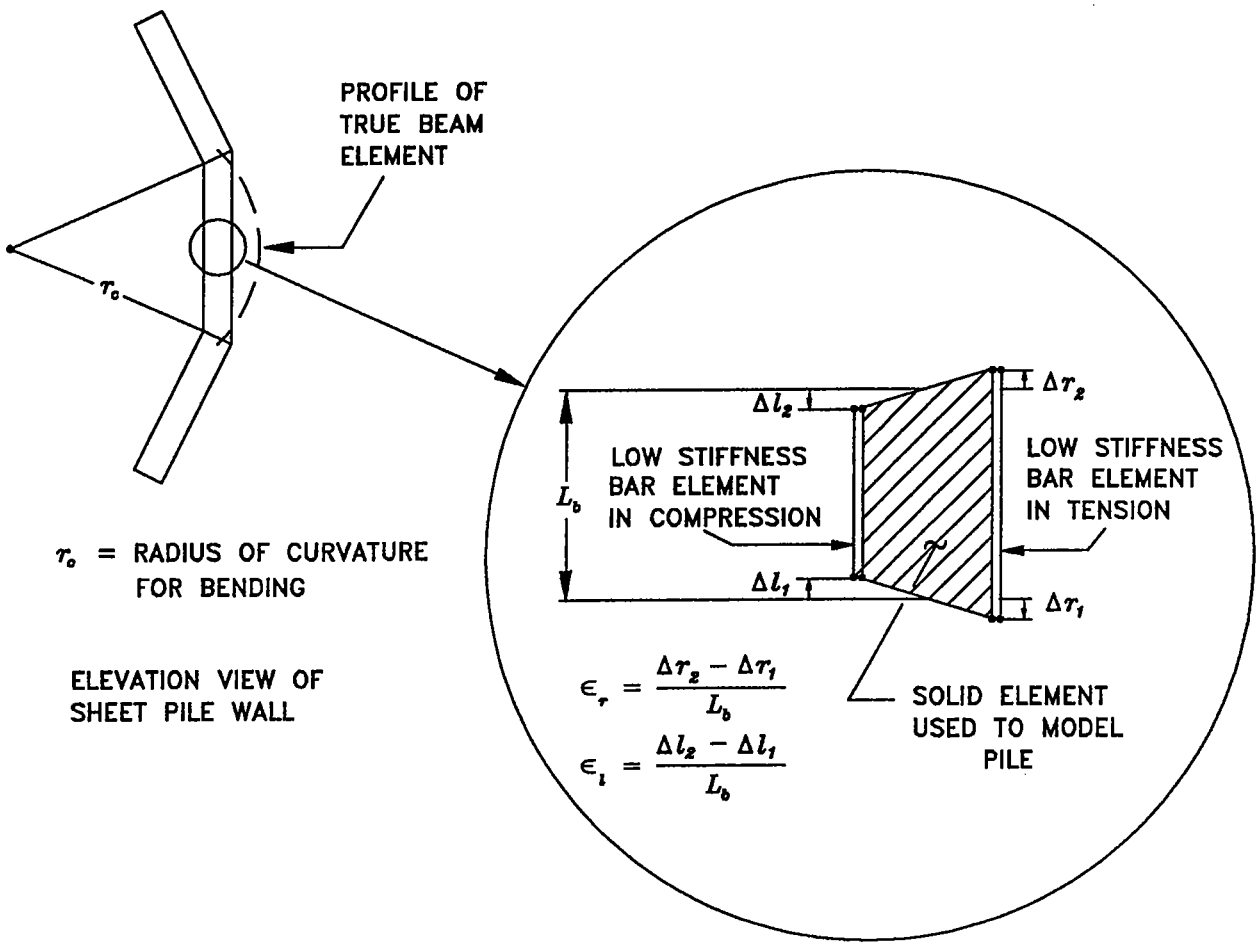

Figure 1. Strain gage method of computing bending moments for four-node solid element

by SOILSTRUCT into a one-dimensional representation such as that provided by CSHTSSI. Experience with this approach has also proved to be unsatisfactory.

21. The method for computing moments that was developed for this study is based on the premise that moments could be computed from beam theory using the "outer fiber strains" computed from displacements of the end nodes. This process is illustrated in Figure 1, which shows the solid elements in a bending pattern. The outer fiber strains are shown to be related to a radius of curvature that a true beam element would conform to. As an expedient, the outer fiber strains are computed by placing bar elements on the edges of the beam elements. These "strain gage" elements are created by using the standard bar element provided by SOILSTRUCT (for modeling anchors and struts, etc.). The bar was given a low stiffness so that there was virtually no interaction between the bar element and surrounding elements. The strains measured in the two bars are therefore the outer fiber strains ϵ_r and ϵ_l. These strains may be related to the

bending strain ϵ_b and axial strain ϵ_a as follows:

$$\epsilon_a = \tfrac{1}{2}(\epsilon_r + \epsilon_l) \tag{5}$$

$$\epsilon_b = \tfrac{1}{2}(\epsilon_r - \epsilon_l) \tag{6}$$

For the case of pure bending (no axial load) $\epsilon_r = -\epsilon_l$ and $\epsilon_a = 0$. For purely axial loads $\epsilon_r = \epsilon_l$ and $\epsilon_b = 0$. [3] Once the strains have been computed the moment per unit width of wall is obtained from the following:

$$M = 2EI\epsilon_b \tag{7}$$

The factor of 2 in the above equation results from the depth to neutral axis of 1/2 corresponding to the 1-ft-wide sheet-pile element.

Accuracy of computed moments

22. The ability of the strain-gage method to accurately predict moments was tested by comparing moments computed in a finite element analysis of a fixed-end beam with hand calculations based on beam theory, Figure 2. Note that the modulus value used in the example problem was not that of steel. The value used is explained in the discussion in paragraph 18. The results from the computer analysis differ from the hand calculations by 0.01 percent. It was found from trial computations that using $\nu = 0.25$ underestimates the displacement by 7.0 percent, a value consistent with the factor $(1 - \nu^2)$ that appears in the relationship for plate stiffness.

23. The displacement along the beam is approximated by the solid element as a series of straight lines. (If, instead, the beam is represented by a true bending element the displacement would be represented by a smooth curve.) As a result, the bending moment computed for the element represents an average value that is presumably indicative of the value at the center of the element. The resolution can be improved by using more elements to represent the pile.

[3] Note that a stiffness could be given to the bar to customize the beam element for unsymmetrically reinforced concrete walls, etc. or to model tensile cracking of walls by using a compression-only bar. Also pure shear deformation of the pile causes no strain in the bars, a fact that could be of some importance since the moment of inertia (I) scales as the cube of the pile thickness whereas the shear stiffness is proportional to thickness. Thus, the bars could be used to add stiffness to bending without changing shear behavior.

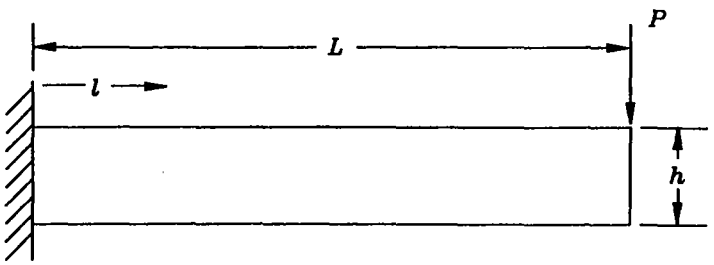

L = 100 ft
$h = b$ = 1 ft
I = 0.00888 ft^4 per ft
E_s = 4.45 * 10^8 lb/ft^2
P = 100 lb
E = 4.18 * 10^9 lb/ft^2

FINITE ELEMENT ANALYSIS	THEORETICAL ANALYSIS
	$I_s = \frac{1}{12} b h^3$
I_s = 0.08333 ft^4	I_s = 0.08333 ft^4
$E_s I_s$ = 3.71 * 10^7 lb–ft^2	$E_s I_s$ = 3.71 * 10^7 lb–ft^2
	$v_{max} = \frac{PL^3}{3 E_s I_s}$
v_{max} = –10.78 in.	v_{max} = –10.78 in.
	$M_l = P(L-l)$
$M_{2.5}$ = 9749 ft–lb	$M_{2.5}$ = 9750 ft–lb

Figure 2. Example problem for comparing moments computed from the strain gage method with hand calculations for a beam having the stiffness of a PZ-27 sheet pile

However, the important feature of the solid elements is that they deform in a manner that is compatible with adjacent soil elements, a consideration of far greater importance than the small error inherent with the linear approximation.

Interface Properties

24. The interface between the soil and pile requires special consideration because unless relative slip is permitted between the soil and pile the stiffness of the combined soil-pile system will be overestimated. The SOILSTRUCT program provides a special-purpose "interface" element to model slip and separation between the soil and pile. Although this element can model complicated stress-displacement behavior, for the analysis presented here a rigid-slip mechanism was assumed;

slip or separation could occur only when the strength was exceeded, at which point the interface offers no further resistance. Thus only the interface strength is required in the model. The shear resistance of the interface is defined by cohesion c, which represents the adhesion between the soil and the steel pile. In general, c should be less than the shear strength of the soil adjacent to the pile. For all analyses it was assumed that $c = 100$ psf, a value that is undoubtedly conservative, particularly for deeper portions of the pile. Separation between the soil and pile occurs when the soil pressure becomes negative (tensile).

Loading History

25. An important feature of soil-structure interaction analyses using SOILSTRUCT is the importance of modeling details of the loading and construction sequence. For I-wall analyses, the sequences consist of the following:

a. The initial stress in the soil created by consolidation under the weight of the levee is computed. This computation was performed as a gravity "turn-on" whereby the stresses induced by the weight of foundation soils and the levee are estimated from an initial elastic analysis. The stresses from this analysis are used to compute stiffness and strength as described in the previous section on soil properties.

b. The sheet pile is inserted. The sheet-pile elements are initially assigned soil properties for the initial stress analysis. Insertion of the pile consists simply of changing the property designation in these elements from soil to steel; the physical details of pile driving are not considered.

c. Water loading is applied as distributed pressures on the soil and pile elements. The water loads are applied in nominally 1-ft increments. This step size was required to maintain stable numerical computations especially as the pile-levee system approached the point of instability.

d. For the wave loading analysis (included in Appendix A), wave loads are applied as concentrated forces.

PART III: ANALYSIS OF FIELD LOAD TEST ON E-99 SHEET-PILE WALL

Introduction

26. The E-99 test section was analyzed using the SOILSTRUCT program to establish the ability of the finite element method to analyze sheet-pile walls in soft clay. The analysis also provided a means to determine the appropriate values for soil stiffness through a comparison of measured and computed displacements and bending moments. As discussed in Part II, the stress-strain properties of the soil are specified by an initial stiffness and the soil strength. Soil strength profiles were obtained from NOD. Thus the principal parameter to be determined from the field load test was the initial stiffness of the soil. To make the determination of initial stiffness more systematic, the initial stiffness was expressed as a ratio of undrained shear strength as in Equation 8.

$$E_i = KS_u \tag{8}$$

where K is known from experience to range from 250 to 1,000 (Clough and Tsui 1977 and Mana 1978).

Finite Element Mesh for E-99 Section

27. The mesh used to model the E-99 test section is shown in Figure 3. The mesh consists of 281 solid elements and 322 nodes and models the foundation between elevations (el) +6.5 to -35 ft. [1] The sheet-pile elements are attached to the soil elements by 19 interface elements. The water loads are applied to the soil surface and pile as linearly varying distributed loads in increments corresponding to water levels of 4.0, 6.0, 7.0, 8.0, and 9.0 ft.

Material Properties

28. The data available for independent assessment of soil properties were severely limited, placing considerable importance on back-analysis of the field test results. Data available from pretest investigations were limited to field classification and Q tests. The specimens tested

[1] All elevations cited herein are in feet and referenced to the National Geodetic Vertical Datum (NGVD).

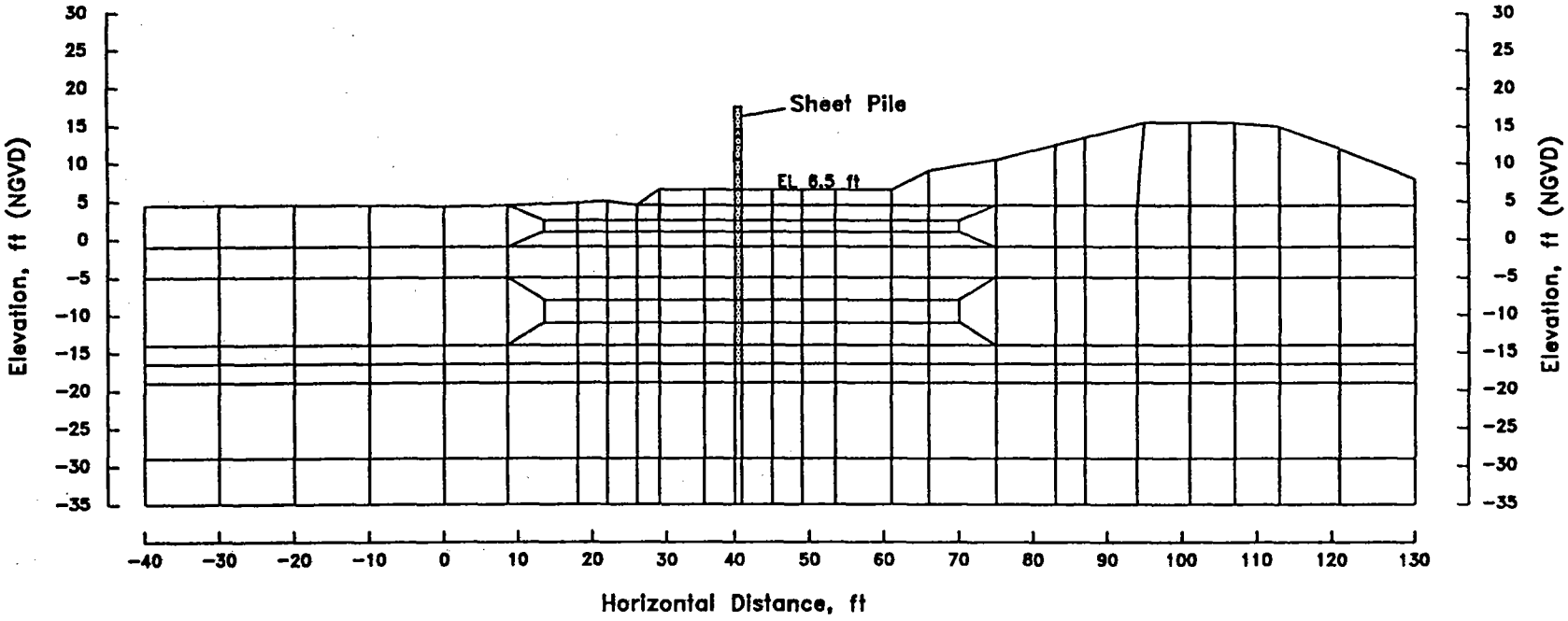

Figure 3. Finite element mesh for analysis of field load test

specifically for this study (see Appendix B) were sampled too far from the pile location to be directly applicable for determination of the strength profile. In the course of the analysis it became readily apparent that the strength profile presented in the field data report overestimated the strength in the upper part of the soil, a conclusion that could be only indirectly supported using the available data.

29. The analysis of the field data was aided by an observed property of the computation procedure: the moment distribution is principally determined by the strength profile whereas the displacement depends on the stiffness factor K. Further, as already noted, the shape of the force-displacement plot was found to be independent of details of the stress-strain curve; thus the stress-strain stiffness parameter K is directly tied to the stiffness of the load-deflection response.

Shear strength profile

30. Soil strengths were entered into the analysis in two ways. First, the upper fill material was assigned a constant undrained shear strength value of 200 psf. Second, the foundation materials were assigned normalized strength values (S_u/p'_c). As discussed in Part II, the strength of these materials depends both on the assigned S_u/p'_c and the initial consolidation stress p'_c which is computed by the program as part of the analysis. The normalizing stress p'_c is the average principal stress $(\sigma'_v + \sigma'_h)/2$ prior to loading (consolidation stress) and is computed from a stress analysis of the initial levee configuration assuming drained conditions. In either case, after the initial stress has been computed, the soil's response to further loading is assumed to be undrained, thus $\phi = 0$.

31. The soil strengths are shown in Figure 4. The strengths shown are those computed at the center of the finite elements corresponding to the sheet pile prior to its insertion into the mesh. The design strengths given in the field data report are shown for comparison. It is seen that the strength used in the analysis is much lower than the design profile as a result of eliminating the "strong" layer between elevations -1.0 and -5.0 ft. The Q-test data shown could, arguably, be used to support either profile. The strength profile used for the finite element analysis is based on the following:

a. The S_u/p'_c ratio for the soils at the site were on the order of 0.45 for the normally consolidated state (see Figure B1 in Appendix B). A strong layer of 200 psf at such a shallow depth implies a strong degree of overconsolidation within the upper layer. The profile used in the finite element analysis is based on the assumption that the soil is normally consolidated.

b. The boring data suggested very soft soils in the upper layer at several locations. In some cases soils with water contents in excess of 100 percent were encountered.

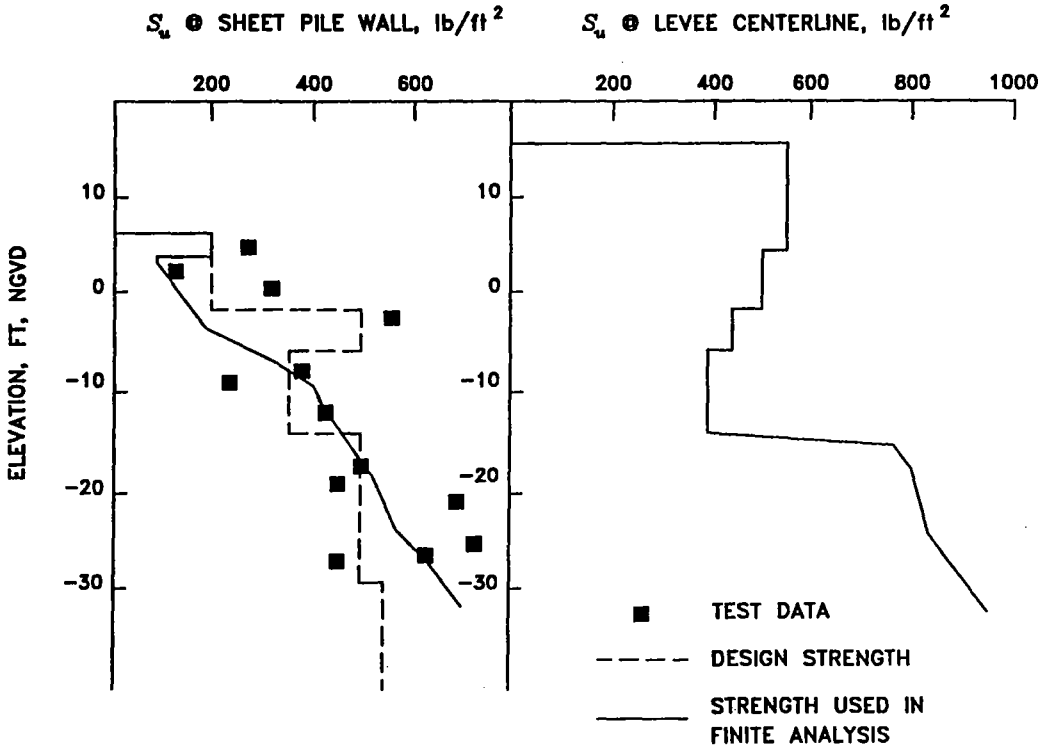

Figure 4. Comparison of design strength profile and strengths from elements at pile location

At other locations samples were not obtained. Therefore, while some Q tests indicated materials with high strength, these samples may not be indicative of the general performance of this layer.

c. The placement of a nominal 2 ft of fill at the top of the levee induced 0.1 - 0.3 in. of movement 60 ft away at the site of the sheet pile (see field data report) indicating soft soil conditions. Trial finite element analyses of this fill loading indicated that the upper soils must have been in their normally consolidated state for the observed movement patterns to have occurred.

d. The measured moments could be obtained from the analysis by assuming these soils to be normally consolidated; use of the design profile resulted in computed moments that were significantly lower than those measured. As noted previously, the moment distribution is controlled by the strength profile, presumably because strengths in the shallow soils are fully mobilized. Based on extensive computations it was concluded that the magnitude of the observed moments could only be obtained by the strength profile shown in Figure 4.

The soil profile for the area under the dike was derived directly from the strength data presented in Appendix B.

Soil stiffness

32. The soil stiffness was derived directly from the field test data based on the assumption that all soils at the site had the same value of K. The nonpredictive nature of the hyperbolic model presents a difficulty in obtaining the stress-strain response from soil tests, particularly for loading under undrained conditions. The stress-strain response depends on the initial consolidation state and the type of loading. For example, the stress-strain response of anisotropically consolidated specimens differs from the conventional isotropically consolidated specimen; generally the anisotropically consolidated specimen is stiffer and displays a pore-pressure-induced softening behavior after the peak strength is reached. The hyperbolic model cannot predict such differences [2] and calibration of the model must be done using tests that replicate the stress path to be experienced by each element. The sophisticated testing program required for such a calibration is clearly not practical and field calibration is therefore required.

Computed Sheet-Pile Displacements and Moments

33. The computed displacements for two values of K are compared to the average displacement measured along the sheet-pile wall in the field test during loading (Figure 5). From the plot two features are apparent:

a. Use of $K = 500$ to estimate soil stiffness overestimates displacements in all phases of loading whereas $K = 1,000$ slightly overestimates displacements in the initial phase of loading and underestimates displacements after the break in the load-versus-deflection curve. In fact, it appears that the displacement is nearly proportional to K since an increase from $K = 500$ to $K = 1,000$ approximately doubles the displacement.

b. Both computed and observed pile displacements begin to increase rapidly with increasing head as the head approaches 8 ft. This second observation suggests that the analysis correctly predicts the ultimate head that the pile can support. However, the structural ductility of the pile-levee system is somewhat overestimated by the finite element model, as seen from the inability to match the curvature in the load-displacement curve. After extensive trial computations it was concluded that to match the displacement near 8 ft of head it is necessary to use a lower stiffness ($K = 500$ or less) whereas the stiffness that best matches the initial loading case is higher ($K = 1,000$ or greater). All of the computations agreed with the field data in indicating that the stiffness decreased rapidly for heads above 6 ft and thus in all cases the allowable load would be predicted properly. Therefore, a stiffness of $K = 1,000$ is adopted to provide a more accurate initial displacement.

[2] The hyperbolic model does not predict softening behavior in any case.

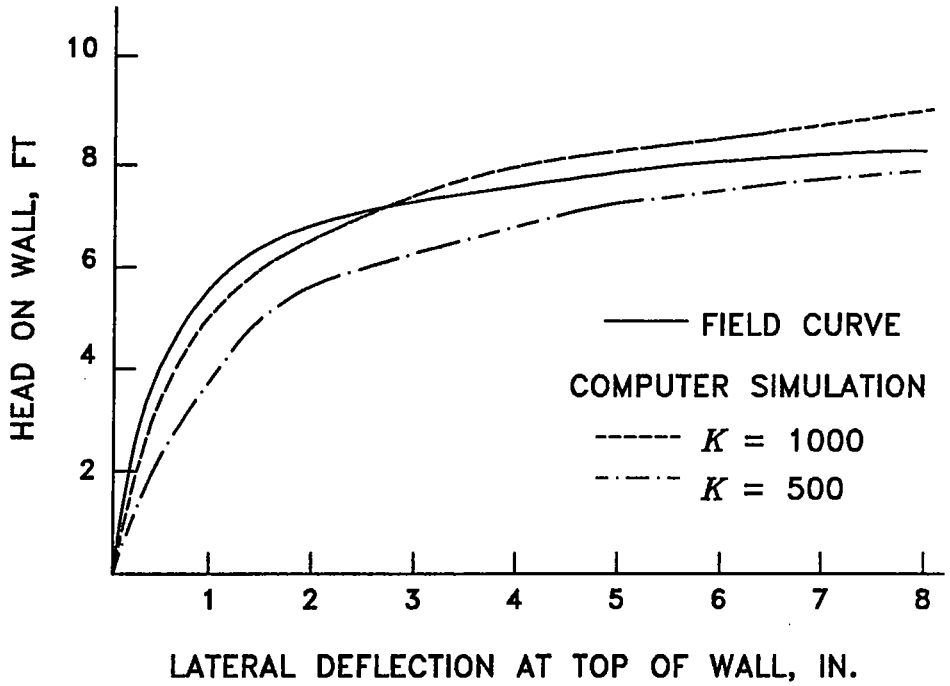

Figure 5. Comparison of measured and computed deflections at top of pile for $K = 500$ and 1,000

34. In Figure 6 the computed deflection is compared with displacements for an inclinometer that was placed 4 ft in front of the pile. The agreement is seen to be quite good for $K = 1,000$. Note that the displacement at the pile tip is shown by both computation and field data to be in the range of 0.25 to 0.50 in. Although this value is small, it does indicate that the entire foundation mass is moving outward from the levee as a result of the water loading. This feature will become important for the analysis of the E-105 section, which displays a deeper profile of soft soils.

35. The computed distribution of bending moments is compared with field measurements in Figure 7. The shape of the computed distribution and the location and magnitude of the maximum moment agree well with the field measurements. The maximum moment computed by the finite element method, however, does not agree with that presented by Jackson (1988) because the CANWAL-derived moments were based on a factor of safety of 1.30 and the design strength profile. Using the appropriate strength profile and a factor of safety of 1.0 produced a maximum moment that was still higher (31,000 versus 21,500 ft-lb) but compared more favorably

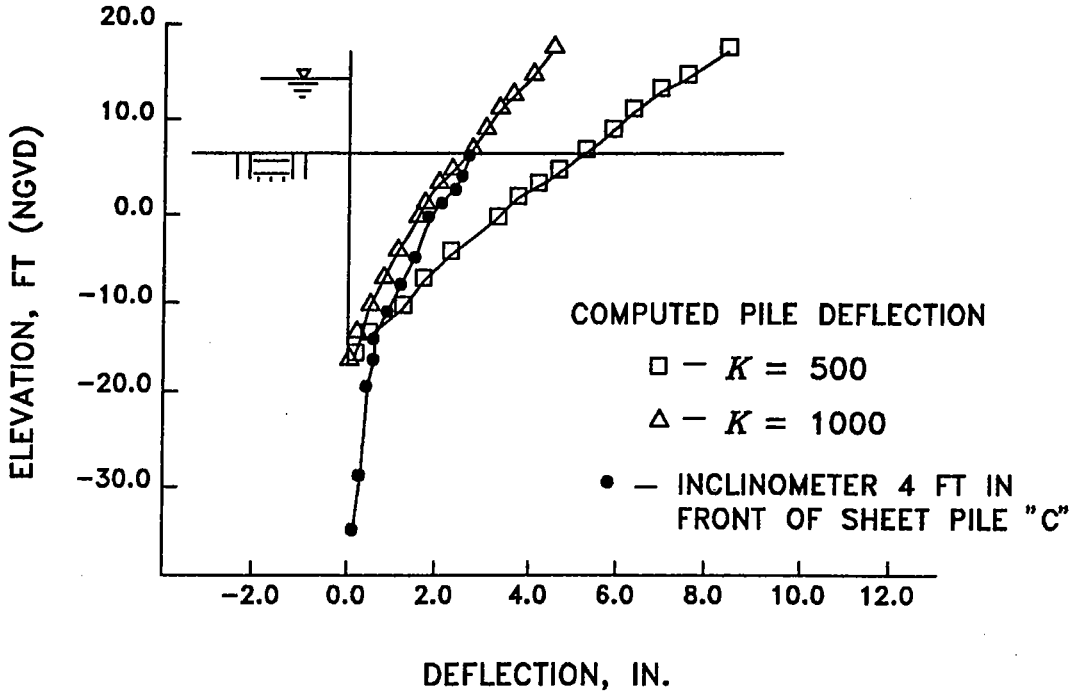

Figure 6. Comparison of computed deflection of "C" pile with displacements of inclinometer at E-99 test section

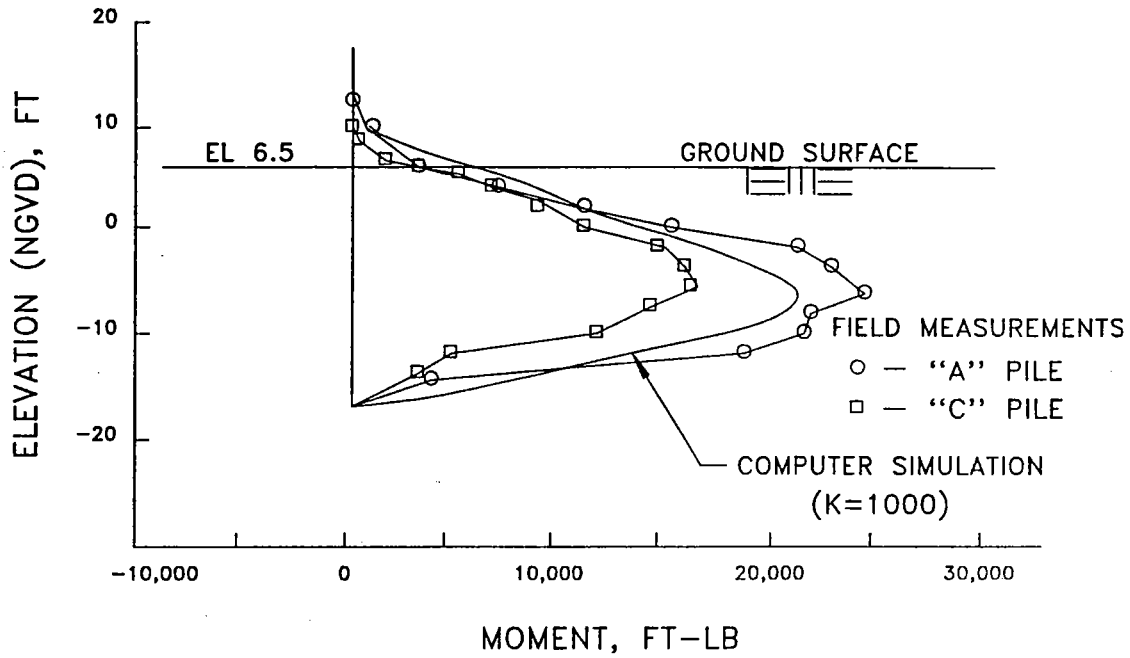

Figure 7. Comparison of measured and computed bending moments for "A" and "C" piles under 8 ft of water loading at E-99 test section

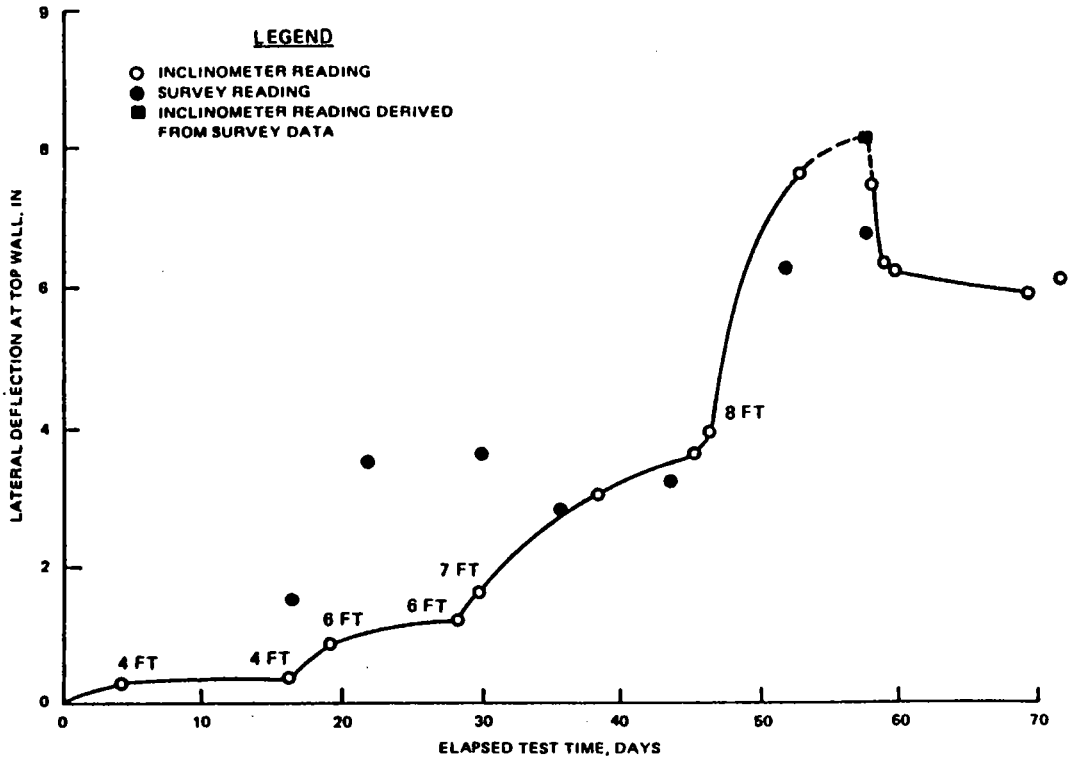

Figure 8. Creep of piles during load test (Jackson 1988)

with the moment distribution and maximum moment location measured in the field. Further investigation showed that when no shear resistance was assumed between the sheet-pile wall and the soil in the finite element analysis (a CANWAL assumption) a maximum moment of 32,500 ft-lb was calculated. This indicates that results from CANWAL and the finite element method are comparable if the same assumptions are imposed on both analyses.

Effect of Load Duration

36. An assessment of the finite element analysis would not be complete without some consideration of the load duration. The loading history in Figure 8 shows displacement plotted as a function of time. The tendency of the soil to creep is apparent from the plot. The simple stress-strain model used in SOILSTRUCT does not allow creep to be included in the analysis in any direct way but its effect can be accounted for by use of a reduced modulus. In essence, the effect of creep has been included because the stiffness was calibrated from the field results. Therefore, the calibration is suitable for a load duration comparable to the load test; it is expected that the stiffness would be greater for short-term loading. Although it would appear that the

stiffness values used may be somewhat conservative for short-term loadings, these results may not be applicable to repeated wave loading. Under such loading, the soil would tend to soften as a result of excess pore pressures thus eliminating any benefit gained from the short duration of the loads.

Conclusions from E-99 Analysis

37. The SOILSTRUCT analysis of the E-99 section clearly shows that the finite element model can be used to predict the behavior of cantilever sheet-pile floodwalls. The following conclusions can be drawn from the analysis:

a. The displacement-versus-head relationship is predicted well. The ability of the analysis to predict the larger displacements as the head approached 8.0 ft is particularly important because it implies that the limit load can be computed accurately.

b. The displacement distribution is predicted well. The ability to predict displacements near the pile tip is significant because in soft-soil foundations deep-seated movements can control the displacements of the pile-levee system.

c. The computed maximum moment and its location agreed well with those measured in the field test.

PART IV: PARAMETRIC ANALYSIS: E-105 SHEET PILE-LEVEE PROFILE

Introduction

38. The analysis of the E-105 section was performed similarly to the analysis of E-99. Soil strengths were inserted into the program as both S_u and S_u/p_c' values based on data provided by NOD and laboratory results. The soil stiffness was based on Equation 8 using $K = 1,000$, a value that was based on analysis of the E-99 section. However, the E-99 and E-105 sections differ in three fundamental aspects that should be kept in mind as the results are described. These are:

a. The soil strengths are generally less for the E-105 section than the E-99 section.

b. The increase in soil strength with depth is less for the E-105 section, making the deep-seated movements more important.

c. The extent of the loaded area behind the sheet-pile wall is much greater for E-105 than for E-99; this tends to increase the depth of significant movement.

39. Another important difference in the analyses of E-99 and E-105 is their purpose. The purpose of the E-99 analysis was to investigate a particular case having specified pile depth, section properties, and loading sequence. E-105 was analyzed to investigate design implications of the soft foundation behavior. As a result, the analysis of E-105 involves six different pile depths, two pile sections, two strength profiles, and four loading heights.

Finite Element Mesh

40. The finite element mesh, shown in Figure 9, was developed in two trials. The first trial consisted of a mesh shown by the insert that was of relatively limited extent. However, the E-105 section displayed large movements that extended to considerable depth. A review of computed results for sheet piles driven to different depths showed that the mesh shown in the insert was too restrictive and caused the computed movements to be too small. A second mesh was therefore constructed that provided for large movements below and in front of the pile.

Material Properties

41. The properties for the E-105 section were treated similarly to the E-99 section. Drained properties were assumed for determination of initial consolidation stress but undrained properties (with $\phi = 0$) were assumed for all loadings thereafter. The upper fill materials were

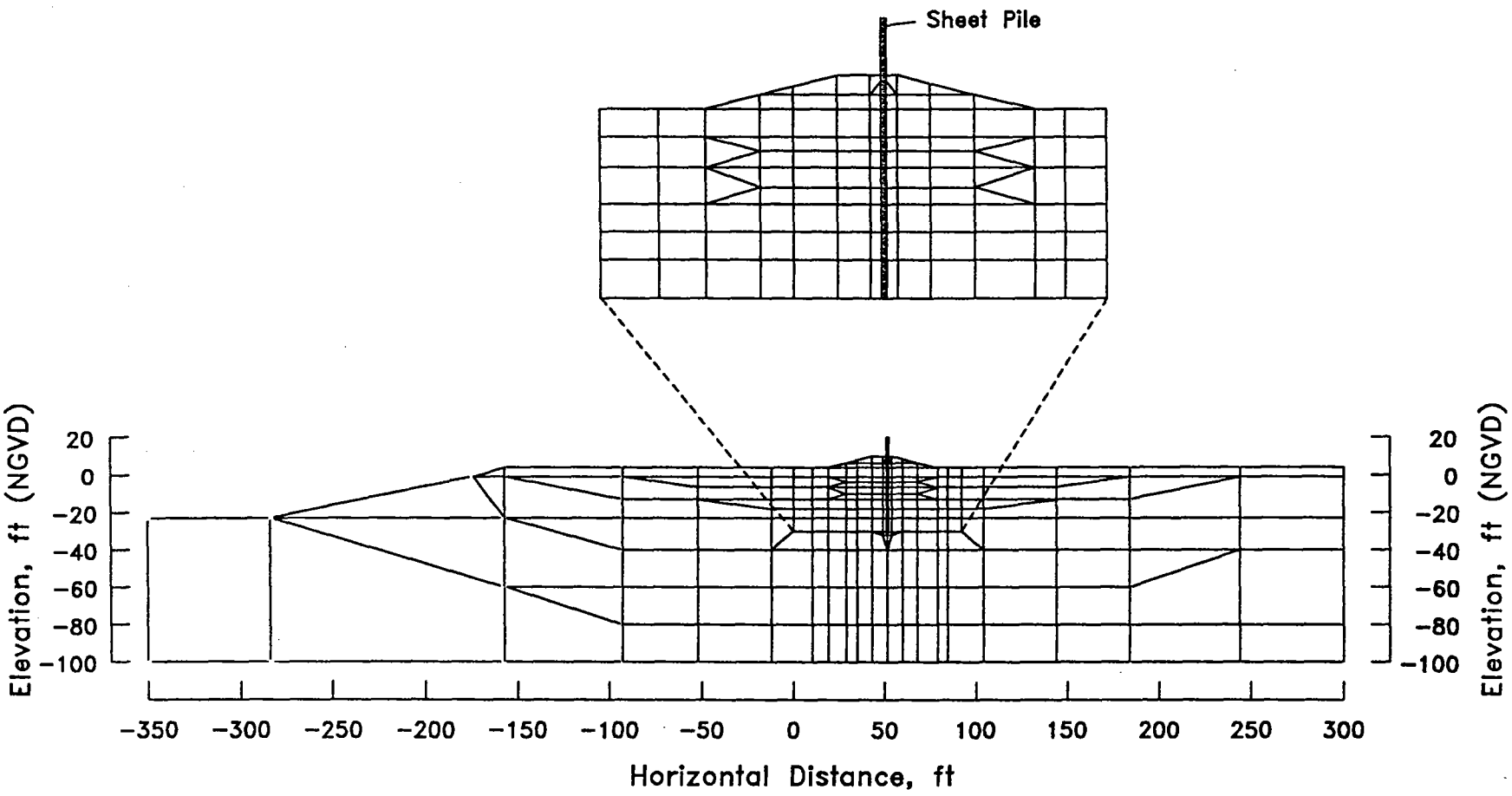

Figure 9. Finite element mesh for E-105 levee section

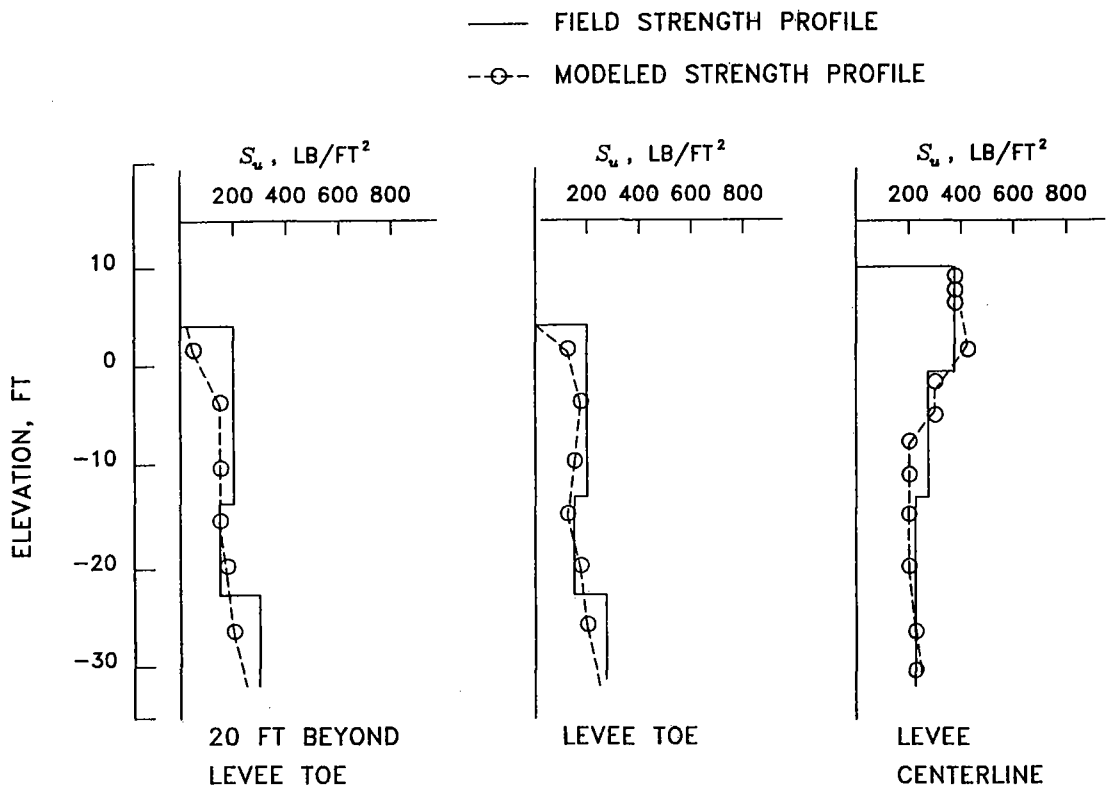

Figure 10. Comparison of design strength profile and strengths from selected elements for "weak" soil profile

assumed to have constant $S_u = 400$ psf. The remainder of the profile was given S_u/p_c' values. The resulting strength profiles are compared in Figure 10 for the levee centerline, toe, and 20 ft beyond the toe. Note that the profile of S_u/p_c' needed to match the E-105 design strength is considerably more complex than that used for E-99.

42. An analysis was also performed for a section geometrically similar to the E-105 section but with a strength profile similar to E-99. The original E-105 section will therefore be referred to as the "weak" section while the higher strength profile will be referred to as the "strong" section. The strength profiles for the strong section are shown in Figure 11.

General Trends from Parametric Analysis

43. All finite element computations are summarized in Appendix A; these results will be summarized here in general terms. Figure 12 shows four stability situations that were observed in the finite element analyses:

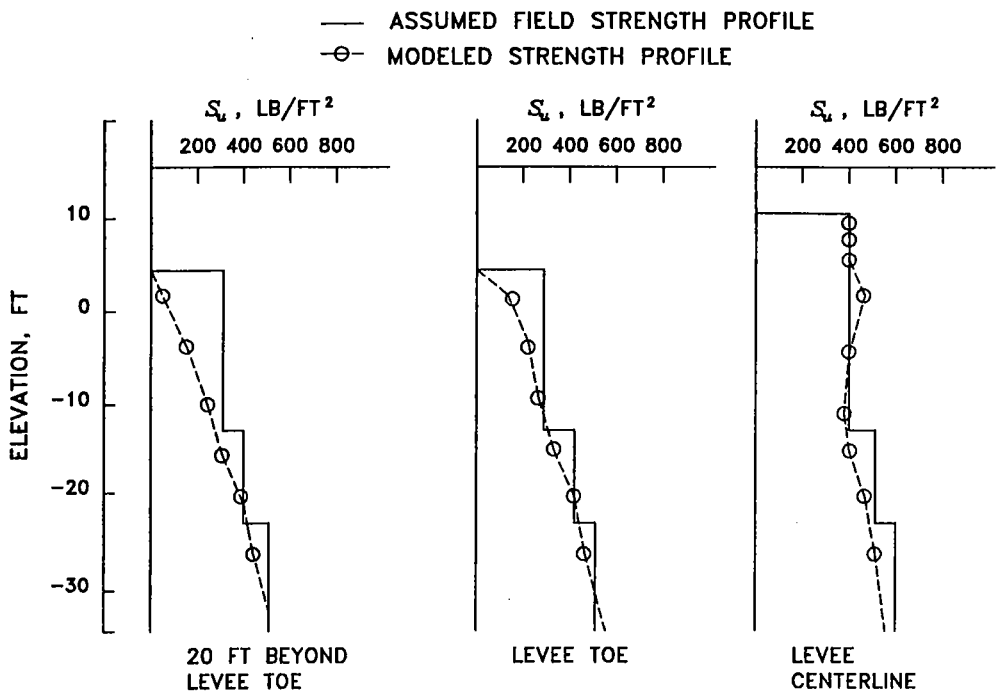

Figure 11. Comparison of design strength profile and strengths from selected elements for "strong" soil profile

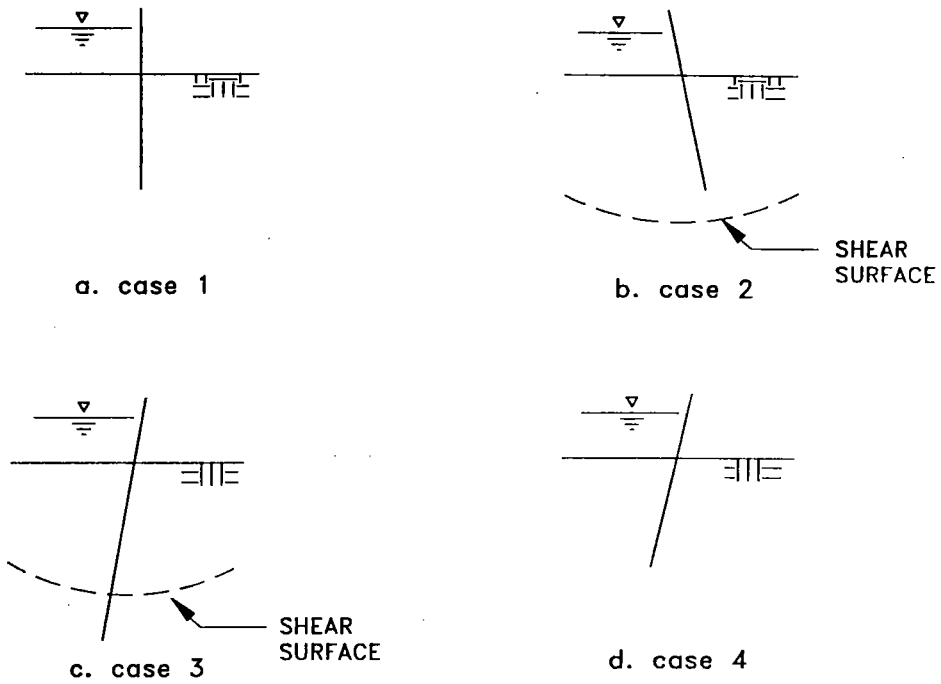

Figure 12. Different cases of levee and sheet pile stability

a. Case 1: The sheet pile and levee are both stable under the current loading condition.

b. Case 2: The levee foundation is unstable and the sheet-pile tip is above the shear surface.

c. Case 3: The levee foundation is unstable and the sheet pile extends below the shear surface.

d. Case 4: The levee foundation is stable but embedment of the sheet pile is insufficient.

Case 1 corresponds to a design that meets all requirements of stability as computed by a slope stability analysis and CANWAL. Cases 2 and 3 occur when an adequate safety factor, as determined by slope stability computations, is not obtained. Note that while extending the sheet pile below the shear surface influences the displacement pattern it does not improve the performance of the levee-pile system. Case 4 occurs when all requirements for foundation stability have been met but the safety factor against overturning, as determined by CANWAL, is too low. In the two sections that follow, the correspondence between the finite element analysis and limit-equilibrium methods (slope stability and CANWAL) will be discussed in detail.

Slope Stability Analyses

44. To complement the finite element analyses, slope stability analyses were performed on the E-105 levee cross section. Both circular arc and wedge-shaped shear surfaces were analyzed using the computer code UTEXAS2 (Edris 1987). The code uses the force equilibrium procedure with the Corps of Engineers modified Swedish side force assumption, which satisfies both the vertical and horizontal force equilibrium requirement. The code also assumes that the side force inclination is constant at a user-selected angle. For these analyses a side force inclination of 0 deg was used, making it similar to the procedure used by the USAE Districts for this type of stability analysis. The objective of these analyses was to determine the correspondence between the displacements computed by the finite element analyses and the safety factor computed by the limit-equilibrium method.

Modeled section

45. The cross section shown in Figure 13 was modeled in the analyses. Typically, for levees founded on soft normally consolidated clay deposits, the material strengths under the levee are higher than those beyond the toe of the embankment. To model the strength variations, the

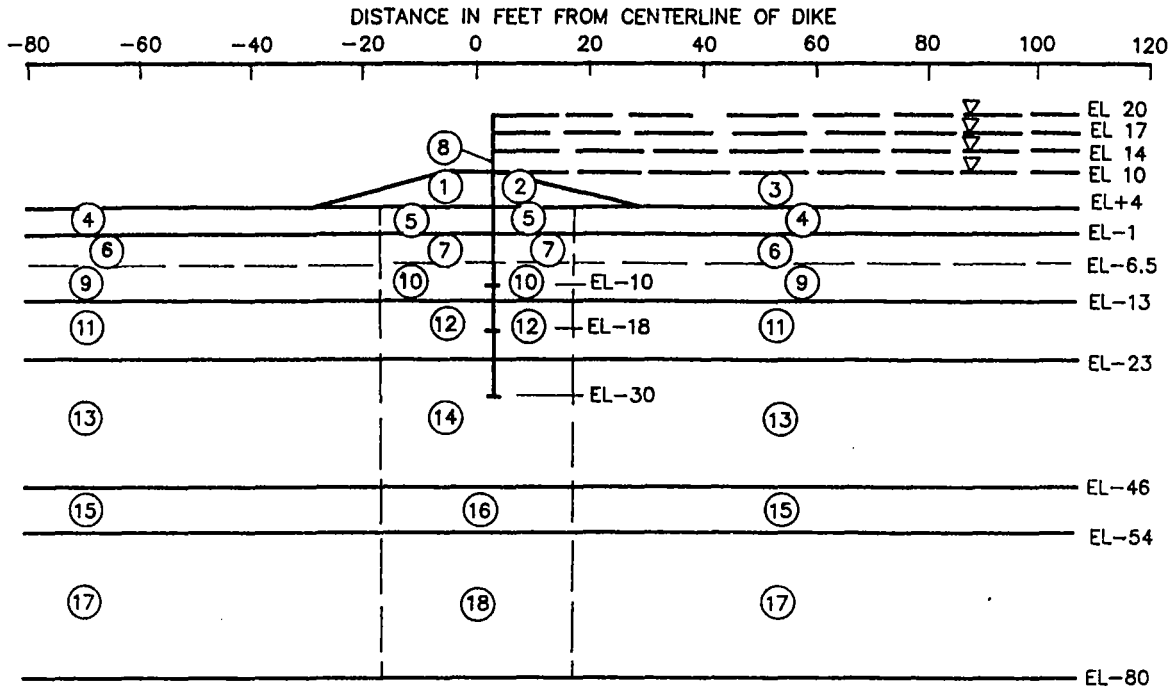

MATERIAL NUMBER	UNIT WEIGHT, PCF	COHESION PSF	REF ELEV, FT	RATE OF CHANGE IN COHESION	COMMENTS
1	100	400	–	–	LEVEE
2	100	400	–	–	LEVEE
3	62.4	0	–	–	WATER
4	38	170	4	12	
5	38	500	1.5	−12	
6	18	190	−10	−4.5	
7	28	375	−3.75	−12	
8	175	3600	0	−200	SHEET PILE
9	18	190	−10	−4.5	
10	28	250	−13	−12	
11	28	230	−20	7	
12	28	250	−13	4	
13	38	300	−29	9.5	
14	38	320	−30	9.5	
15	28	480	−50	7	
16	28	500	−49	7	
17	38	510	−54	9.5	
18	38	600	−60	9.5	

Figure 13. E-105 section and assumed material properties used in stability analyses

material under the levee was modeled as having a higher strength. Because of the large number of soil strata, the UTEXAS2 code was modified to handle up to 40 profile layers.

46. The field strength profile of the E-105 weak section was modeled for these analyses. Figure 14 shows the slope stability strength profile, the profile used in the finite element analyses, and the field strength profile obtained from the LMVD. The field strength profile was well matched for both analyses. The UTEXAS2 code required that the shear strengths be represented by a cohesion value and a rate of change in cohesion with depth. The cohesion is the value at the top of each soil layer and the rate of change in cohesion is taken to be from top to bottom of that layer.

47. The sheet pile was modeled as a soil layer having the unit weight of steel and a strength equal to the pull-out resistance that can be developed below the shear surface. The pull-out resistance is modeled as a function of the pile surface area and soil shear strength. For a PZ-27 sheet pile section, its pull-out resistance was assumed to increase at a rate of 200 lb/ft along its embedment depth, a value consistent with the interface resistance used in the finite element analysis.

48. The water loads on the soil layers could be applied either as surface load or as a soil layer with zero friction and cohesion. In these analyses, the water loads were modeled as a soil layer with zero cohesion and friction. Representing water loads this way ensured that the proper horizontal pressures were applied to the sheet pile. Several different water loads were evaluated in the analyses. These loads represent different flood levels and range from el +10 (6 ft of head on the levee with no head on the pile) to +20 ft.

Analysis variables

49. The variables in the analyses included the water loads and the pile length (Figure 13). Five different water loading cases were considered, water level at el +10, +12, +14, +17, and +20 ft. The pile embedments were 40, 28, 20, and 11 ft, with the pile extending 10 ft above the levee surface for all cases.

Results

50. The stability results were compared with those from the NOD for the same shear surface configuration. The differences in the resulting safety factors are attributed to the differences in the methods used to model the shear strengths, the strength values themselves, and the sheet pile being represented as part of the levee in these analyses. In the NOD analyses the shear

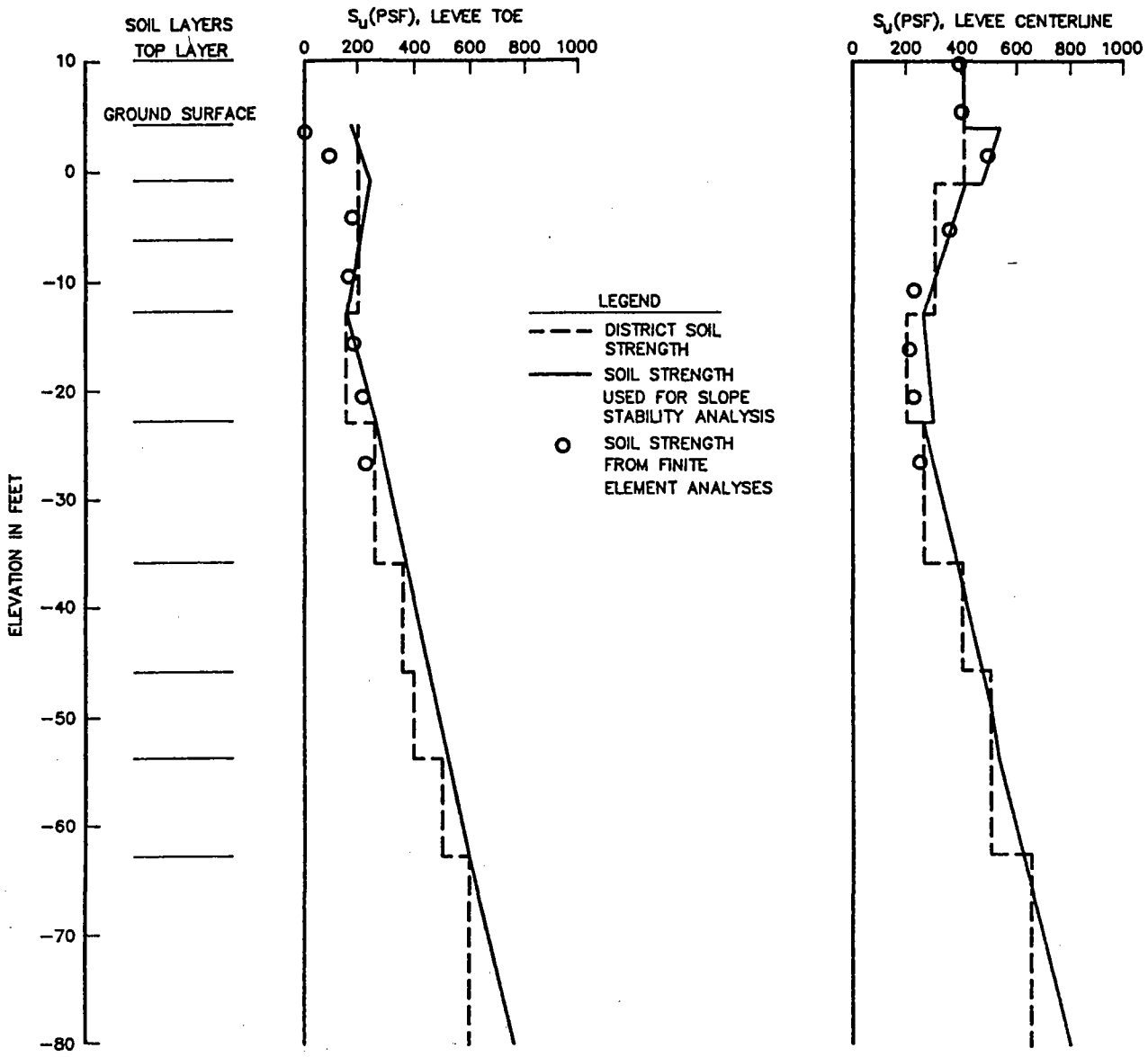

Figure 14. Comparison of design strength profile with stability and finite element analyses

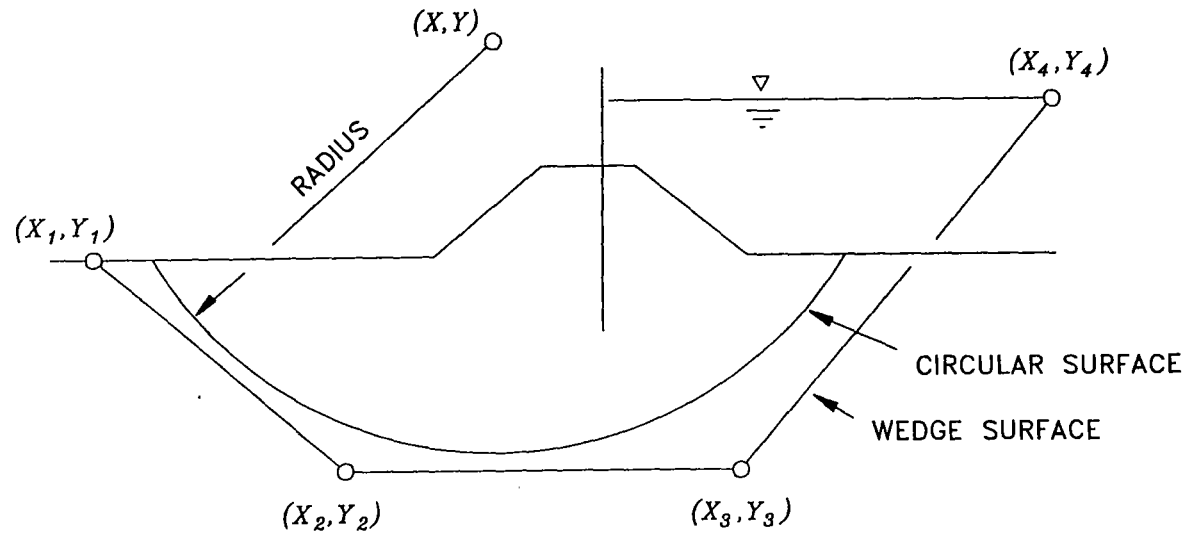

ORIGIN $\begin{cases} X_o = \text{CENTERLINE OF LEVEE} \\ Y_o = 0.0 \text{ FT (NGVD)} \end{cases}$

$Y_4 = \text{WATER LOADING ELEVATION}$

Figure 15. Definition of shear surface coordinates in Tables 1, 2, and 3

strength varied linearly under the levee from the centerline to the toe, but remained constant with depth in each soil layer.

51. The results of the slope stability analyses are listed in Tables 1 through 3. Table 1 lists the results for the circular arc surfaces. Along with safety factors, the radius and rotational center of the potential failure arc are given. In Table 2 results for general wedge-shaped surfaces are given whereas Table 3 presents results for wedge-shaped sliding surfaces that have nearly horizontal basal sliding surfaces. The coordinates used to define the wedge-shaped surfaces in Tables 2 and 3 are defined in Figure 15. The results shown in Table 3 correspond most nearly to the conventional wedge analysis used for design by NOD. It was found that the wedge-shaped surface with a non-horizontal basal sliding plane gave the lowest safety factor but tended to approximate the shape of the corresponding circular sliding surface. Therefore, it appears that when compared on the basis of the same strength profile, the potential sliding surface is nearly circular, an assessment supported by the displacement patterns computed by the finite element analysis illustrated in Figure 16.

52. Safety factors versus water elevations for the circular and wedge-shaped shear surfaces are plotted in Figure 17. It is seen that the various assumptions for potential failure surfaces give

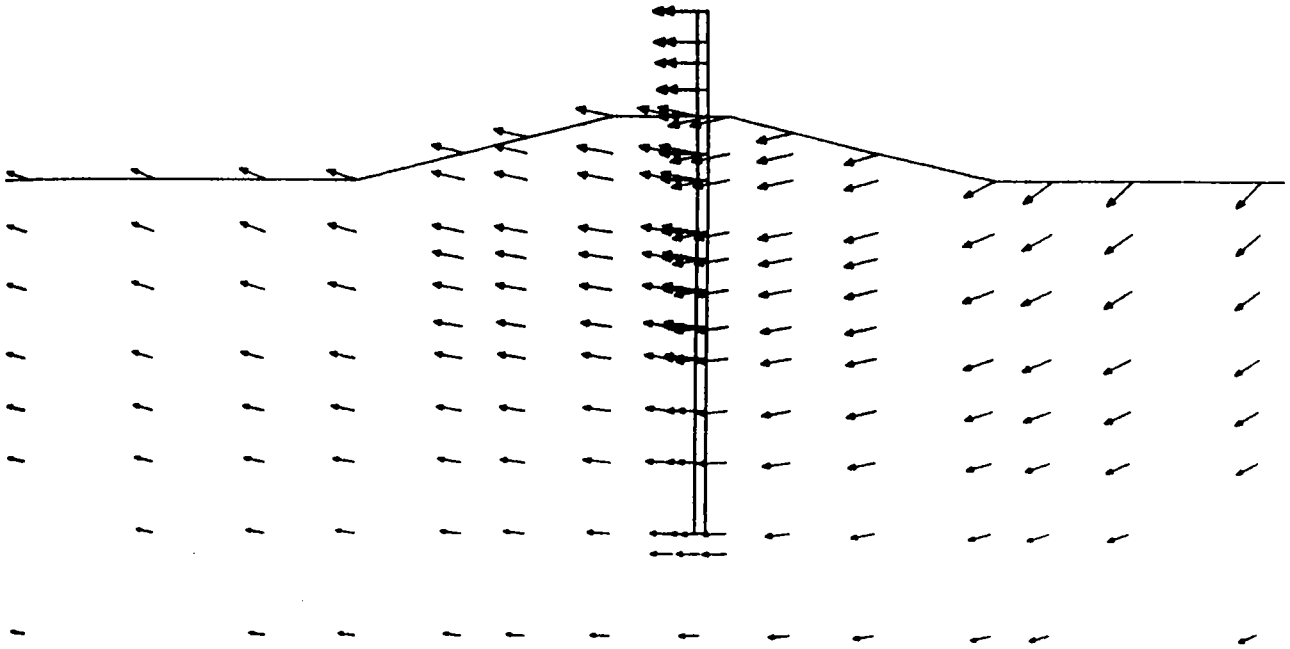

Figure 16. Circular displacement pattern predicted by finite element analysis for E-105 "weak" soil profile

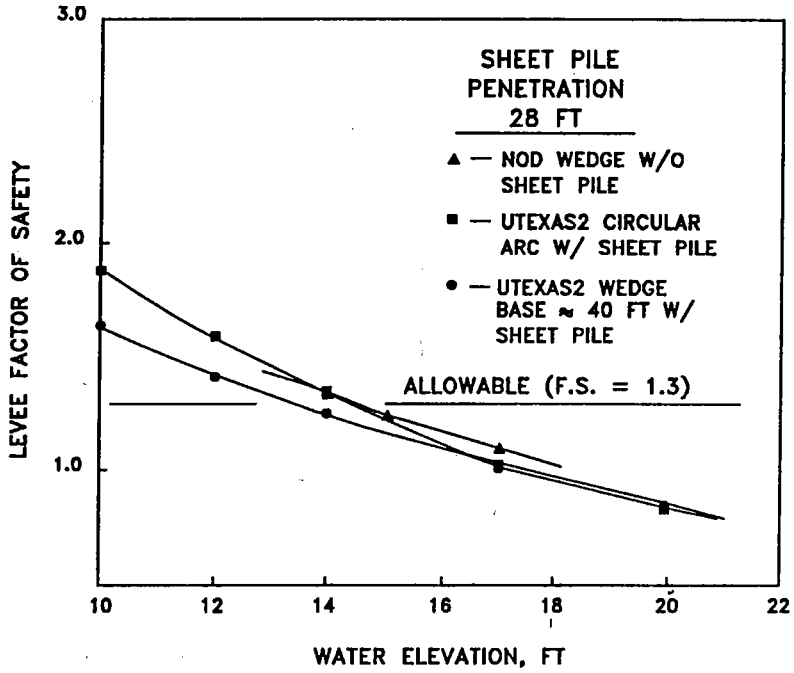

Figure 17. Safety factor versus water elevation based on slope stability analyses using the computer code UTEXAS2 and the "weak" soil profile

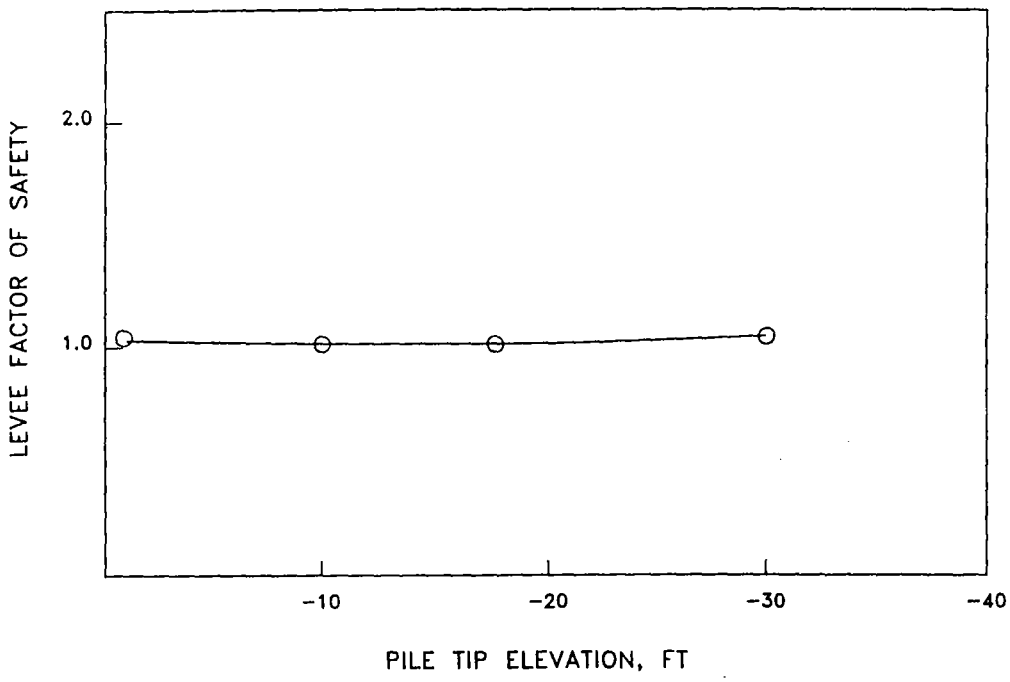

Figure 18. Safety factor versus pile tip elevation based on slope stability analyses for circular shear surface using the "weak" soil profile with water level at elevation +17 ft

approximately the same results for safety factors at or below the allowable of 1.3.

53. Comparisons between safety factors and pile embedments are plotted in Figure 18. It may be seen that increasing the pile depth does not increase the stability of the levee significantly. In fact, the safety factor is reduced slightly by embedment unless the pile is extended well below the potential shear surface that would be obtained without the pile. This reduction may be the result of the low pull-out resistance assumed for the pile, whereby the pile was weaker than the soil it replaced.

Comparison to finite element analyses

54. Displacement computed by the finite element method is compared to the safety factor as computed by UTEXAS2 in Figure 19. The comparisons are based on three different embedment depths assuming the potential failure surface to be a circular arc. The comparison is affected little by the embedment depth with the greatest scatter among the results occurring as the safety factor fell below the allowable. The most important observation to be made is that displacements increase rapidly as the safety factor falls below the allowable. Thus, the safety factors computed by the limit-equilibrium method are consistent with the computed load-displacement behavior.

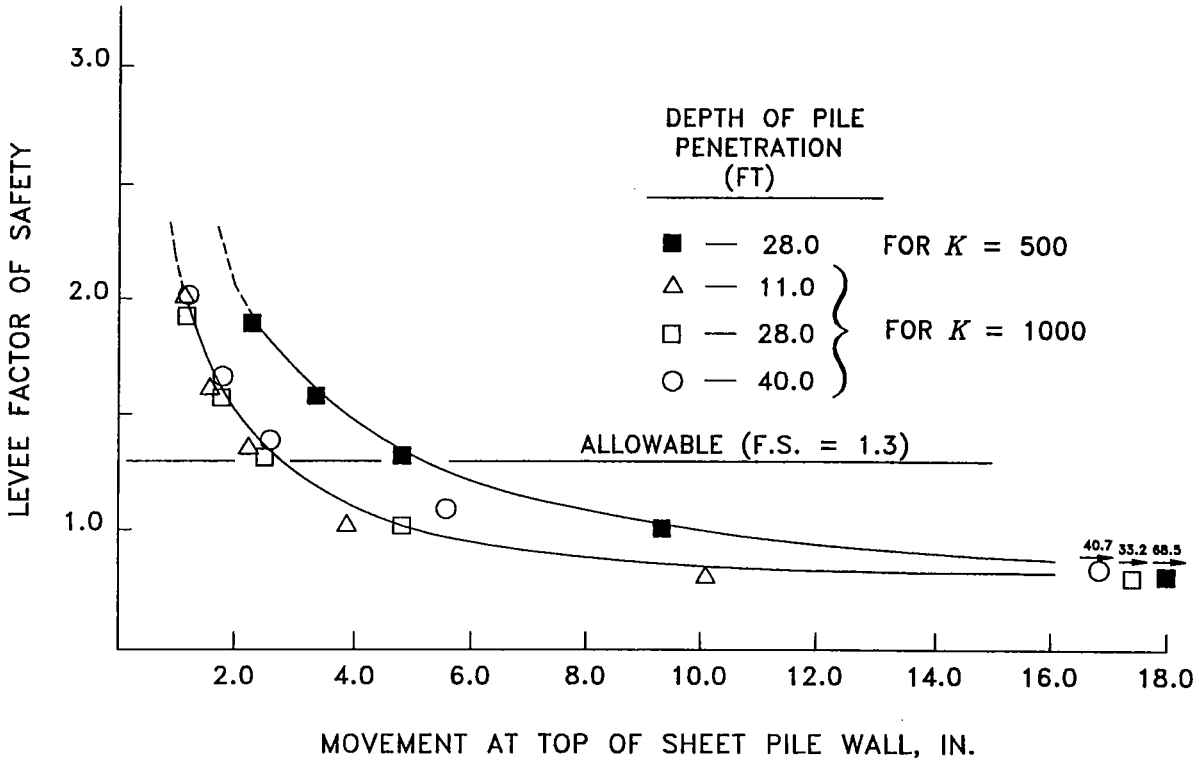

Figure 19. Displacement computed by finite element method versus safety factor computed by limit-equilibrium method

Comparison of SOILSTRUCT and CANWAL Analyses

55. A comparison was made between the finite element analysis using SOILSTRUCT and the conventional analysis using CANWAL. The CANWAL analyses, which are presented in Table 4, were provided by Mr. Rich Jackson of LMVD. The finite element results are presented in Appendix A.

56. A comparison of results in Table 4 and the maximum moments shown on the plots in Appendix A indicate that as the safety factor against overturning approaches 1.0, the moments from the finite element analysis approach those computed by CANWAL; this is a finding consistent with the results of the E-99 analysis, which showed that the moment distribution was primarily determined by the strength distribution. The displacements computed by the two types of analysis, in contrast, differ both in magnitude and in the predicted relationship to pile section stiffness. The displacements will be discussed first.

Displacements

57. The displacements obtained from CANWAL are based on the computed moment distribution and an assumed fixed point on the sheet pile. Therefore, the CANWAL analysis ignores the deep-seated foundation movement and pile tip rotation that are evident in all of the finite element analyses. Even for cases having adequate safety factors against foundation instability the computed foundation movements are much greater than those derived from cantilever action of the pile. The displacement caused by cantilever action is directly proportional to the section stiffness, a fact easily verified by inspection of the displacements given in Table 4. Thus, displacements computed by CANWAL tend to support the conclusion that displacements can be reduced by using larger pile sections. In contrast, the finite element analysis shows that the sheet pile is not effective in limiting foundation movements. In general, the deep-seated movements are resisted by the pile through axial (pullout) resistance and shear stiffness, which act within the limited zone of shear movement. Flexural action is not an efficient means of resisting these movements because they are carried over such a long section of the pile. Therefore, the CANWAL-computed displacements are not appropriate for soft clay foundations where deep-seated movements are significant and pile tip rotation occurs.

Moments

58. Figure 20 shows that as pile penetration is increased so is the maximum moment that a pile can develop. However, as the pile embedment exceeds 11 ft the moment becomes constant for a given load. Thus, the pile begins to behave as a clamped beam for embedments greater than 11 ft. Once this virtually clamped condition is reached, further embedment does little to increase the clamping effect; thus, it does little to increase the moment.

59. It is important to note that the maximum moments shown on Figure 20 correlate to those computed by CANWAL for a safety factor of 1.0 and water loads of less than 6 ft. The effect of shear resistance between the sheet pile and soil, discussed previously in paragraphs 24 and 35, does not appear to affect results until water loads are above 6 ft and the sheet pile has reached its limit load. In general, for a given water load, there is a point on the pile above which all soil strength is fully mobilized. Therefore, the moments above that point can be determined because all water and soil loads are known. Further, the moment at that point is the maximum that can be applied for a given water load because it represents the condition where the soil can supply no further resistance. For a safety factor of 1.0, loads applied below that point equilibrate the loads above, with the result that the beam could be statically analyzed as though it is clamped at the point of maximum moment. Because soil strengths around the upper portion of the pile are close

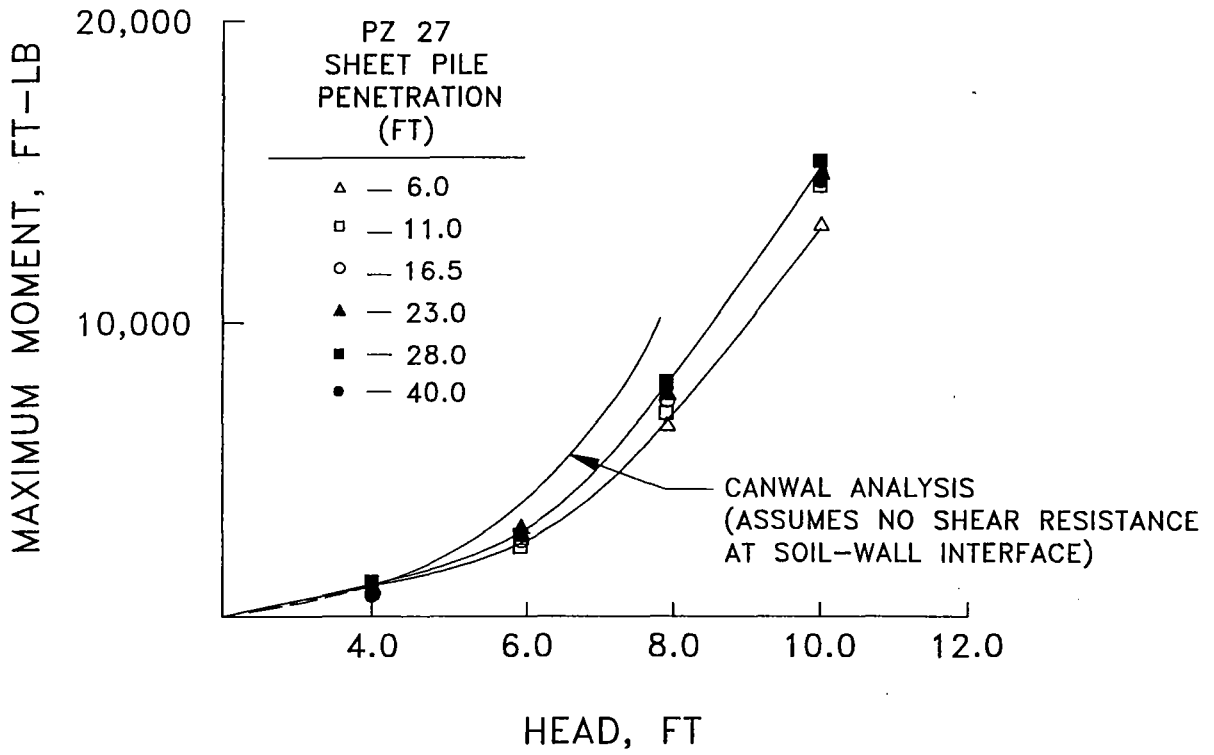

Figure 20. Maximum moment versus head from finite element analysis for different pile penetration depths in "strong" soil profile

to being fully mobilized regardless of the embedment depth, the maximum moment computed from the finite element analysis approaches that of the limiting (fully mobilized) case computed by CANWAL for a safety factor of 1.0.

Correction to CANWAL Displacements

60. A method to combine the finite element results with those from CANWAL was developed from the reasoning outlined in the preceding section. Because the moment distribution along the pile, *above the point of maximum moment*, is computed accurately by CANWAL, the displacements computed above that point are reasonably accurate; that is, if the displacement and slope of the point on the pile that CANWAL considers to be fixed are known, the total displacement of the pile can be computed. The computational procedure is illustrated in Figure 21.

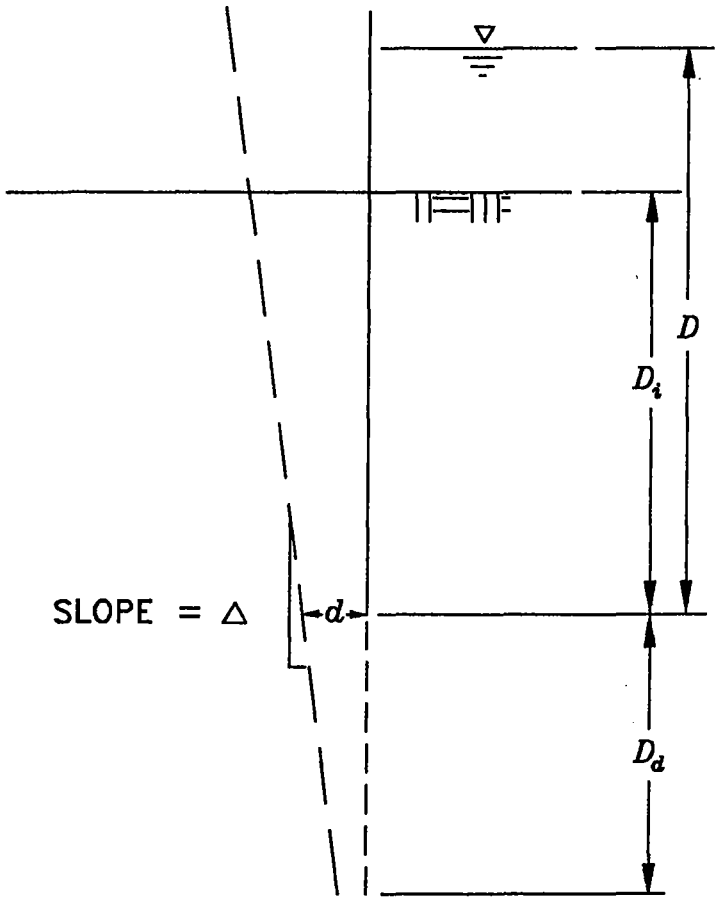

Figure 21. Schematic of slope in pile and movements at pile tip due to movements in the foundation

61. The procedure amounts to adding a "correction" to the displacement computed by CANWAL. First, the embedment and displacement corresponding to a safety factor of 1.0 are computed by CANWAL. The computed embedment depth is D_i and the total length of pile is D as shown in Figure 21. As discussed above, this displacement corresponds to the correct moment distribution. Second, the additional embedment depth D_d needed to obtain the required safety factor is computed using CANWAL. Next the appropriate plots in Figures 22 to 25 are used to determine the displacement and slope at the pile tip. The displacement at the top of the pile is thus the sum of the CANWAL displacement and the quantity $d + (\Delta \times D)$.

Conclusions

62. Task III was to perform detailed analyses and develop recommendations for new sheet-pile wall design procedures. The analyses were performed using the E-105 sheet pile-levee

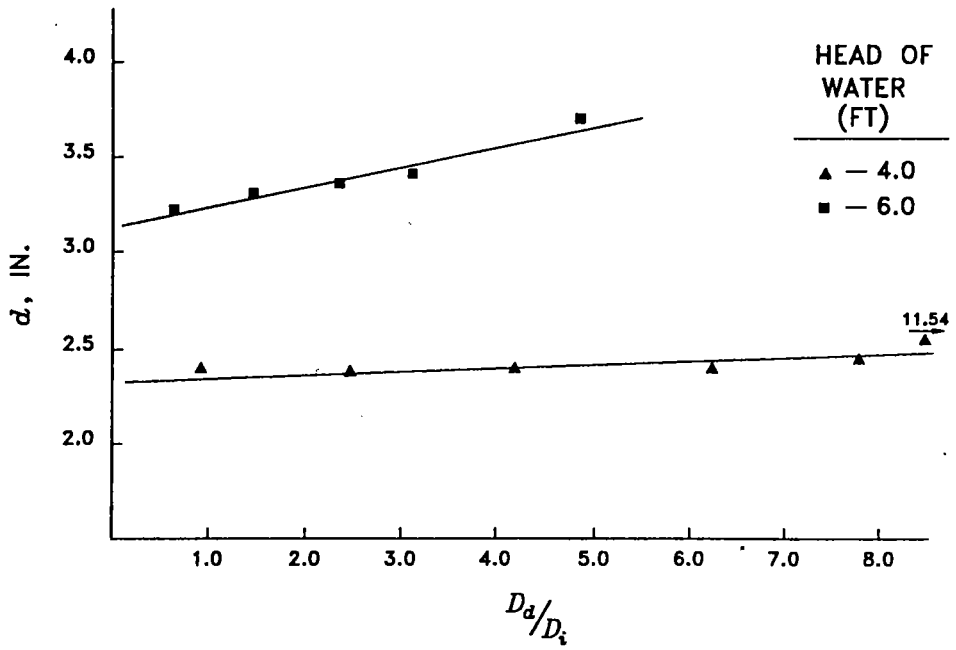

Figure 22. Movement at pile tip due to movements in foundation for the E-105 "weak" soil profile

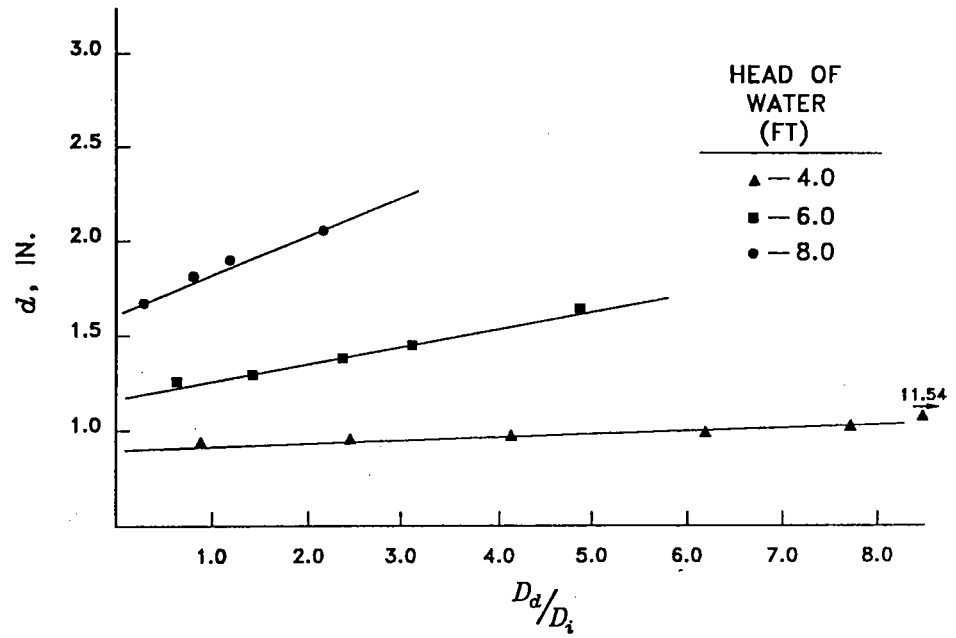

Figure 23. Movement at pile tip due to movements in the foundation for the E-105 "strong" soil profile

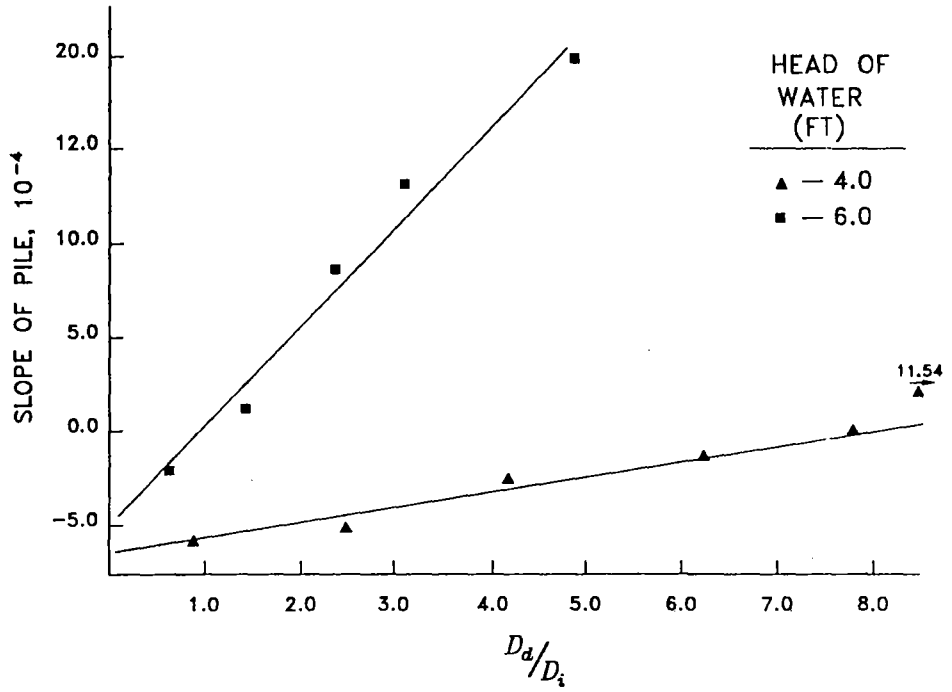

Figure 24. Slope in pile at pile tip due to movements in the foundation for the E-105 "weak" soil profile

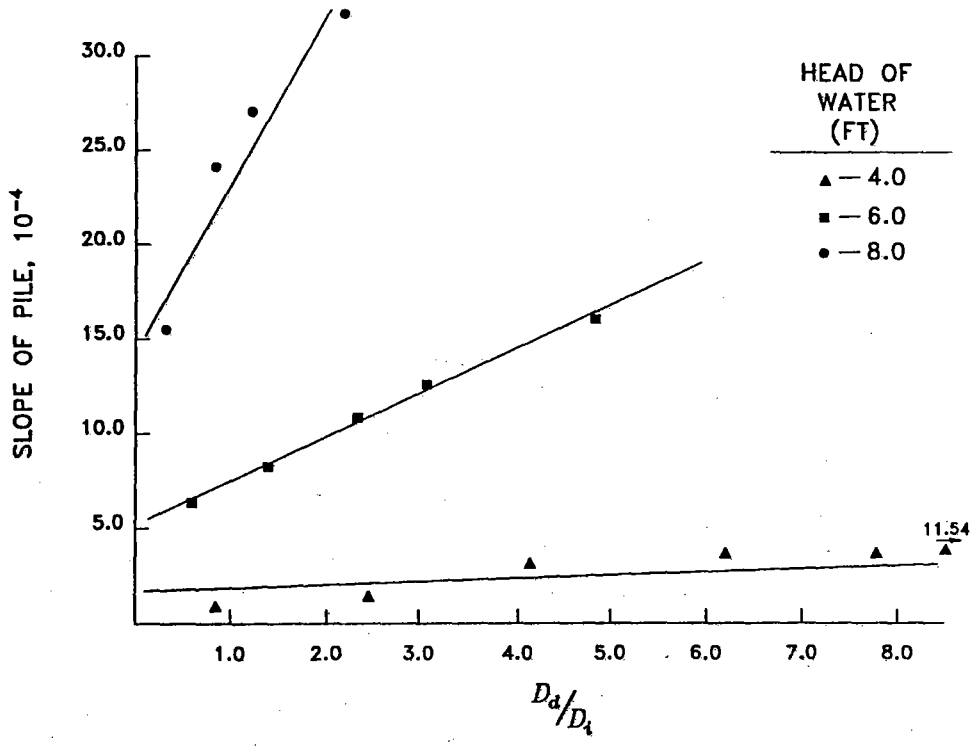

Figure 25. Slope in pile at pile tip due to movements in the foundation for the E-105 "strong" soil profile

profile, Figure 9. An analysis of the E-105 profile has been completed and the following basic conclusions have been reached.

a. Deep-seated movements in the levee foundation control the magnitude of sheet-pile deflection, particularly in soft soils. As a result, the height of water loading that can be sustained by a particular I wall is controlled by the stability of the foundation, as determined by a slope stability analysis.

b. The stability of the levee implied by the displacements is consistent with the safety factor computed by limit-equilibrium methods.

c. Increased sheet-pile penetration does not improve the stability of the levee.

d. The stability of the sheet pile relative to overturning, as implied by computed displacements, is consistent with the safety factors computed by CANWAL.

e. Penetration of the sheet pile below that needed to meet requirements for resistance against overturning does not improve performance of the sheet pile.

f. Pile stiffness has little effect on total displacements.

g. Deflection of the sheet-pile wall, as conventionally determined using the CANWAL program, is a poor criterion for design of sheet-pile walls because movements are caused by shear deformation in the foundation and not the cantilever action of the pile.

h. The moments computed by CANWAL for a safety factor of 1.0 agree best with those obtained from the finite element analysis.

PART V: RECOMMENDATIONS

63. Based on the findings outlined in Part IV, it is recommended that sheet-pile wall design be based on the static equilibrium of the sheet pile-levee system. The stability of the levee would be based on a conventional analysis preferably using a circular arc method (although both circular arc and wedge-shaped cases should be checked). This analysis would determine a maximum water loading that could be tolerated. The pile embedment would be determined using the conventional criteria for static equilibrium of a cantilever wall (i.e. by CANWAL). This analysis would determine the embedment needed. The strength parameter to be used for the analysis should be consistent with the unconsolidated undrained (end-of-construction) condition (i.e. $c = S_u$ and $\phi = 0$). If wall displacement is an important design parameter, the semi-empirical technique based on Figure 21 can be used. If site conditions differ significantly from those considered in this report, displacements should be determined by a complete finite element analysis unless the safety factor for deep-seated movement is high. If the safety factor for the foundation (as computed by slope stability methods) is high, displacements can be computed by CANWAL based on the embedment corresponding to a safety factor of 1.0. It is estimated from Figure 19 that the safety factor for foundation stability must be well above 2.0 before the displacements computed by CANWAL are appropriate. Because of complicating factors there is no known general procedure that can be used to correct the maximum moments computed by CANWAL at this time.

REFERENCES

Clough, W. G. 1984. "User's Manual for Program SOILSTRUCT," Virginia Polytechnical Institute, Blacksburg, Va.

Clough, W. G. and Tsui, Y. 1977. "Static Analysis of Earth Retaining Structures," *Numerical Methods in Geotechnical Engineering*, edited by Desai, C. S. and Christian, J. T., McGraw-Hill Book Company, New York, pp 506-527.

Dawkins, W. P. 1983. "User's Guide: Computer program for Soil-Structure Interaction Analysis of Sheet Pile Retaining Walls (CSHTSSI)," Instruction Report K-83-3, US Army Engineer Waterways Experiment Station, CE, Vicksburg, Miss.

Edris, E. V. 1987. "User's Guide: UTEXAS2 Slope-Stability Package, Volume I: User's Manual," Instruction Report GL-87-1, US Army Engineer Waterways Experiment Station, CE, Vicksburg, Miss.

Jackson, R. B. 1988. "E-99 Sheet Pile Wall Field Load Test Report," Technical Report No. 1, US Army Engineer Division, Lower Mississippi Valley, Vicksburg, Miss.

Mana, A. I. 1978. "Finite Element Analyses of Deep Excavation Behavior in Soft Clay," Ph. D. dissertation submitted to the Dept. of Civil Engineering and the Committee on Graduate Studies, Stanford University, Calif.

Manson, L. H. 1978. "User's Guide: Cantilever Retaining Wall Design and Analysis - CANWAL (X0026)," Automatic Data Processing Center, US Army Engineer Waterways Experiment Station, CE, Vicksburg, Miss.

Timoshenko, S. and Woinowsky-Krieger, S. 1959. *Theory of Plates and Shells*, Second Edition, McGraw-Hill Book Company, New York, p 5.

Table 1. Circular Shear Surfaces

Pile Tip Elevation	Water Level	Center X	Center Y	Radius	Safety Factor
- 1	20	-8	26	43	0.82
	17	-10	27	45	1.04
	14	-13	27	46	1.35
	12	-15	26	46	1.63
	10	-18	26	47	1.98
-10	20	-7	24	41	0.82
	17	-10	27	45	1.03
	14	-13	27	46	1.33
	12	-16	27	47	1.60
	10	-19	27	48	1.94
-18	20	-9	24	43	0.82
	17	-11	25	45	1.02
	14	-14	26	47	1.32
	12	-17	26	48	1.58
	10	-21	26	50	1.90
-30	20	-8	24	42	0.86
	17	-11	25	45	1.07
	14	-14	26	48	1.38
	12	-17	25	49	1.64
	10	-20	25	49	1.98

Table 2. Non-Circular Shear Surface With Sloping Base

Pile Tip Elevation	Water Level	Shear Surface Coordinates						Safety Factor
		X_1	X_2	Y_2	X_3	Y_3	X_4	
- 1	20	-49.6	-15.0	-25.6	25.0	- 2.7	47.2	0.84
	17	-52.0	-15.7	-27.0	24.3	- 1.9	42.3	1.03
	14	-54.4	-16.5	-28.5	23.8	- 1.1	39.2	1.26
	12	-56.1	-16.9	-29.6	23.4	- 0.4	39.2	1.46
	10	-57.6	-17.4	-30.3	22.7	0.7	40.2	1.70
-10	20	-49.6	-15.1	-25.6	24.8	- 2.4	46.5	0.83
	17	-51.9	-15.8	-27.0	24.1	- 1.5	41.7	1.01
	14	-54.3	-16.5	-28.5	23.8	- 1.0	39.4	1.24
	12	-56.0	-16.9	-29.6	23.3	- 0.2	39.8	1.43
	10	-57.4	-17.4	-30.3	22.8	0.6	39.8	1.66
-18	20	-51.7	-15.4	-27.7	26.1	- 4.4	50.3	0.83
	17	-54.0	-16.1	-29.2	25.1	- 3.2	44.8	1.01
	14	-56.4	-16.7	-30.7	23.9	- 1.5	38.5	1.23
	12	-58.1	-17.1	-31.8	23.9	- 1.1	37.1	1.41
	10	-60.2	-17.5	-33.2	23.5	- 0.3	36.6	1.64
-30	20	-52.3	-15.8	-28.1	26.5	- 5.4	51.7	0.87
	17	-54.6	-16.5	-29.6	25.5	- 4.0	46.2	1.06
	14	-56.8	-17.0	-31.0	24.2	- 2.1	39.5	1.29
	12	-58.6	-17.5	-32.0	23.9	- 1.5	36.6	1.49
	10	-60.8	-18.0	-33.5	23.5	- 0.7	36.0	1.73

Table 3. Non-Circular Shear Surface with Nearly Horizontal Base

Pile Tip	Water	Shear Surface Coordinates						Safety
Elevation	Level	X_1	X_2	Y_2	X_3	Y_3	X_4	Factor
- 1	20	-50.0	-23.0	-23.0	7.0	-23.0	50.0	0.82
	17	-50.0	-23.0	-23.0	7.0	-23.0	47.0	1.03
	14	-54.2	-24.1	-25.2	4.3	-18.3	40.1	1.28
	12	-55.9	-24.7	-26.4	3.8	-17.5	38.4	1.52
	10	-56.3	-24.8	-26.5	2.8	-15.8	32.3	1.77
-10	20	-50.0	-23.0	-23.0	7.0	-23.0	50.0	0.82
	17	-50.0	-23.0	-23.0	7.0	-23.0	47.0	1.03
	14	-54.4	-24.2	-25.3	4.1	-18.0	40.2	1.27
	12	-56.1	-24.7	-26.6	3.6	-17.2	38.6	1.51
	10	-54.8	-24.5	-25.2	2.7	-15.7	30.9	1.72
-18	20	-50.0	-23.0	-23.0	7.0	-23.0	50.0	0.82
	17	-50.0	-23.0	-23.0	7.0	-23.0	47.0	1.03
	14	-54.9	-24.2	-25.2	3.9	-17.7	40.6	1.26
	12	-56.6	-24.9	-27.0	3.9	-17.6	38.3	1.49
	10	-54.7	-24.5	-25.2	2.8	-15.8	30.7	1.70
-30	20	-50.0	-23.0	-23.0	7.0	-23.0	50.0	0.83
	17	-53.8	-24.0	-25.0	5.4	-23.2	41.8	1.03
	14	-55.6	-24.6	-26.2	4.9	-19.3	39.3	1.31
	12	-57.1	-25.1	-27.5	4.4	-18.5	37.7	1.55
	10	-59.6	-25.7	-29.3	3.8	-17.5	35.3	1.85

Table 4. CANWAL Analysis for E-105 Section

Soil	Head ft	Safety Factor	Required Tip Elevation ft	u, in PZ-27	u, in PZ-40	Maximum Moment, ft-lb
Weak	4	1.50	5.47	0.01	0.003	1,078
	6	1.50	-0.85	0.13	0.05	5,141
	8	1.50	-	-	-	-
	10	1.50	-	-	-	-
	4	1.25	6.20	0.005	0.002	975
	6	1.25	1.20	0.08	0.03	4,298
	8	1.25	-7.91	0.85	0.32	13,772
	10	1.25	-	-	-	-
	4	1.00	6.81	0.004	0.001	889
	6	1.00	3.16	0.05	0.02	3,640
	8	1.00	-3.08	0.42	0.16	10,803
	10	1.00	-	-	-	-
Strong	4	1.50	5.40	0.007	0.003	1,078
	6	1.50	-0.81	0.13	0.05	5,141
	8	1.50	-12.50	1.57	0.59	17,655
	10	1.50	-	-	-	-
	4	1.25	6.20	0.005	0.002	975
	6	1.25	1.20	0.084	0.032	4,298
	8	1.25	-7.32	0.813	0.305	13,772
	10	1.25	-	-	-	-
	4	1.0	6.81	0.004	0.001	889
	6	1.0	3.16	0.052	-	3,640
	8	1.0	-2.73	0.420	0.157	10,803
	10	1.0	-	-	-	-

APPENDIX A: SUMMARY OF COMPUTED PILE DISPLACEMENTS AND MOMENTS FOR E-105 SECTION

A1. This appendix presents Table A1, which summarizes the parametric analyses and plots of the computed displacements and moments for the E-105 "weak" and "strong" soil profiles. Each displacement plot presents results for a particular water height with the results for different embedments being compared on each plot. The displacement plot shows the lateral (horizontal) displacement of the pile (shown as a solid line) and the soil below the pile (shown as a dashed line). To aid in interpretation, view the dashed line as the displacement that would be measured by a slope inclinometer inserted in the soil below the pile. The moment diagrams are presented for each embedment depth with the results for different water heights compared on each plot. The plots for wave loading include two embedment depths.

A2. Because computed displacements and moments for the PZ-27 and PZ-40 sections were approximately the same, no displacement or moment plots for the PZ-40 section are presented.

Table A1. Results From E105 Sheet-Pile Wall Parametric Analysis

Type Loading	Soil Profile	Pile Depth ft	PZ-27 Lateral Def in	PZ-27 Max Moment ft-lb	PZ-27 El of Max Moment ft, NGVD	PZ-40 Lateral Def in	PZ-40 Max Moment ft-lb	PZ-40 El of Max Moment ft, NGVD
Flood:	Weak	6.0	2.28	1,000	8.5			
4-ft head		11.0	2.30	1,000	8.0			
K = 1,000		16.5	2.36	900	8.5			
		23.0	2.37	800	8.5			
		28.0	2.45	900	8.5			
		40.0	2.57	900	8.5	2.65	800	9.0
	Strong	6.0	0.96	900	8.5	0.95	900	9.0
		11.0	0.98	1,000	7.5	0.97	1,000	8.0
		16.5	1.02	900	8.0	1.02	800	8.5
		23.0	1.06	800	7.5	1.07	750	8.0
		28.0	1.09	900	8.0	1.10	800	7.5
		40.0	1.14	900	8.5	1.16	750	9.0
Flood:	Weak	6.0	3.25	3,000	9.0			
6-ft head		11.0	3.28	3,000	8.0			
K = 1,000		16.5	3.41	3,000	8.0			
		23.0	3.58	3,100	8.0			
		28.0	3.74	3,000	8.0			
		40.0	4.14	2,900	7.5	4.20	3,000	8.0
	Strong	6.0	1.46	2,700	8.5	1.47	2,700	9.0
		11.0	1.50	3,100	8.0	1.41	3,300	8.0
		16.5	1.52	3,000	8.0	1.47	3,000	8.5
		23.0	1.65	3,000	7.5	1.59	2,900	8.0
		28.0	1.75	3,000	7.5	1.72	3,100	8.0
		40.0	2.00	3,000	7.5	1.94	2,900	8.0

Table A1. (Continued)

Type Loading	Soil Profile	Pile Depth ft	PZ-27 Lateral Def in	PZ-27 Max Moment ft-lb	PZ-27 El of Max Moment ft, NGVD	PZ-40 Lateral Def in	PZ-40 Max Moment ft-lb	PZ-40 El of Max Moment ft, NGVD
Flood:	Weak	6.0	5.50	6,600	9.0			
8-ft head		11.0	4.85	7,000	8.0			
K = 1,000		16.5	5.15	7,800	7.0			
		23.0	5.90	7,500	7.0			
		28.0	6.20	7,500	7.0			
		40.0	8.30	7,200	6.5	8.07	7,200	7.5
	Strong	6.0	2.91	6,500	8.5	2.84	6,300	8.5
		11.0	2.28	7,200	7.5	2.15	7,400	8.0
		16.5	2.45	7,400	7.0	2.27	7,500	6.0
		23.0	2.76	7,500	7.0	2.62	7,600	5.5
		28.0	2.96	7,800	6.5	2.82	7,800	5.5
		40.0	3.35	7,500	6.5	3.15	7,800	5.5
Flood:	Weak	6.0	-	13,000	8.0			
10-ft head		11.0	10.17	15,000	9.0			
K = 1,000		16.5	11.35	16,000	5.5			
		23.0	23.69	14,200	5.5			
		28.0	33.20	14,000	6.0			
		40.0	40.73	14,100	6.0			
	Strong	6.0	-	13,300	6.5	-	13,500	8.0
		11.0	4.12	14,700	6.5	3.69	14,400	6.5
		16.5	4.27	15,000	6.5	3.85	15,100	5.5
		23.0	4.82	15,200	6.5	4.40	14,500	5.5
		28.0	5.10	15,200	6.5	4.25	15,600	5.5
		40.0	5.85	14,800	6.0	5.34	15,800	5.5

Table A1. (Continued)

Type Loading	Soil Profile	Pile Depth ft	PZ-27 Lateral Def in	PZ-27 Max Moment ft-lb	PZ-27 El of Max Moment ft, NGVD	PZ-40 Lateral Def in	PZ-40 Max Moment ft-lb	PZ-40 El of Max Moment ft, NGVD
Flood:	Weak	23.0	4.72	800	8.5			
4-ft head		28.0	4.83	800	8.5			
K = 500								
	Strong	23.0	2.05	800	8.5			
		28.0	2.10	800	8.5			
Flood:	Weak	23.0	6.96	3,000	8.0			
6-ft head		28.0	7.31	3,000	8.0			
K = 500								
	Strong	23.0	3.21	3,100	8.0			
		28.0	3.43	3,100	8.0			
Flood:	Weak	23.0	11.30	7,600	6.0			
8-ft head		28.0	12.10	7,300	6.0			
K = 500								
	Strong	23.0	5.37	7,600	5.5			
		28.0	5.74	7,600	5.5			
Flood:	Weak	23.0	48.80	14,500	6.0			
10-ft head		28.0	68.57	14,000	6.0			
K = 500								
	Strong	23.0	9.14	15,400	5.5			
		28.0	9.73	15,500	5.5			

Table A1. (Concluded)

Type Loading	Soil Profile	Pile Depth ft	PZ-27 Lateral Def in	PZ-27 Max Moment ft-lb	PZ-27 El of Max Moment ft, NGVD	PZ-40 Lateral Def in	PZ-40 Max Moment ft-lb	PZ-40 El of Max Moment ft, NGVD
Wave:	Weak	23.0	4.58	23,700	5.5			
4,100 lb		28.0	4.70	23,700	5.5			
K = 1,000								
	Strong	23.0	3.15	23,500	5.0			
		28.0	3.20	23,500	5.0			
Wave:	Weak	16.5	5.65	28,000	5.5			
4,700 lb		23.0	5.35	28,000	5.5			
K = 1,000		28.0	5.50	28,000	5.5			
		40.0	5.59	28,000	5.5			
	Strong	16.5	4.05	28,200	5.5	2.91	27,000	5.5
		23.0	3.67	28,500	5.5	2.24	23,000	5.5
		28.0	3.75	28,600	5.5	2.48	25,500	5.5
		40.0	4.08	28,800	5.5	2.74	27,500	5.5

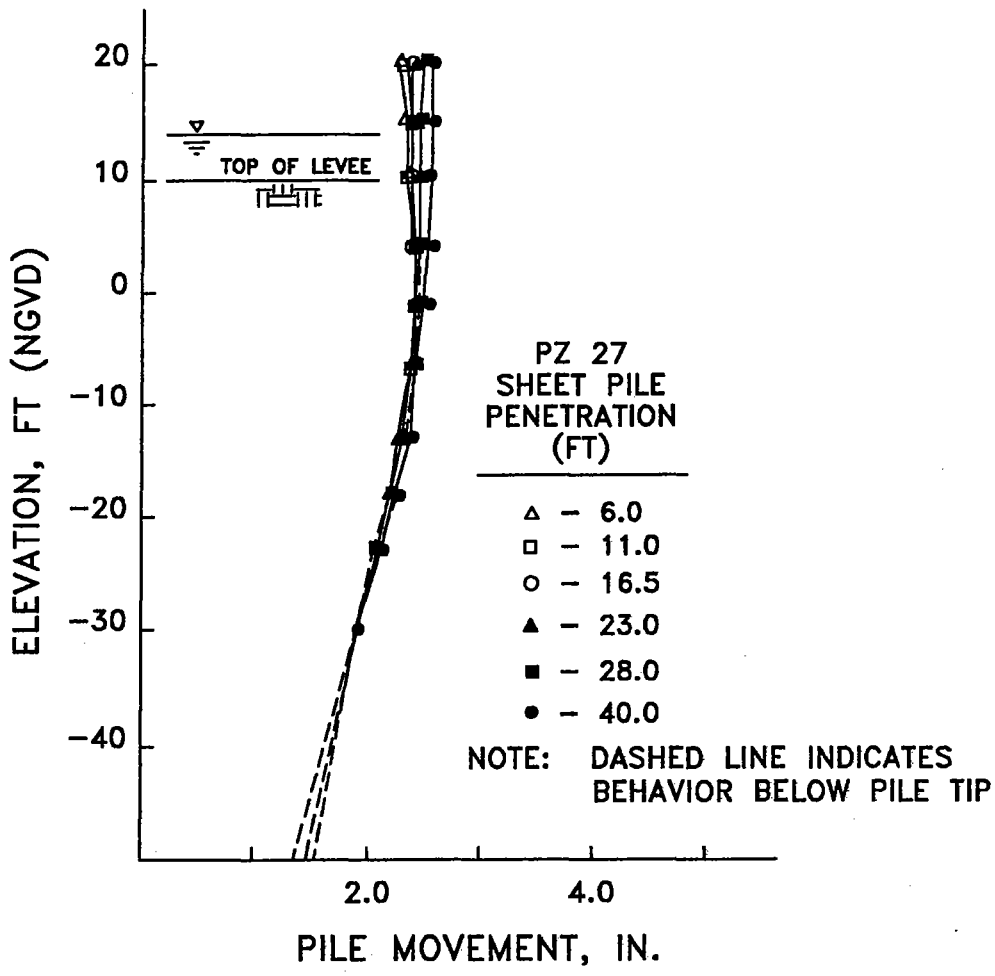

Figure A1. Pile movement for different pile penetration depths in the E-105 "weak" soil profile for a loading of 4.0 ft of head

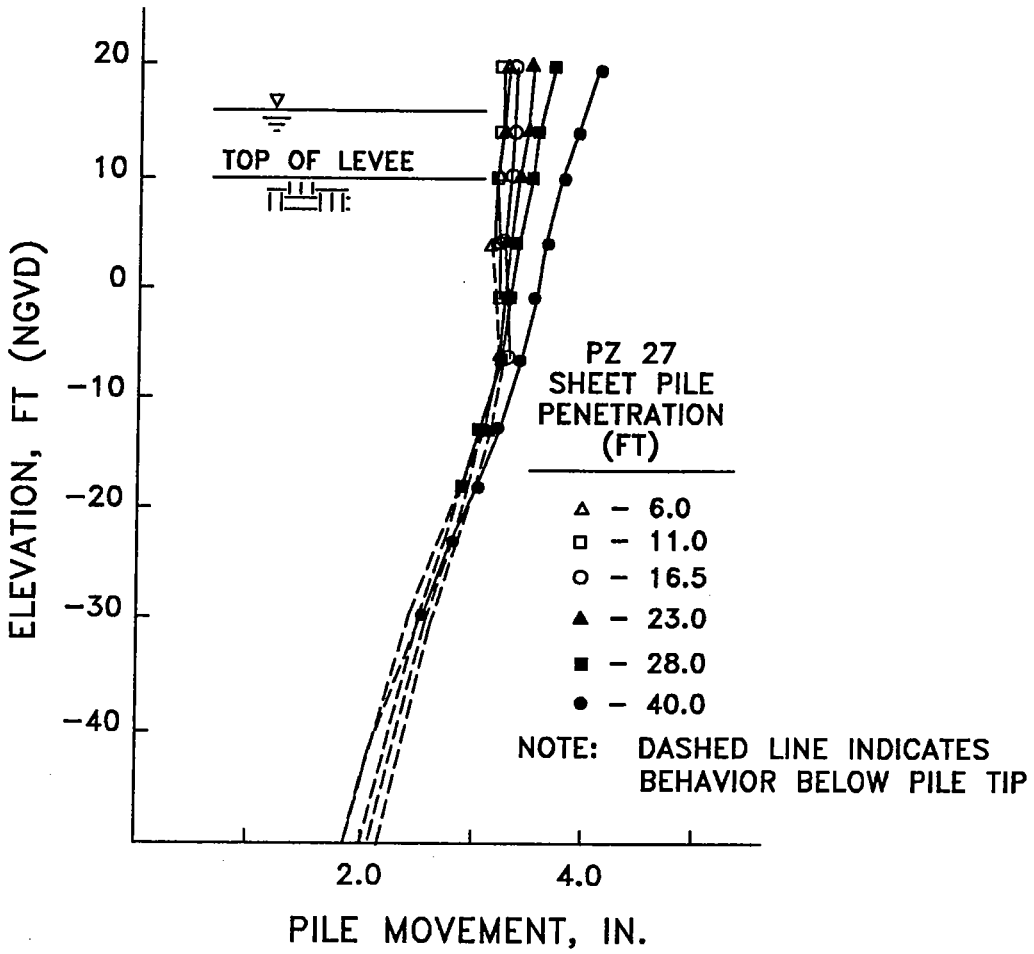

Figure A2. Pile movement for different pile penetration depths in the E-105 "weak" soil profile for a loading of 6.0 ft of head

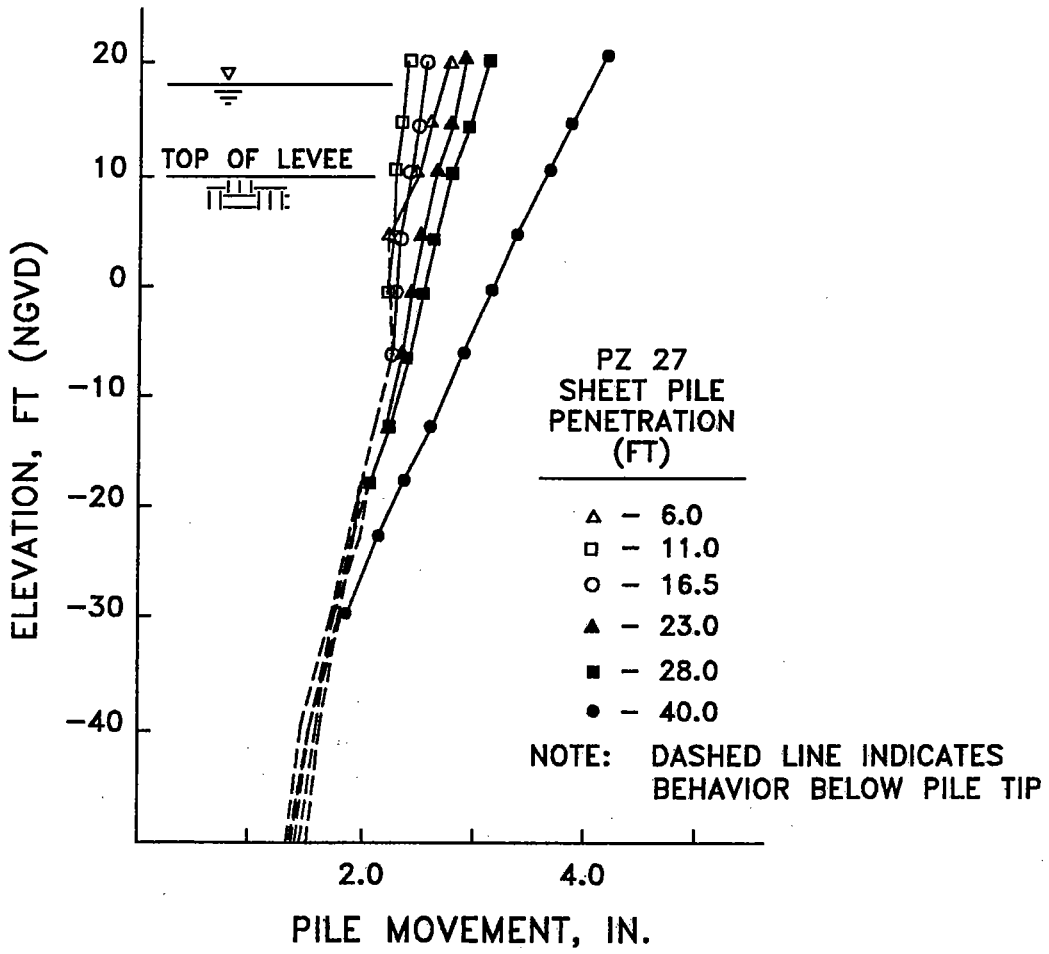

Figure A3. Pile movement for different pile penetration depths in the E-105 "weak" soil profile for a loading of 8.0 ft of head

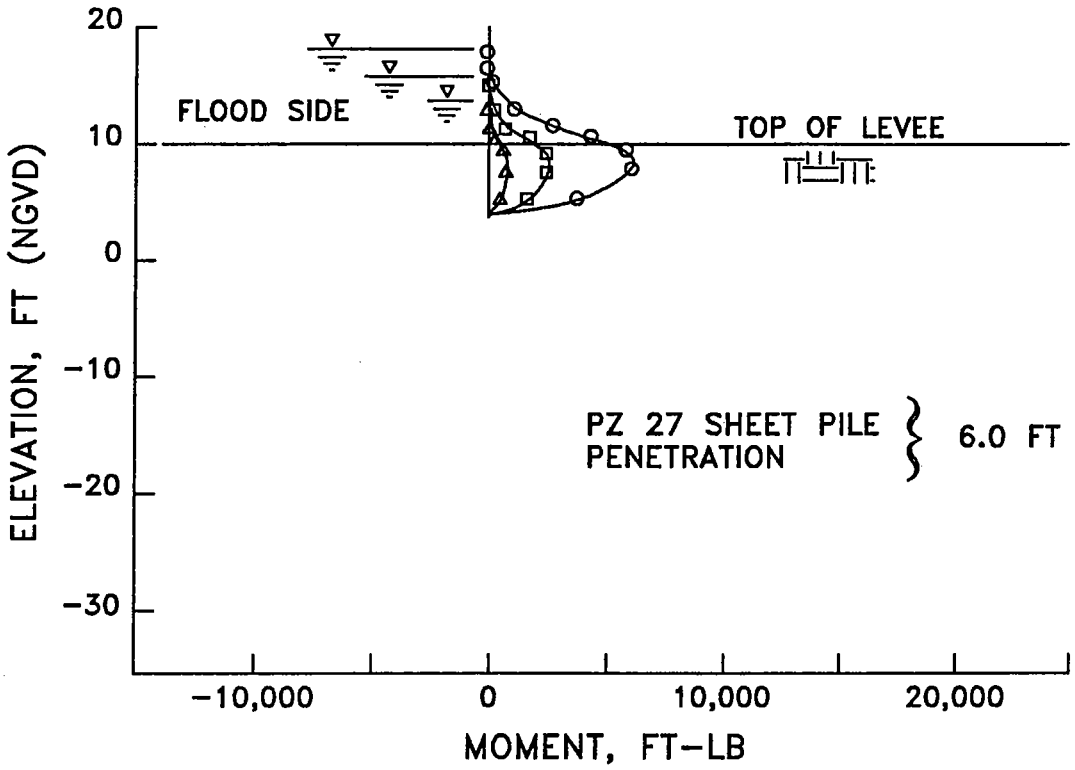

Figure A4. Pile moments for a pile penetration depth of 6.0 ft in the E-105 "weak" soil profile for loadings of 4.0, 6.0, and 8.0 ft of head

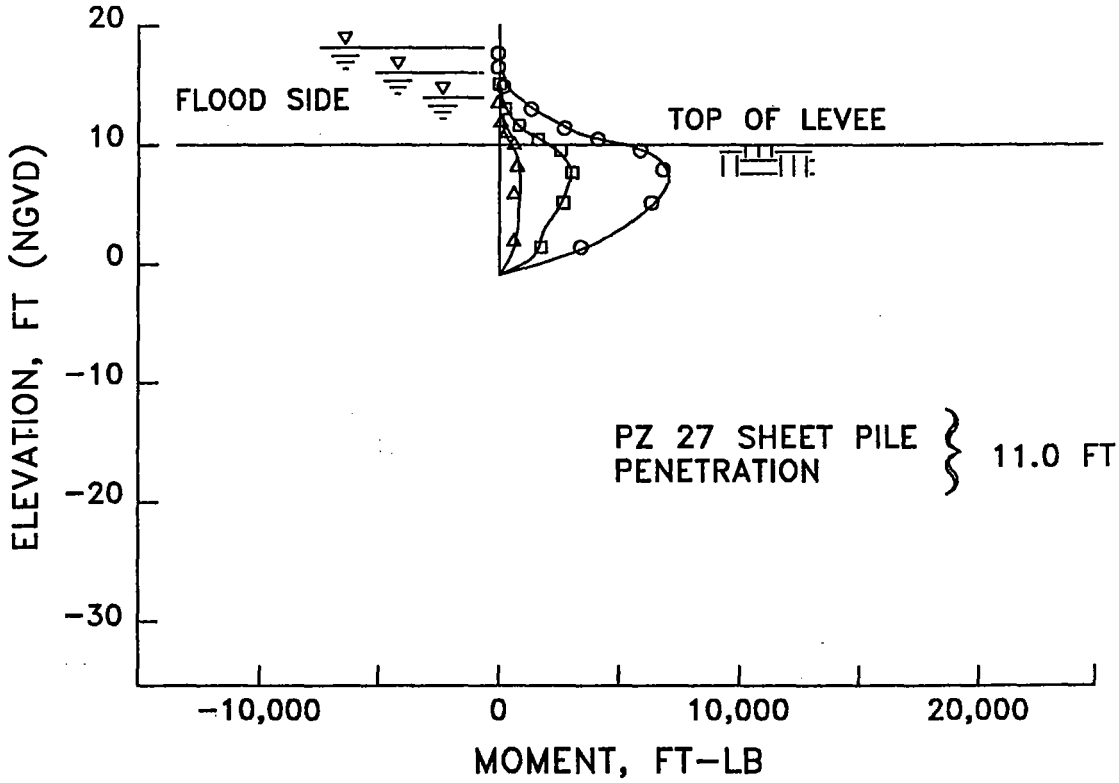

Figure A5: Pile moments for a pile penetration depth of 11.0 ft in the E-105 "weak" soil profile for loadings of 4.0, 6.0, and 8.0 ft of head

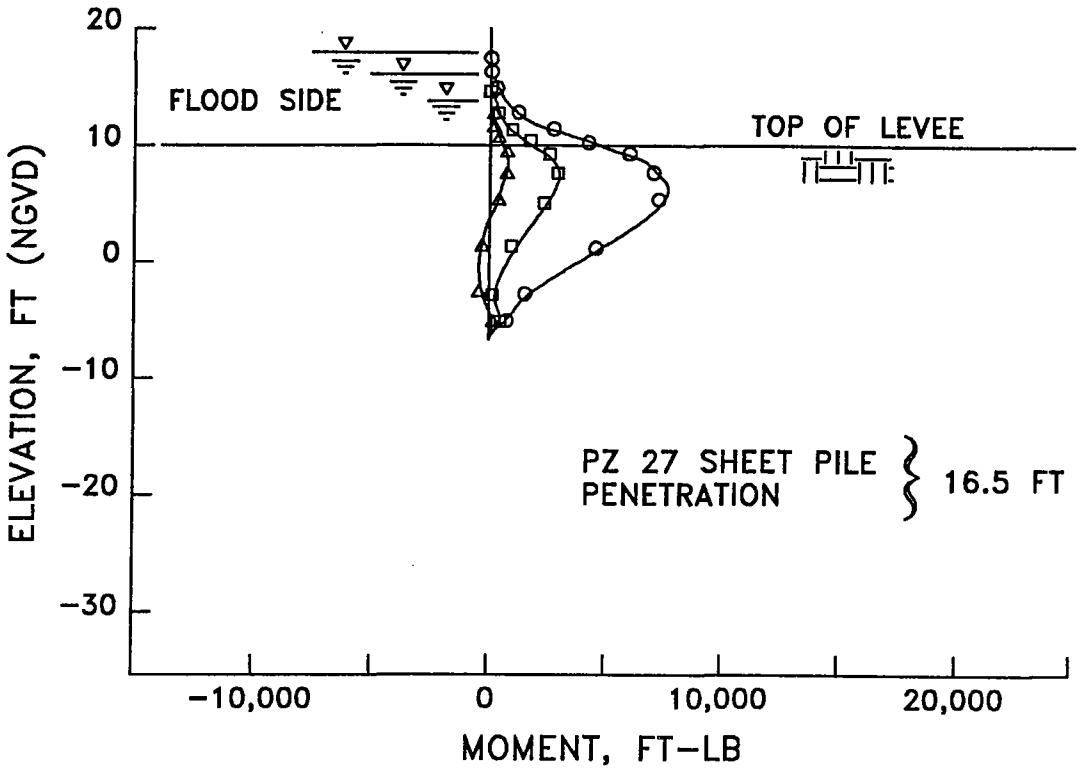

Figure A6. Pile moments for a pile penetration depth of 16.5 ft in the E-105 "weak" soil profile for loadings of 4.0, 6.0, and 8.0 ft of head

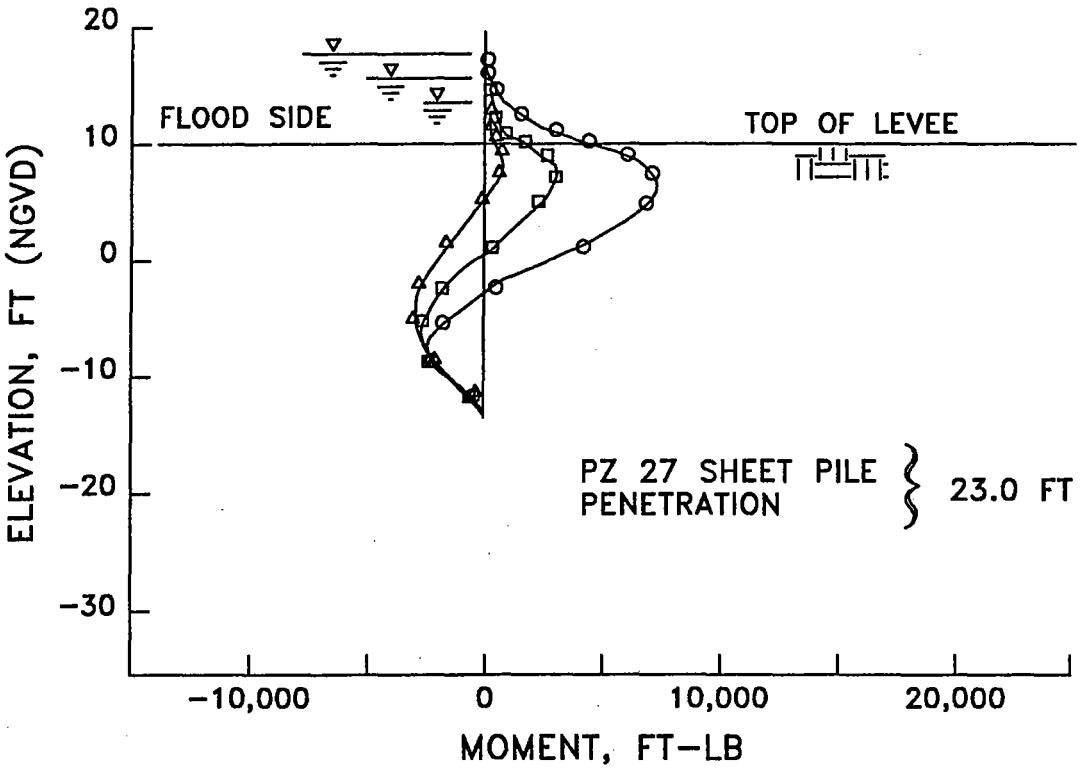

Figure A7. Pile moments for a pile penetration depth of 23.0 ft in the E-105 "weak" soil profile for loadings of 4.0, 6.0, and 8.0 ft of head

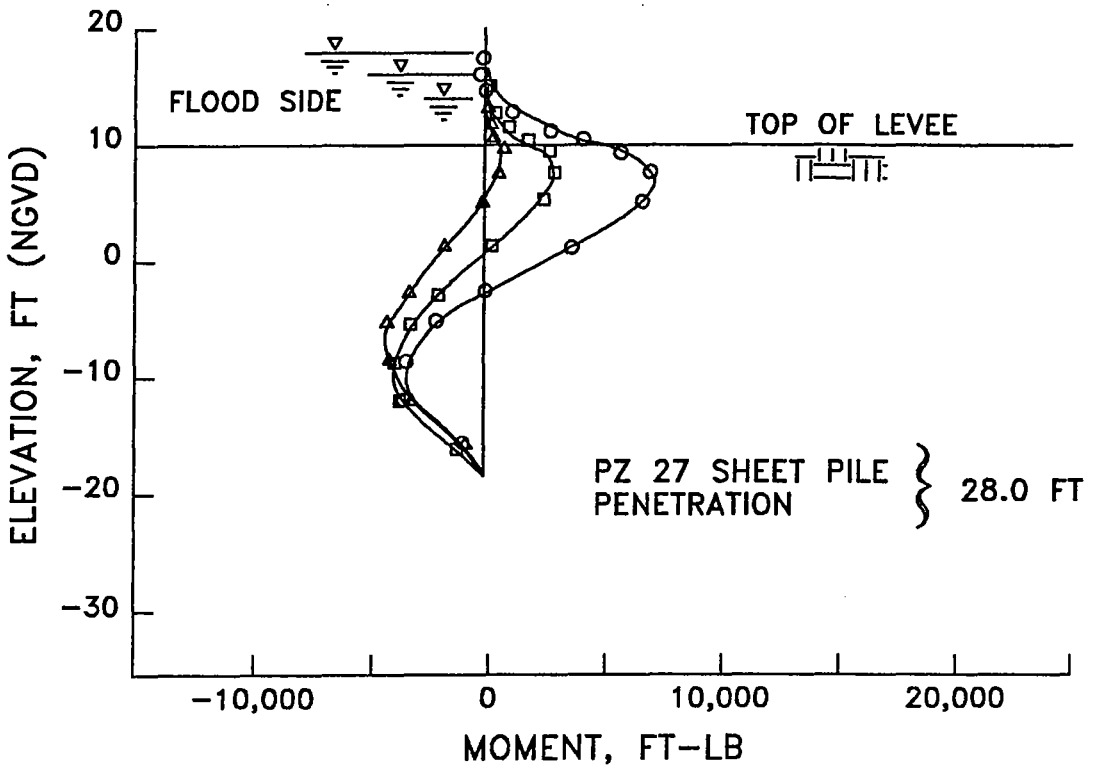

Figure A8. Pile moments for a pile penetration depth of 28.0 ft in the E-105 "weak" soil profile for loadings of 4.0, 6.0, and 8.0 ft of head

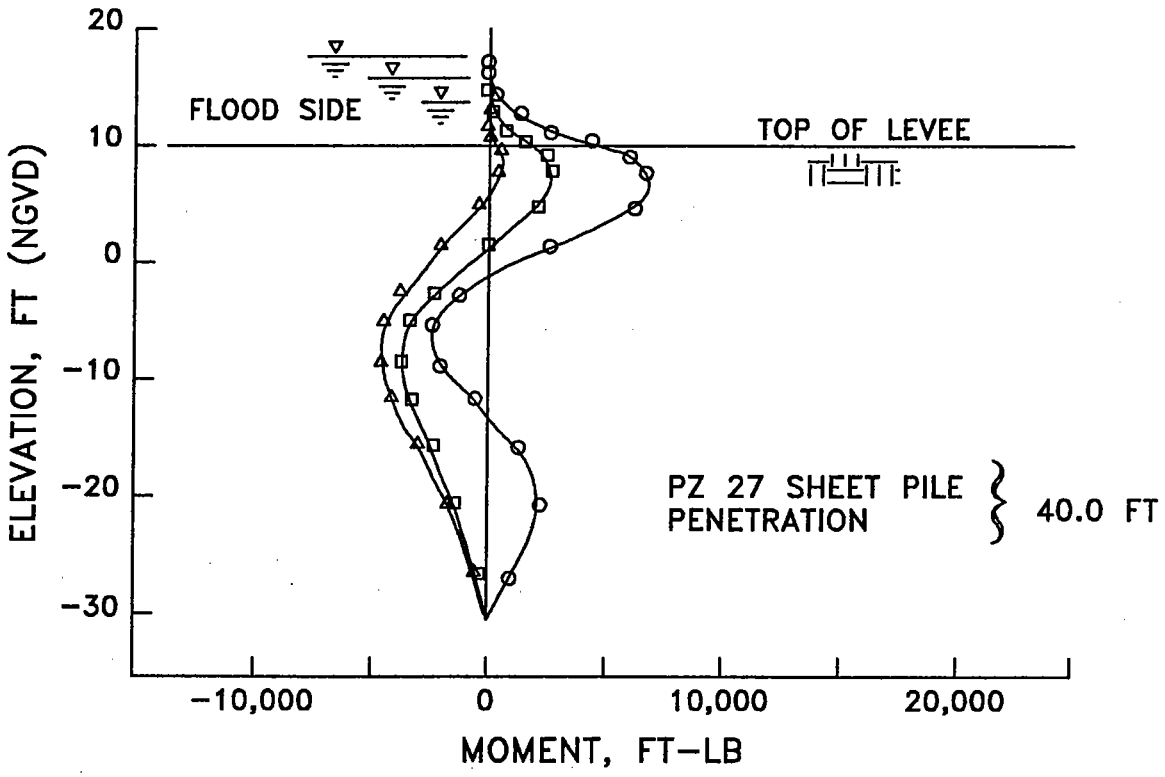

Figure A9. Pile moments for a pile penetration depth of 40.0 ft in the E-105 "weak" soil profile for loadings of 4.0, 6.0, and 8.0 ft of head

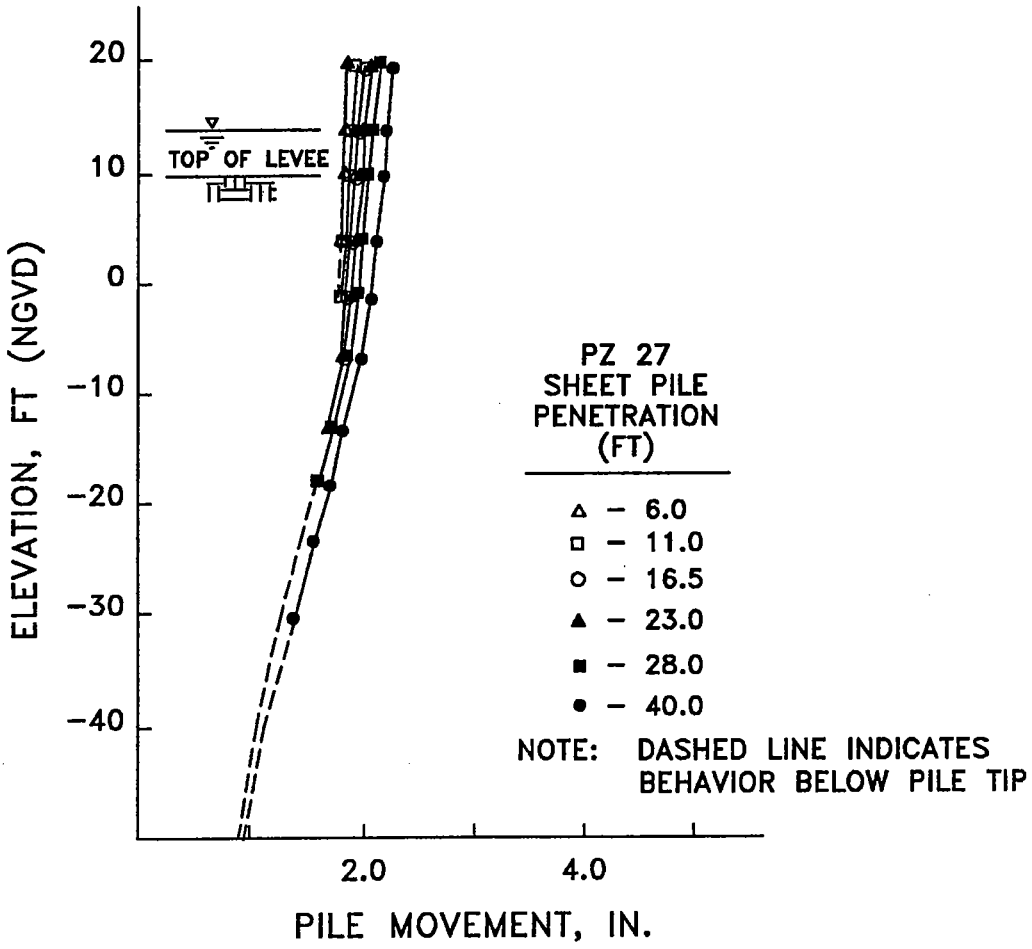

Figure A10. Pile movement for different pile penetration depths in the E-105 "strong" soil profile for a loading of 4.0 ft of head

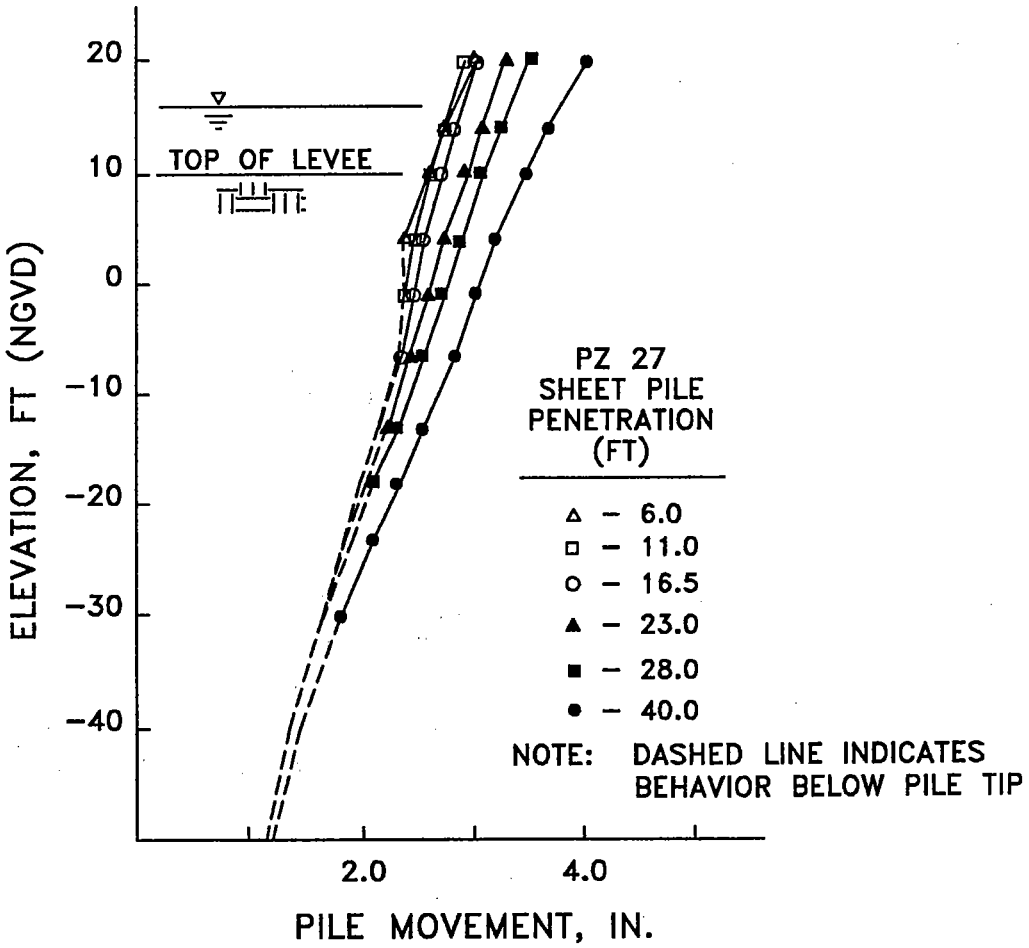

Figure A11. Pile movement for different pile penetration depths in the E-105 "strong" soil profile for a loading of 6.0 ft of head

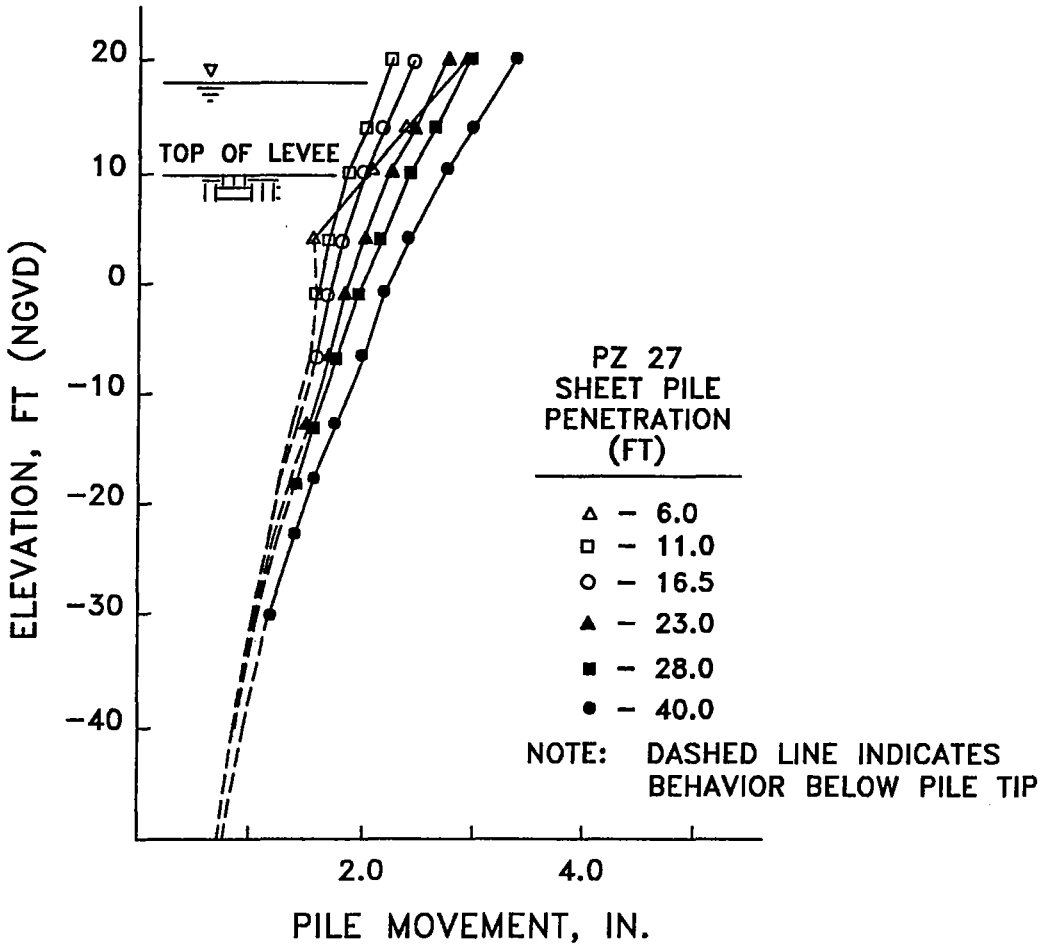

Figure A12. Pile movement for different pile penetration depths in the E-105 "strong" soil profile for a loading of 8.0 ft of head

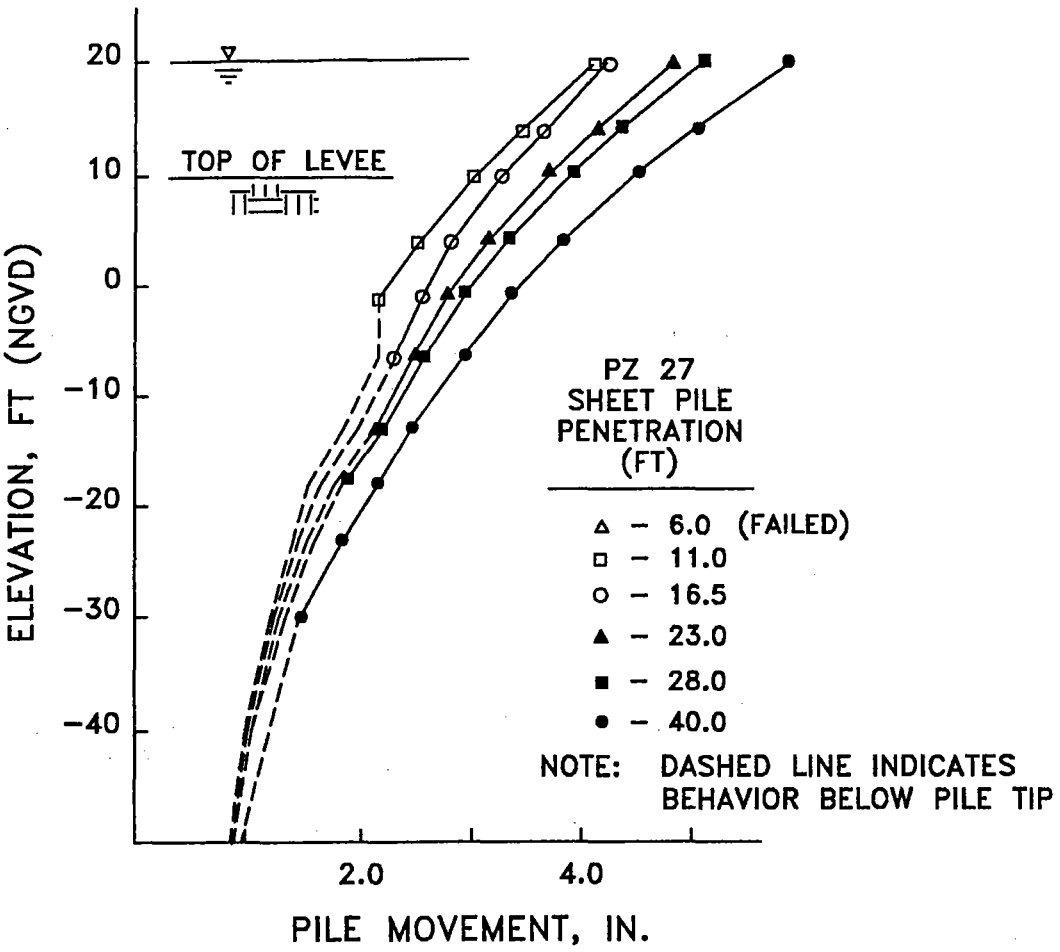

Figure A13. Pile movement for different pile penetration depths in the E-105 "strong" soil profile for a loading of 10.0 ft of head

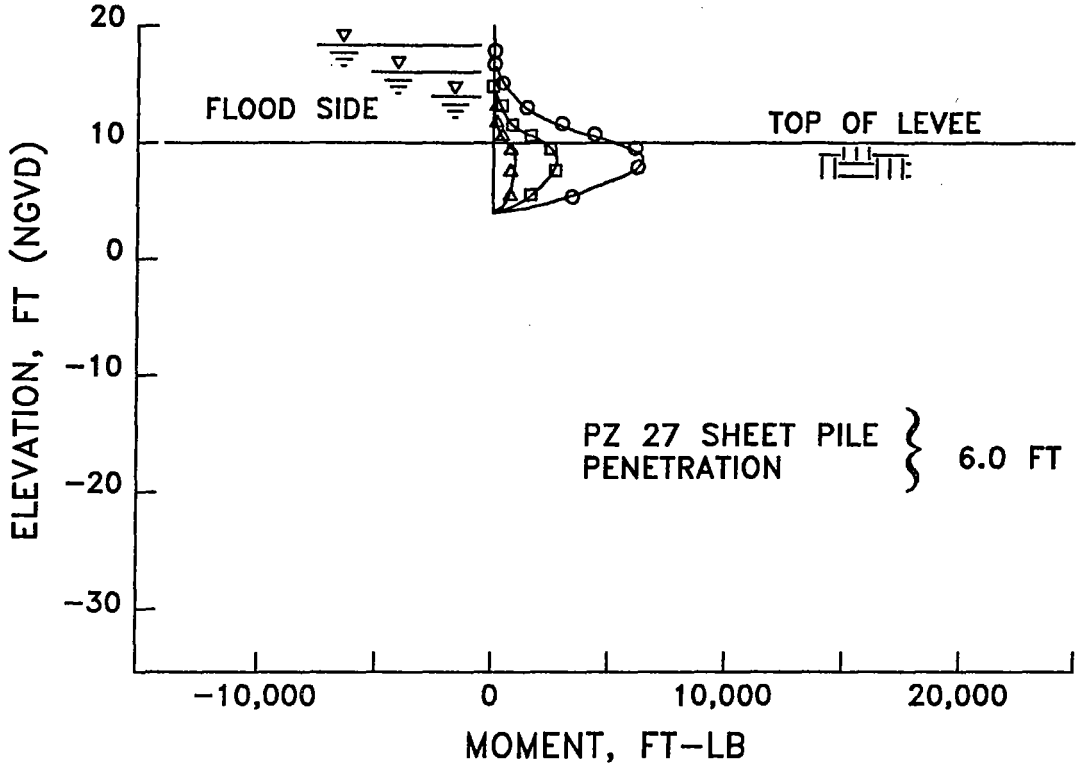

Figure A14. Pile moments for a pile penetration depth of 6.0 ft in the E-105 "strong" soil profile for loadings of 4.0, 6.0, 8.0, and 10.0 ft of head

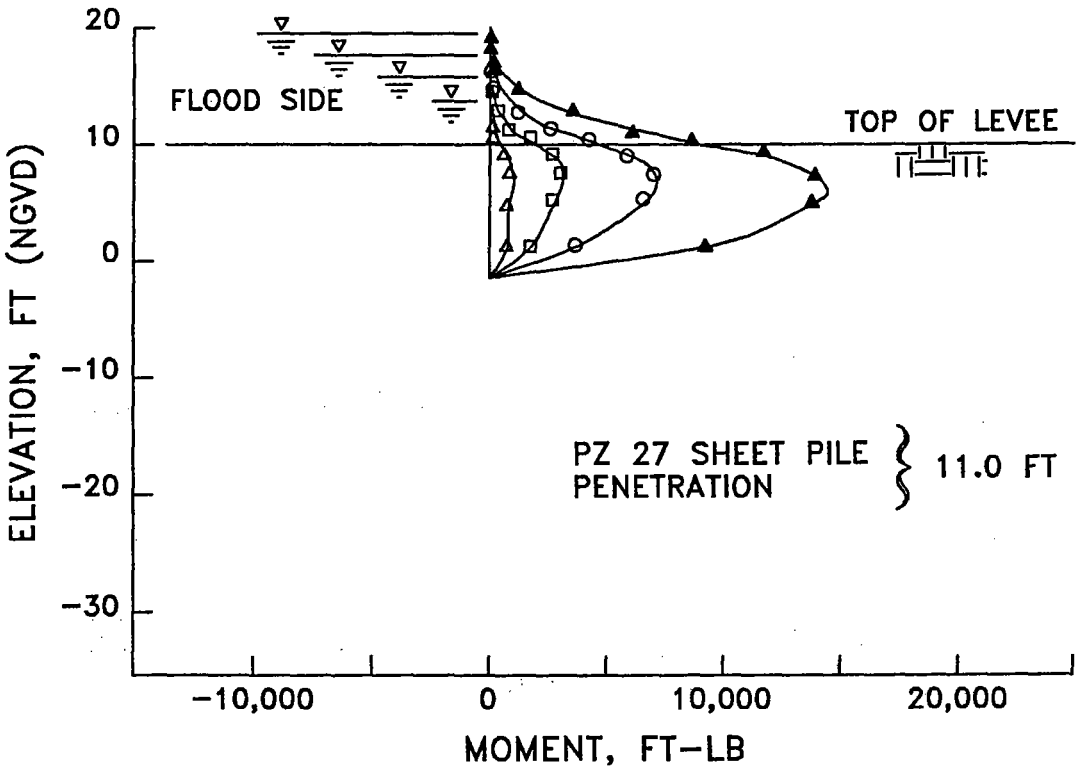

Figure A15. Pile moments for a pile penetration depth of 11.0 ft in the E-105 "strong" soil profile for loadings of 4.0, 6.0, 8.0, and 10.0 ft of head

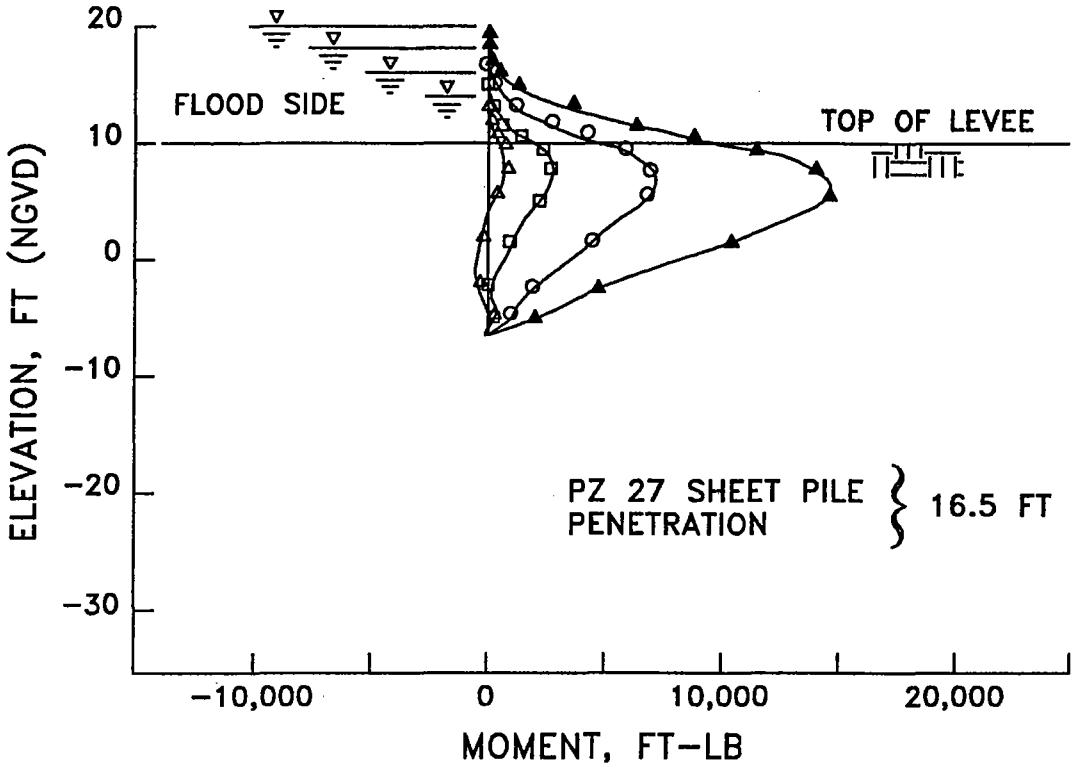

Figure A16. Pile moments for a pile penetration depth of 16.5 ft in the E-105 "strong" soil profile for loadings of 4.0, 6.0, 8.0, and 10.0 ft of head

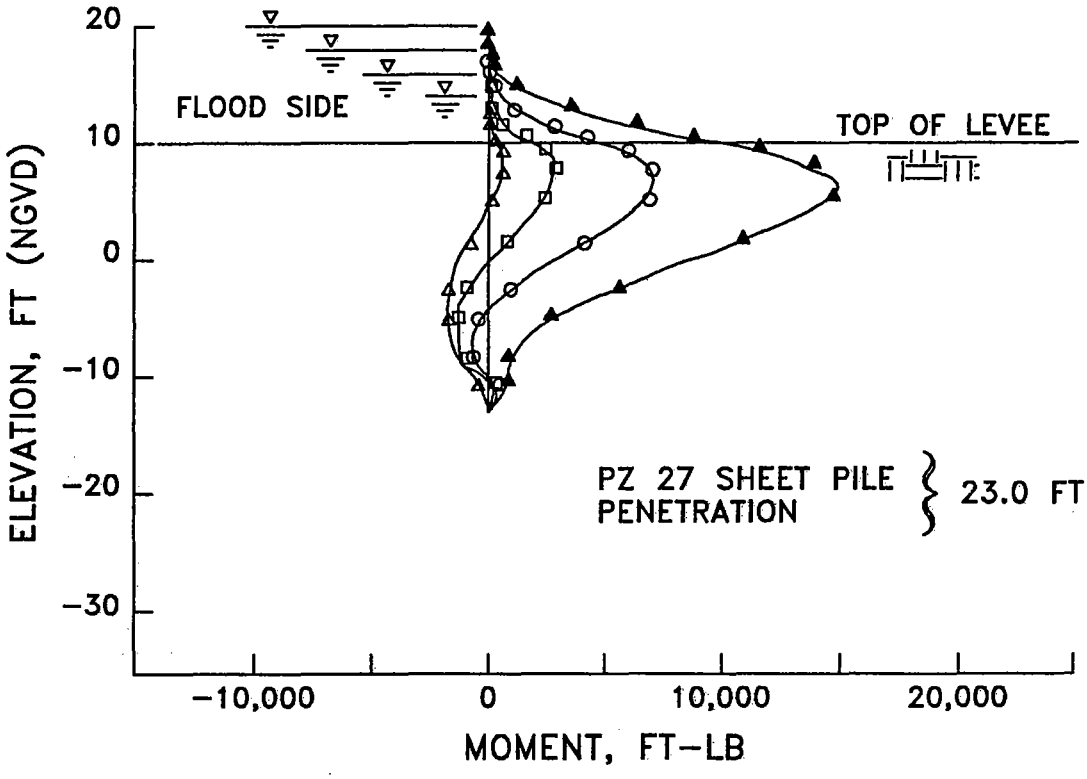

Figure A17: Pile moments for a pile penetration depth of 23.0 ft in the E-105 "strong" soil profile for loadings of 4.0, 6.0, 8.0, and 10.0 ft of head

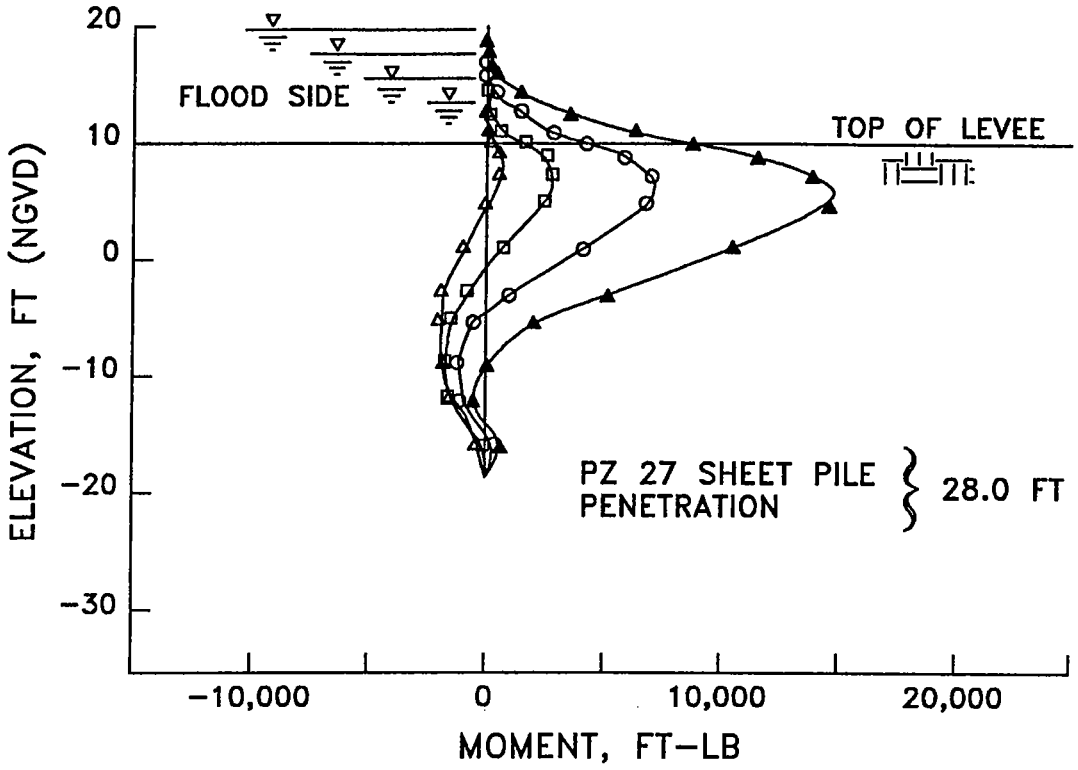

Figure A18. Pile moments for a pile penetration depth of 28.0 ft in the E-105 "strong" soil profile for loadings of 4.0, 6.0, 8.0, and 10.0 ft of head

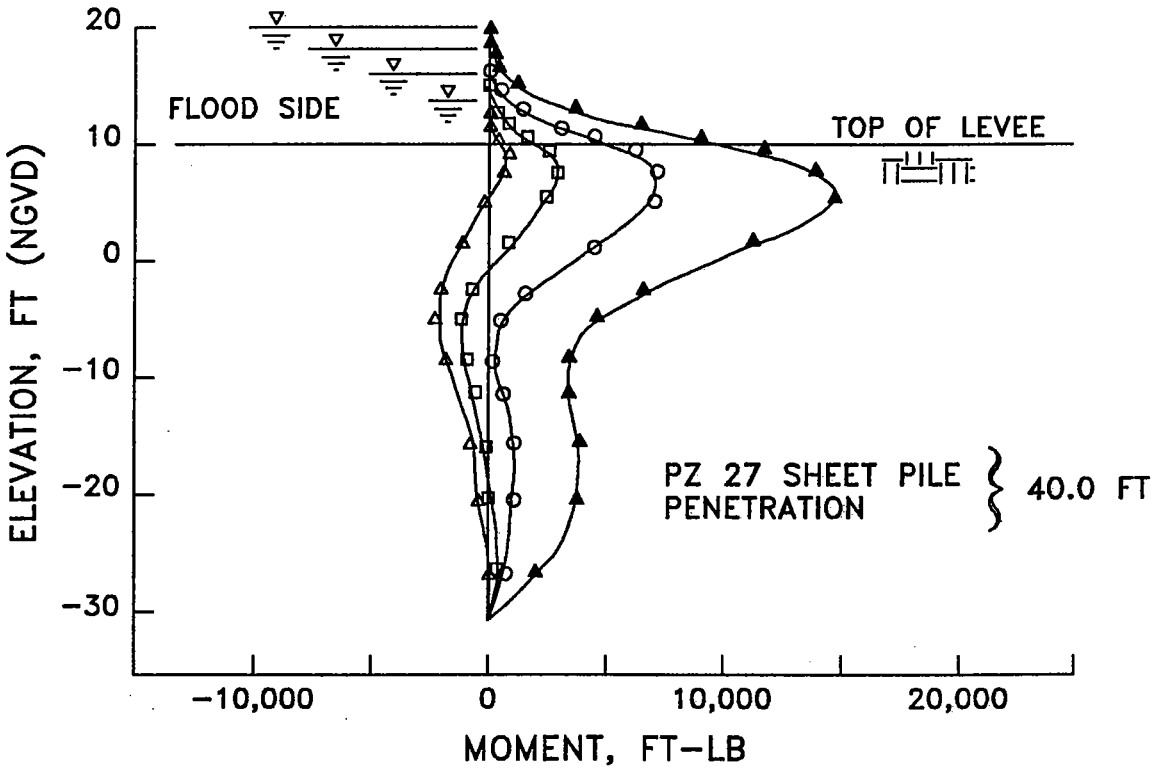

Figure A19. Pile moments for a pile penetration depth of 40.0 ft in the E-105 "strong" soil profile for loadings of 4.0, 6.0, 8.0, and 10.0 ft of head

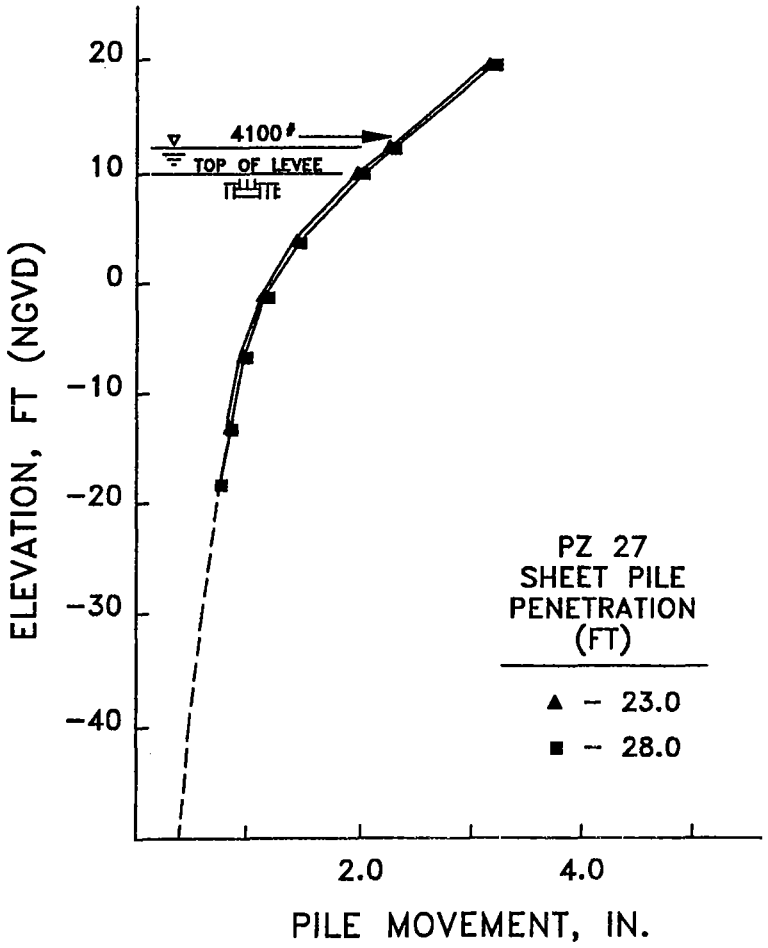

Figure A20. Pile movement for different pile penetration depths in the E-105 "strong" soil profile; for an equivalent lumped wave load of 4,100.0 lb at 3.5 ft above the levee surface with 2.5 ft of head

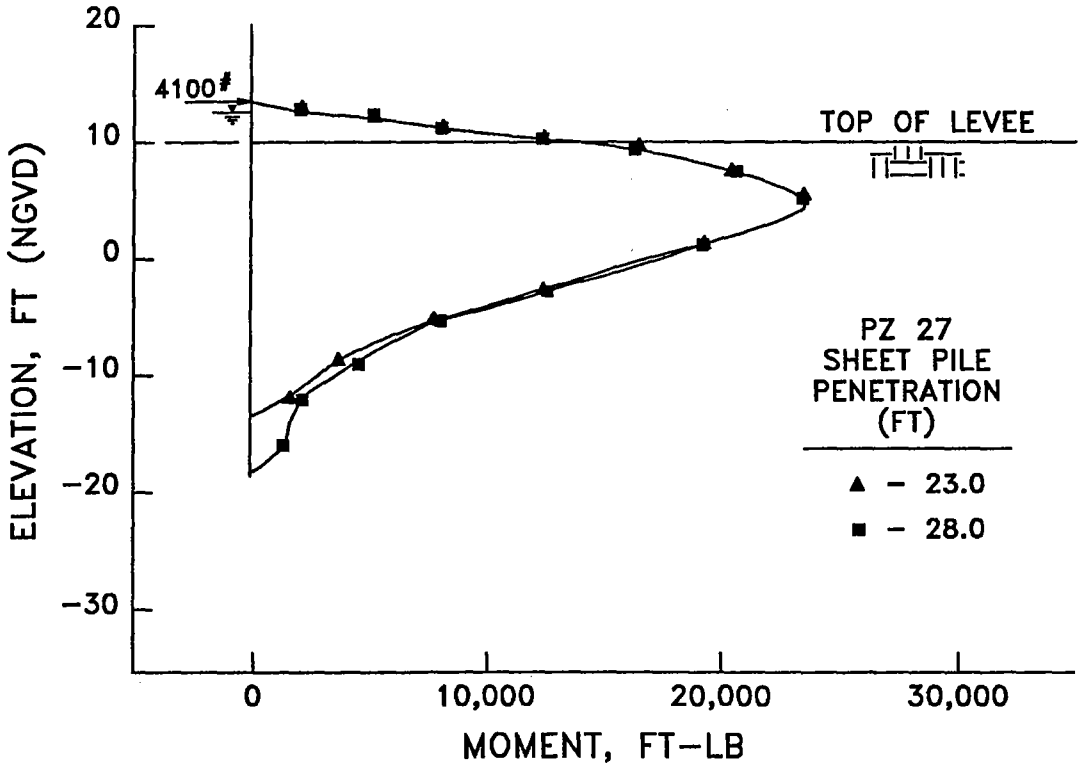

Figure A21. Pile moments for different pile penetration depths in the E-105 "strong" soil profile; for an equivalent lumped wave load of 4,100.0 lb at 3.5 ft above the levee surface with 2.5 ft of head

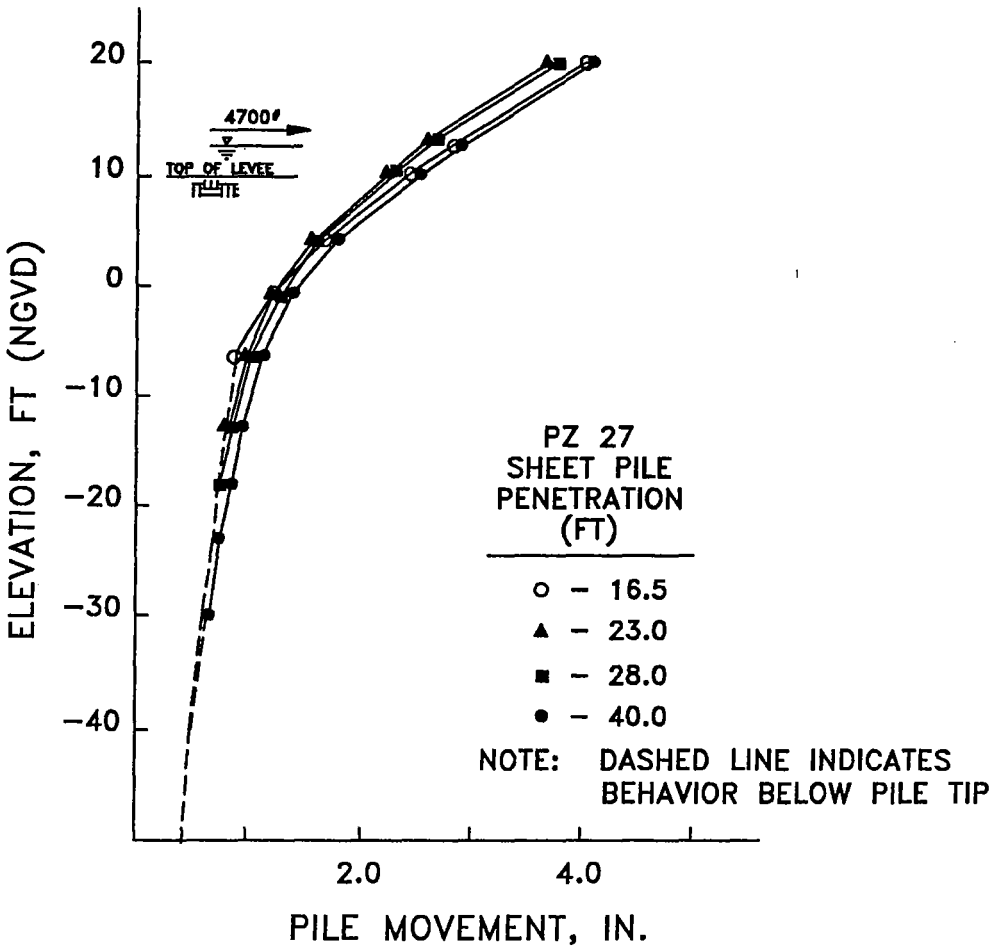

Figure A22. Pile movement for different pile penetration depths in the E-105 "weak" soil profile; for an equivalent lumped wave load of 4,700.0 lb at 3.5 ft above the levee surface with 2.5 ft of head

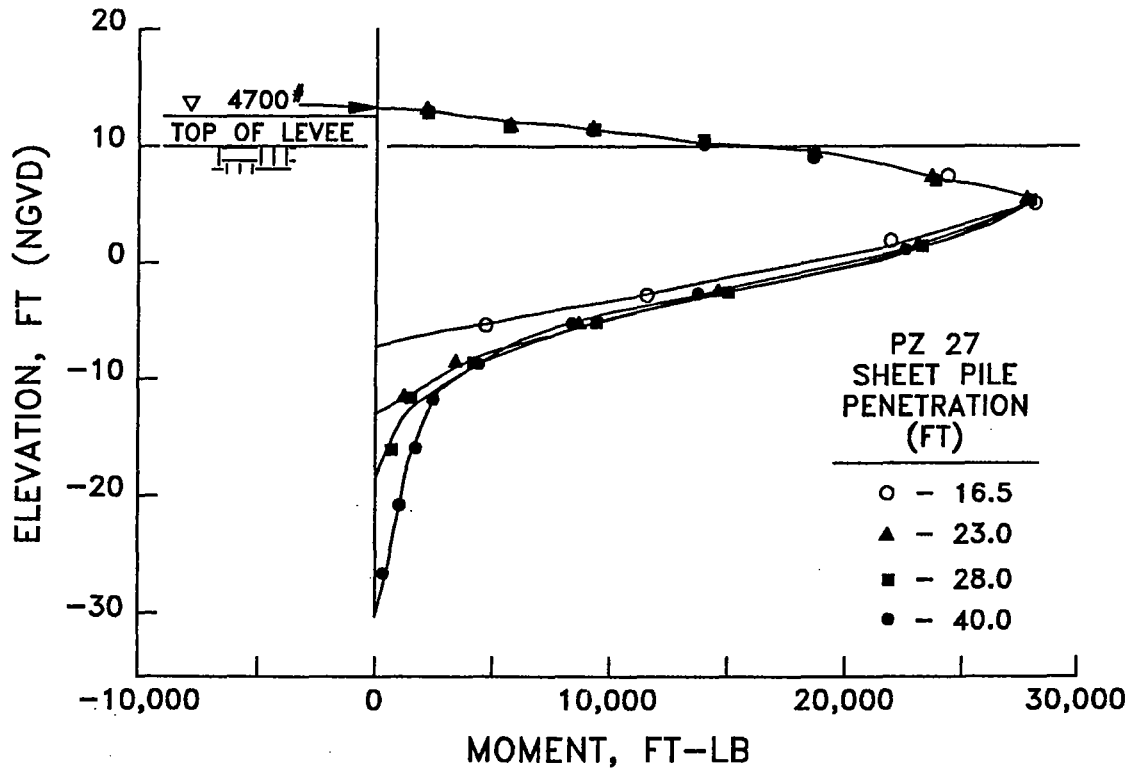

Figure A23. Pile moments for different pile penetration depths in the E-105 "weak" soil profile; for an equivalent lumped wave load of 4,700.0 lb at 3.5 ft above the levee surface with 2.5 ft of head

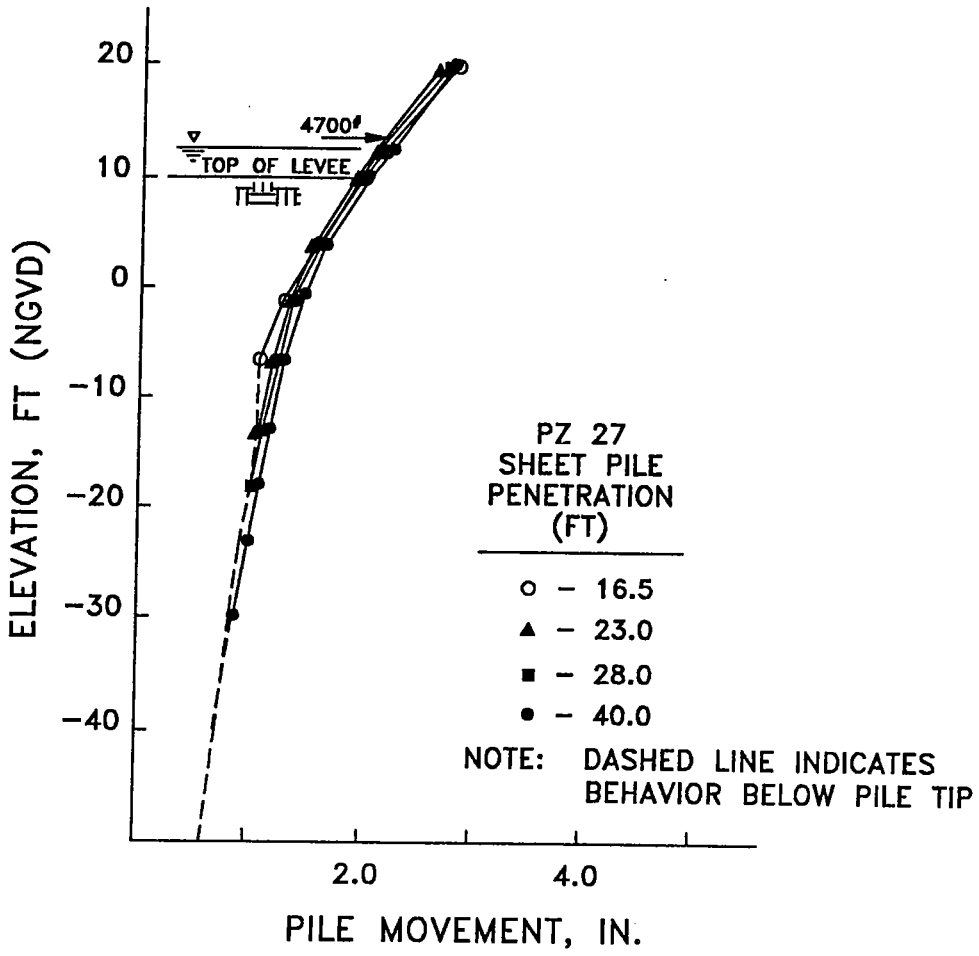

Figure A24. Pile movement for different pile penetration depths in the E-105 "strong" soil profile; for an equivalent lumped wave load of 4,700.0 lb at 3.5 ft above the levee surface with 2.5 ft of head

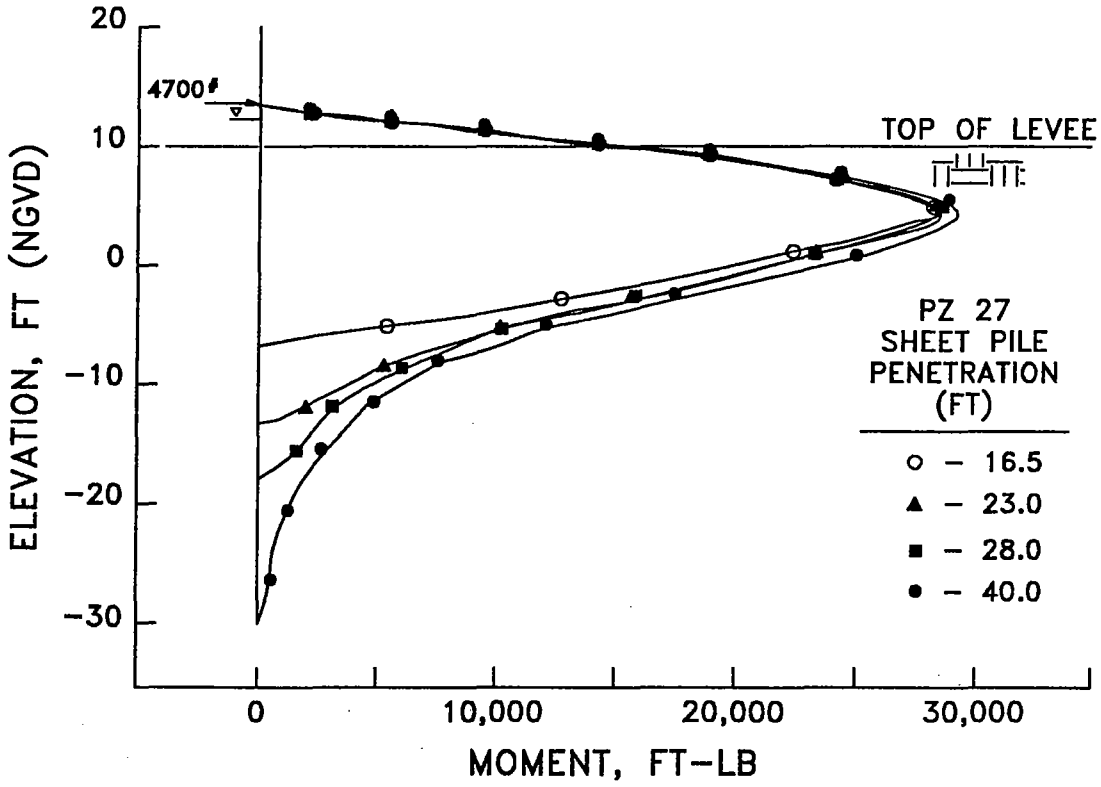

Figure A25. Pile moments for different pile penetration depths in the E-105 "strong" soil profile; for an equivalent lumped wave load of 4,700.0 lb at 3.5 ft above the levee surface with 2.5 ft of head

APPENDIX B: SUMMARY OF SOIL TESTS

B1. A summary of the boring is presented in Table B1 and the laboratory test results are summarized in Table B2 and Figure B1. The laboratory test data for soil specimens taken from each sample of boring NSD-1UT have been grouped into individual data packets. Each packet is designated by the sample number from which the data were derived. From Figure B1 it is seen that the two samples from shallow depths, 1-C and 4-C, are overconsolidated while the two deeper samples, 6-D and 9-D, are normally consolidated. These results are indicative of samples taken from the toe of the levee and therefore justify the use of the high S_u/p'_c values selected for this part of the soil profile. For other portions of the foundation, the strength can be determined from the following relationship:

$$S_u = 0.45 p'_c \left(\frac{p'_m}{p'_c} \right)^{0.81} \tag{B1}$$

Table B1. Summary of Boring NSD-1UT

Sample [a]	Depth ft	w %	γ_t pcf	σ_v psf	p_u psf	σ'_v psf
1-C	2.3	47.3	107.0	246.0	0.0	246.0
4-C	13.0	32.1	115.0	1,450.0	474.0	976.0
6-D	21.6	67.3	98.0	2,310.0	1,010.0	1,300.0
9-D	33.9	63.1	100.0	3,580.0	1,780.0	1,800.0

[a] Boring located at station 102+00, 63.0 ft landside of centerline; ground surface el at 9.4 ft; ground water el at 4.0 ft

Table B2. Summary of Laboratory Test Data

Sample	Specimen	p'_o psf	p_m psf	p'_c psf	S_u psf	p'_c/p_m	S_u/p'_c	p'_o/p_m
1-C	1	185.0	1,730.0	1,220.0	700.0	0.706	0.574	0.107
	2	185.0	1,730.0	4,300.0	1,680.0	2.488	0.391	0.107
	3	185.0	1,730.0	800.0	560.0	0.463	0.700	0.107
	4	185.0	1,730.0	680.0	740.0	0.394	1.090	0.107
4-C	1	732.0	1,600.0	2,400.0	1,140.0	1.502	0.475	0.458
	2	732.0	1,600.0	600.0	620.0	0.375	1.030	0.458
	3	732.0	1,600.0	1,340.0	840.0	1.839	0.627	0.458
	4	732.0	1,600.0	240.0	550.0	0.150	2.290	0.458
6-D	1	964.0	850.0	260.0	240.0	0.306	0.920	1.134
	2	964.0	850.0	1,900.0	1,000.0	2.235	0.526	1.134
	3	964.0	850.0	920.0	560.0	1.082	0.609	1.134
9-D	1	1,210.0	1,210.0	500.0	480.0	0.413	0.960	1.116
	2	1,210.0	1,210.0	2,620.0	1,180.0	2.165	0.450	1.116
	3	1,210.0	1,210.0	1,320.0	740.0	1.091	0.561	1.116
	4	1,210.0	1,210.0	2,620.0	1,200.0	2.165	0.458	1.116

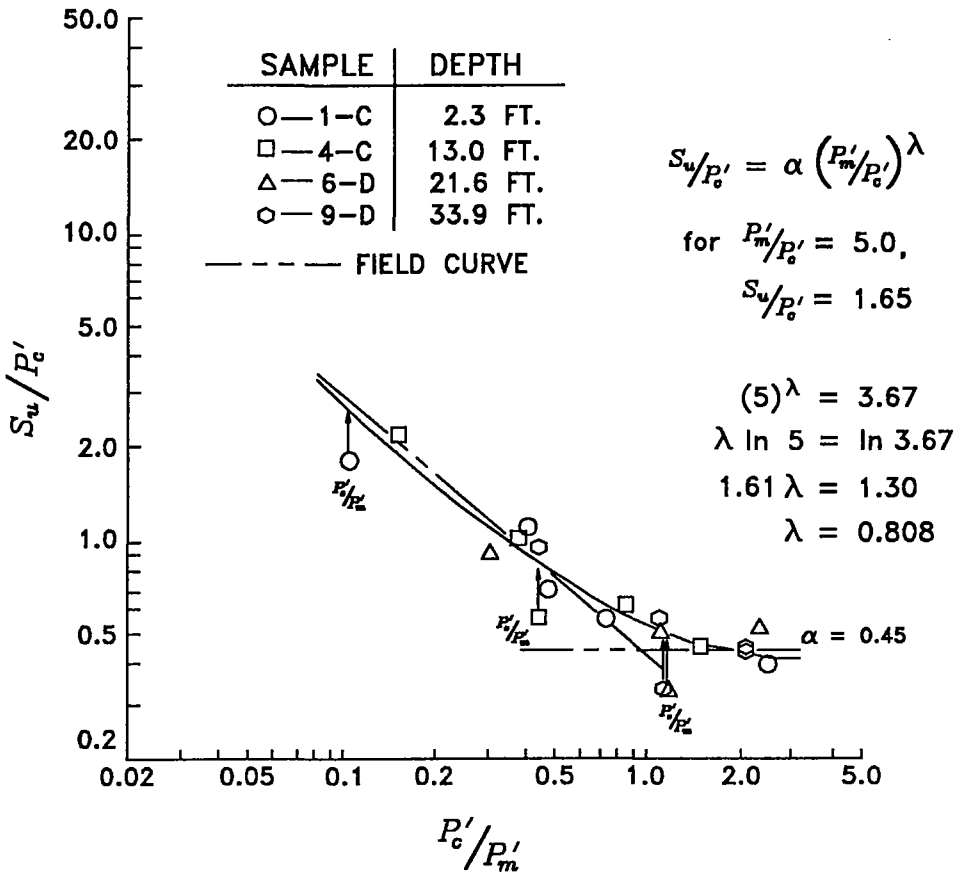

Figure B1. Effect of consolidation state on undrained shear strength

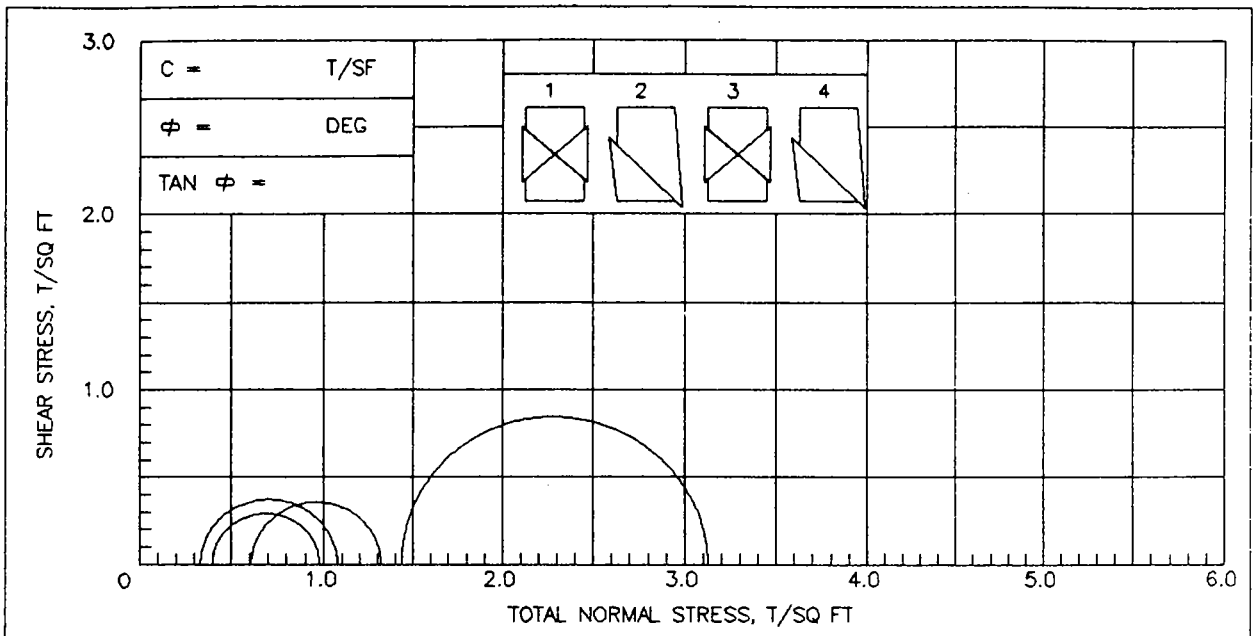

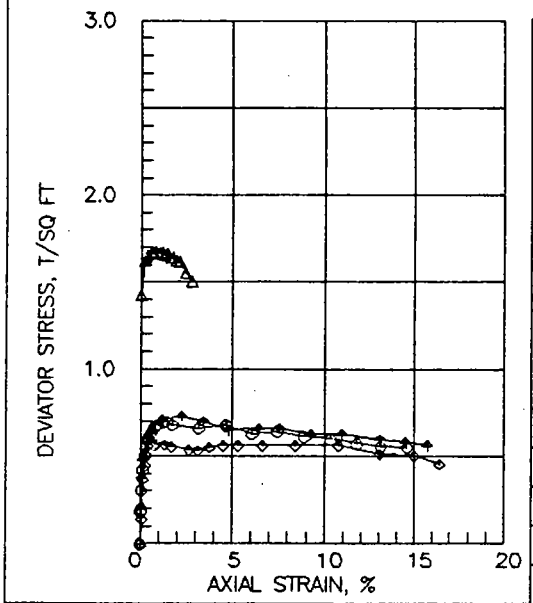

SPECIMEN NO.		⊙ 1	△ 2	◇ 3	+ 4
INITIAL	WATER CONTENT, %	46.5	48.4	46.1	48.1
	DRY DENSITY, PCF	72.9	73.0	73.0	71.8
	SATURATION, %	95.8	99.8	95.1	96.4
	VOID RATIO	1.311	1.310	1.309	1.348
BEFORE SHEAR	WATER CONTENT, %	48.2	41.8	48.4	50.8
	DRY DENSITY, PCF	73.1	78.9	73.0	71.8
	SATURATION, %	99.7	99.2	99.8	100+
	VOID RATIO	1.305	1.137	1.309	1.348
	BACK PRESS., TSF	.11	3.60	−.04	−.22
MIN PRIN. STRESS, TSF		.61	1.44	.40	.34
MAX. DEV. STRESS, TSF		.70	1.68	.57	.73
TIME TO FAILURE, MIN.		72	785	46	115
RATE OF STRAIN, %/MIN		.020	.001	.020	.020
INITIAL DIAMETER, IN.		1.41	1.40	1.41	1.40
INITIAL HEIGHT, IN.		3.50	3.50	3.50	3.50

CONTROLLED−STRAIN TEST

DESCRIPTION OF SPECIMENS:

LL	PL	PI	GS 2.70 (ESTIMATED)	UNDISTURBED SPECIMEN	$\bar{R}$ TEST

REMARKS:	PROJECT E−99 SHEETPILE TEST	
	BORING NO. NSD−1UT	SAMPLE NO. 1C
	DEPTH/ELEV 2.3	TECH. LRC
	LABORATORY USAE WES	DATE 31 OCT 88
	$\bar{R}$−TRIAXIAL COMPRESSION TEST REPORT	

Figure B2. Data packet for sample 1-C

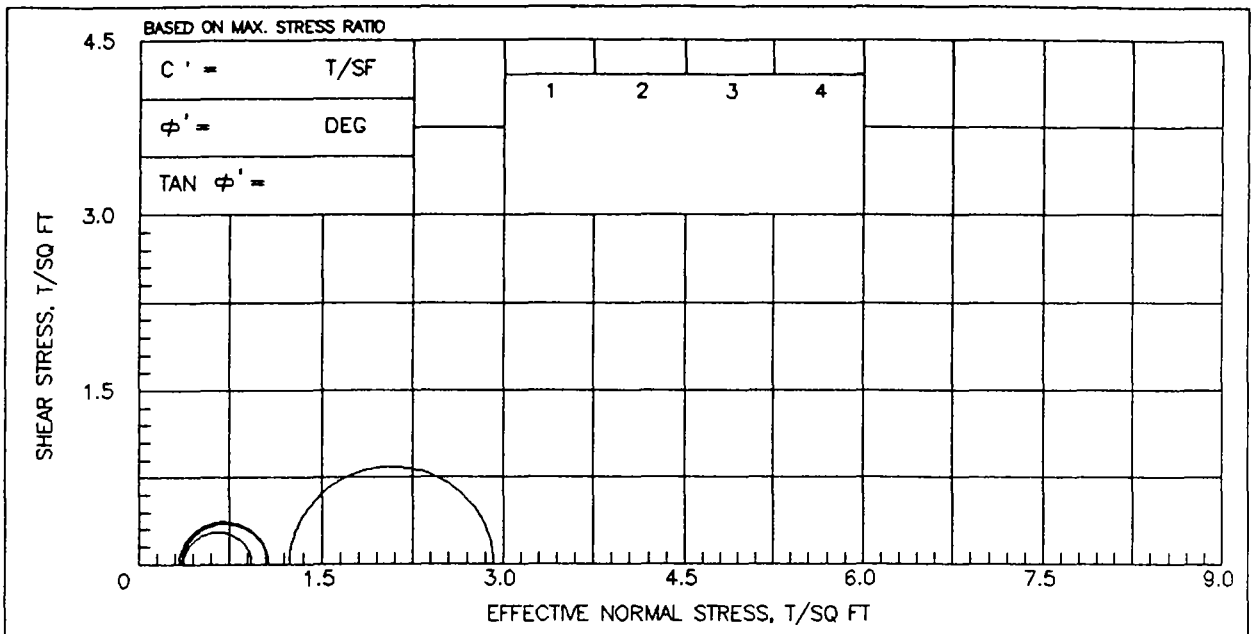

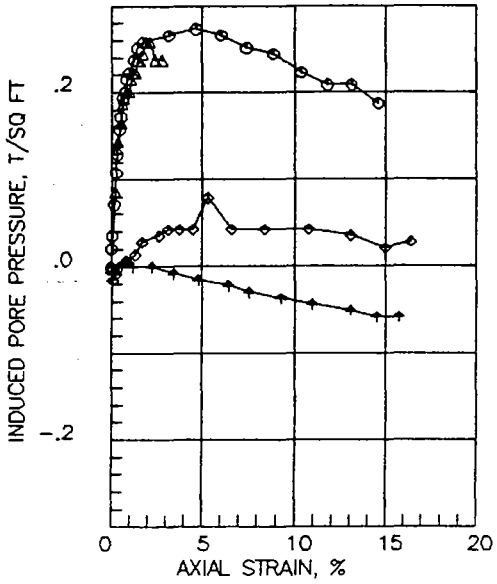

SPECIMEN NO.		◇ 1	△ 2	○ 3	+ 4
INITIAL	WATER CONTENT, %	46.5	48.4	46.1	48.1
	DRY DENSITY, PCF	72.9	73.0	73.0	71.8
	SATURATION, %	95.8	99.8	95.1	96.4
	VOID RATIO	1.311	1.310	1.309	1.348
BEFORE SHEAR	WATER CONTENT, %	48.2	41.8	48.4	50.8
	DRY DENSITY, PCF	73.1	78.9	73.0	71.8
	SATURATION, %	99.7	99.2	99.8	100+
	VOID RATIO	1.305	1.137	1.309	1.348
	BACK PRESS., TSF	.11	3.60	-.04	-.22
MIN PRIN. STRESS, TSF		.36	1.24	.37	.34
MAX. DEV. STRESS, TSF		.70	1.68	.56	.73
TIME TO FAILURE, MIN.		72	785	87	115
RATE OF STRAIN, %/MIN		.020	.001	.020	.020
INITIAL DIAMETER, IN.		1.41	1.40	1.41	1.40
INITIAL HEIGHT, IN.		3.50	3.50	3.50	3.50

CONTROLLED-STRAIN TEST

DESCRIPTION OF SPECIMENS:

LL	PL	PI	GS 2.70 (ESTIMATED)	UNDISTURBED SPECIMEN	$\bar{R}$ TEST

REMARKS:	PROJECT E-99 SHEETPILE TEST	
	BORING NO. NSD-1UT	SAMPLE NO. 1C
	DEPTH/ELEV 2.3	TECH. LRC
	LABORATORY USAE WES	DATE 31 OCT 88
	$\bar{R}$-TRIAXIAL COMPRESSION TEST REPORT	

Figure B2. (Continued)

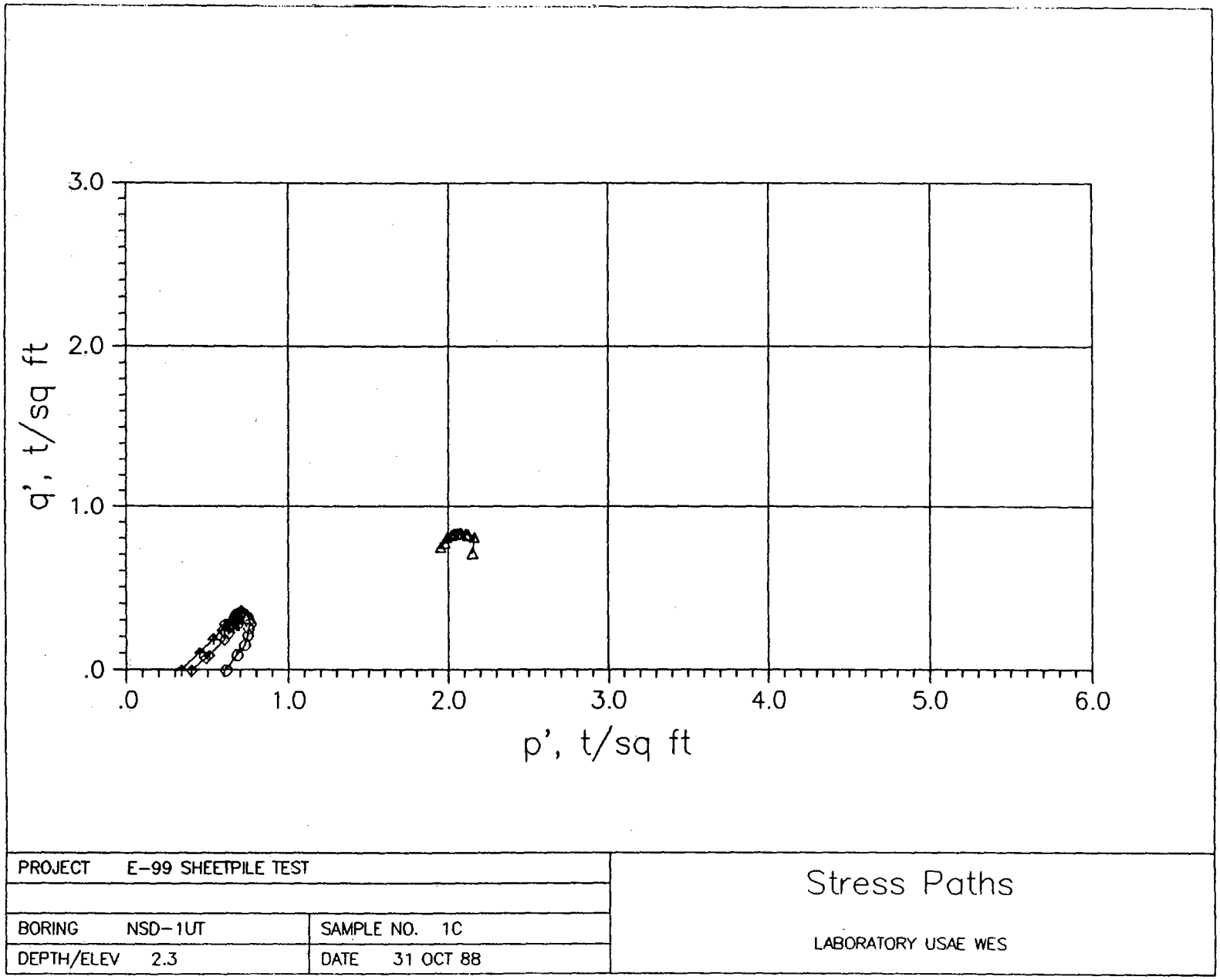

Figure B2: (Continued)

R-BAR TRIAXIAL COMPRESSION TEST REPORT

TLE: E-99 SHEETPILE TEST

BOR: NSD-1UT SAM: 1C DEP: 2.3 DAT: 31 OCT 88 TEC: LRC
DES:

SAMPLE TYPE - UNDISTURBED
GS: 2.70 (ESTIMATED)
LL: 0 PL: 0 PI: 0

WEIGHT OF SOLIDS - 103.88 I. HEIGHT - 3.500" I. DIAMETER - 1.405"

HEIGHT CHANGES: PRE-CONS. - .00300" DURING CONS. - .00000"

VOLUME CHANGE DURING CONS. - .0 CC TIME OF TEST - 740 MINS.

BACK PRESSURE - 1.50 PSI (.11 TSF) CHAMBER PRESSURE - 10.00

EFF CONFINING PRESSURE, TSF - .61

	INITIAL	BEFORE SHEAR
WATER CONTENT, %	46.50	48.20
VOID RATIO	1.311	1.305
SATURATION, %	95.76	99.71
DRY DENSITY, PCF	72.94	73.12

V DEF IN.	AXIAL LOAD LBS	PORE PRESS PSI	STRAIN %	IND POR PRESS TSF	DEVIAT STRESS TSF	EFFECTIVE E1 - TSF -	E3	RATIO E1/ E3	NORML STRES TSF	SHEAR STRES TSF
.000	.0	1.5	.0	.00	.00	.612	.612	1.000	.61	.00
.001	4.0	1.8	.0	.02	.19	.776	.590	1.315	.68	.09
.002	6.6	2.0	.1	.04	.31	.883	.576	1.533	.73	.15
.005	9.1	2.5	.1	.07	.42	.963	.540	1.783	.75	.21
.009	10.9	3.0	.3	.11	.51	1.010	.504	2.003	.76	.25
.012	12.1	3.3	.3	.13	.56	1.043	.482	2.163	.76	.28
.016	13.0	3.7	.5	.16	.60	1.056	.454	2.327	.75	.30
.019	13.5	3.9	.5	.17	.62	1.064	.439	2.422	.75	.31
.023	13.9	4.2	.7	.19	.64	1.060	.418	2.538	.74	.32
.026	14.4	4.3	.7	.20	.66	1.075	.410	2.620	.74	.33
.029	14.6	4.5	.8	.22	.67	1.069	.396	2.701	.73	.34
.033	14.8	4.6	.9	.22	.68	1.071	.389	2.754	.73	.34
.043	15.1	4.8	1.2	.24	.69	1.068	.374	2.853	.72	.35
.050	15.3	5.0	1.4	.25	.70	1.061	.360	2.949	.71	.35
.061	14.9	5.1	1.7	.26	.68	1.034	.353	2.930	.69	.34
.111	14.7	5.2	3.2	.27	.66	1.008	.346	2.916	.68	.33
.163	15.3	5.3	4.7	.27	.68	1.017	.338	3.005	.68	.34
.211	14.4	5.2	6.0	.27	.63	.975	.346	2.821	.66	.31
.260	14.9	5.0	7.4	.25	.64	1.002	.360	2.782	.68	.32
.311	14.5	4.9	8.9	.24	.61	.982	.367	2.674	.67	.31
.362	14.4	4.6	10.4	.22	.60	.989	.389	2.545	.69	.30
.412	14.0	4.4	11.8	.21	.57	.978	.403	2.425	.69	.29
.458	13.8	4.4	13.1	.21	.56	.961	.403	2.384	.68	.28
.510	13.9	4.1	14.6	.19	.55	.977	.425	2.300	.70	.28

RATE OF STRAIN - .020

Figure B2. (Continued)

R-BAR TRIAXIAL COMPRESSION TEST REPORT

TLE: E-99 SHEETPILE TEST

BOR: NSD-1UT SAM: 1C DEP: 2.3 DAT: 31 OCT 88 TEC: LRC
DES:

SAMPLE TYPE - UNDISTURBED
GS: 2.70 (ESTIMATED)
LL: 0 PL: 0 PI: 0

WEIGHT OF SOLIDS - 103.78 I. HEIGHT - 3.500" I. DIAMETER - 1.404"

HEIGHT CHANGES: PRE-CONS. - -.01200" DURING CONS. - .27100"

VOLUME CHANGE DURING CONS. - 7.6 CC TIME OF TEST - 2450 MINS.

BACK PRESSURE - 50.00 PSI (3.60 TSF) CHAMBER PRESSURE - 70.00

EFF CONFINING PRESSURE, TSF - 1.44

	INITIAL	BEFORE SHEAR
WATER CONTENT, %	48.40	41.80
VOID RATIO	1.310	1.137
SATURATION, %	99.76	99.25
DRY DENSITY, PCF	72.97	78.87

V DEF IN.	AXIAL LOAD LBS	PORE PRESS PSI	STRAIN %	IND POR PRESS TSF	DEVIAT STRESS TSF	EFFECTIVE E1 - TSF -	E3	RATIO E1/ E3	NORML STRES TSF	SHEAR STRES TSF
.000	30.7	50.0	.0	.00	1.43	2.869	1.440	1.992	2.15	.71
.006	35.0	51.2	.2	.09	1.63	2.979	1.353	2.201	2.17	.81
.010	35.5	51.9	.3	.14	1.65	2.950	1.303	2.264	2.13	.82
.012	35.8	52.0	.4	.14	1.66	2.956	1.296	2.281	2.13	.83
.018	36.1	52.3	.6	.17	1.67	2.945	1.274	2.311	2.11	.84
.020	36.1	52.6	.6	.19	1.67	2.923	1.253	2.333	2.09	.83
.023	36.1	52.7	.7	.19	1.67	2.914	1.246	2.339	2.08	.83
.027	36.4	52.8	.8	.20	1.68	2.918	1.238	2.357	2.08	.84
.032	36.2	52.8	1.0	.20	1.67	2.907	1.238	2.347	2.07	.83
.035	36.3	53.0	1.1	.22	1.67	2.895	1.224	2.366	2.06	.84
.038	36.4	53.1	1.2	.22	1.67	2.891	1.217	2.376	2.05	.84
.043	36.1	53.1	1.3	.22	1.66	2.875	1.217	2.363	2.05	.83
.047	36.4	53.3	1.5	.24	1.67	2.872	1.202	2.389	2.04	.83
.052	36.0	53.3	1.6	.24	1.65	2.851	1.202	2.371	2.03	.82
.058	36.1	53.4	1.8	.24	1.65	2.845	1.195	2.381	2.02	.83
.063	35.7	53.6	1.9	.26	1.63	2.810	1.181	2.380	2.00	.81
.069	35.6	53.6	2.1	.26	1.62	2.802	1.181	2.373	1.99	.81
.080	34.3	53.3	2.5	.24	1.56	2.759	1.202	2.295	1.98	.78
.091	33.3	53.3	2.8	.24	1.51	2.709	1.202	2.253	1.96	.75

RATE OF STRAIN - .001

Figure B2. (Continued)

R-BAR TRIAXIAL COMPRESSION TEST REPORT

TLE: E-99 SHEETPILE TEST

BOR: NSD-1UT SAM: 1C DEP: 2.3 DAT: 31 OCT 88 TEC: LRC
DES:

SAMPLE TYPE - UNDISTURBED
GS: 2.70 (ESTIMATED)
LL: 0 PL: 0 PI: 0

WEIGHT OF SOLIDS - 105.00 I. HEIGHT - 3.500" I. DIAMETER - 1.412"

HEIGHT CHANGES: PRE-CONS. - .00000" DURING CONS. - .00000"

VOLUME CHANGE DURING CONS. - .0 CC TIME OF TEST - 842 MINS.

BACK PRESSURE - -.60 PSI (-.04 TSF) CHAMBER PRESSURE - 5.00

EFF CONFINING PRESSURE, TSF - .40

	INITIAL	BEFORE SHEAR
WATER CONTENT, %	46.10	48.40
VOID RATIO	1.309	1.309
SATURATION, %	95.07	99.81
DRY DENSITY, PCF	72.99	72.99

V DEF IN.	AXIAL LOAD LBS	PORE PRESS PSI	STRAIN %	IND POR PRESS TSF	DEVIAT STRESS TSF	EFFECTIVE E1 - TSF -	E3	RATIO E1/ E3	NORML STRES TSF	SHEAR STRES TSF
.000	.0	-.6	.0	.00	.00	.403	.403	1.000	.40	.00
.003	3.1	-.8	.1	-.01	.14	.560	.418	1.341	.49	.07
.003	4.0	-.8	.1	-.01	.18	.601	.418	1.440	.51	.09
.006	8.0	-.8	.2	-.01	.37	.785	.418	1.879	.60	.18
.009	9.8	-.7	.3	-.01	.45	.860	.410	2.095	.64	.22
.012	11.0	-.7	.3	-.01	.50	.914	.410	2.228	.66	.25
.016	11.6	-.6	.5	.00	.53	.934	.403	2.317	.67	.27
.026	12.3	-.5	.7	.01	.56	.957	.396	2.418	.68	.28
.032	12.5	-.5	.9	.01	.57	.965	.396	2.438	.68	.28
.047	12.5	-.4	1.3	.01	.57	.956	.389	2.458	.67	.28
.060	12.3	-.2	1.7	.03	.56	.930	.374	2.485	.65	.28
.093	12.0	-.1	2.7	.04	.54	.904	.367	2.463	.64	.27
.110	12.0	.0	3.1	.04	.53	.894	.360	2.485	.63	.27
.131	12.5	.0	3.7	.04	.55	.913	.360	2.537	.64	.28
.158	12.8	.0	4.5	.04	.56	.922	.360	2.561	.64	.28
.186	12.9	.5	5.3	.08	.56	.886	.324	2.733	.60	.28
.231	13.1	.0	6.6	.04	.56	.923	.360	2.563	.64	.28
.295	13.4	.0	8.4	.04	.56	.924	.360	2.567	.64	.28
.376	13.7	.0	10.7	.04	.56	.922	.360	2.562	.64	.28
.457	12.9	-.1	13.1	.04	.52	.883	.367	2.404	.62	.26
.525	12.9	-.3	15.0	.02	.50	.886	.382	2.321	.63	.25
.575	11.9	-.2	16.4	.03	.46	.832	.374	2.221	.60	.23

RATE OF STRAIN - .020

Figure B2: (Continued)

R-BAR TRIAXIAL COMPRESSION TEST REPORT

TLE: E-99 SHEETPILE TEST

BOR: NSD-1UT SAM: 1C DEP: 2.3 DAT: 31 OCT 88 TEC: LRC
DES:

SAMPLE TYPE - UNDISTURBED
GS: 2.70 (ESTIMATED)
LL: 0 PL: 0 PI: 0

WEIGHT OF SOLIDS - 102.11 I. HEIGHT - 3.500" I. DIAMETER - 1.404"

HEIGHT CHANGES: PRE-CONS. - .00000" DURING CONS. - .00000"

VOLUME CHANGE DURING CONS. - .0 CC TIME OF TEST - 805 MINS.

BACK PRESSURE - -3.00 PSI (-.22 TSF) CHAMBER PRESSURE - 1.70

EFF CONFINING PRESSURE, TSF - .34

	INITIAL	BEFORE SHEAR
WATER CONTENT, %	48.10	50.80
VOID RATIO	1.348	1.348
SATURATION, %	96.36	101.77
DRY DENSITY, PCF	71.80	71.80

V DEF IN.	AXIAL LOAD LBS	PORE PRESS PSI	STRAIN %	IND POR PRESS TSF	DEVIAT STRESS TSF	EFFECTIVE E1 - TSF -	E3	RATIO E1/ E3	NORML STRES TSF	SHEAR STRES TSF
.000	.0	-3.0	.0	.00	.00	.338	.338	1.000	.34	.00
.002	4.6	-3.1	.1	-.01	.21	.559	.346	1.619	.45	.11
.003	8.1	-3.1	.1	-.01	.38	.722	.346	2.089	.53	.19
.006	10.4	-3.1	.2	-.01	.48	.828	.346	2.397	.59	.24
.010	11.7	-3.1	.3	-.01	.54	.888	.346	2.570	.62	.27
.013	12.7	-3.0	.4	.00	.59	.927	.338	2.739	.63	.29
.017	13.2	-3.0	.5	.00	.61	.949	.338	2.805	.64	.31
.020	13.9	-3.0	.6	.00	.64	.981	.338	2.899	.66	.32
.030	14.8	-2.9	.9	.01	.68	1.014	.331	3.060	.67	.34
.042	15.5	-3.0	1.2	.00	.71	1.051	.338	3.105	.69	.36
.079	16.1	-3.0	2.3	.00	.73	1.070	.338	3.163	.70	.37
.120	15.6	-3.1	3.4	-.01	.70	1.046	.346	3.027	.70	.35
.169	14.7	-3.2	4.8	-.01	.65	1.003	.353	2.844	.68	.33
.224	15.1	-3.3	6.4	-.02	.66	1.017	.360	2.826	.69	.33
.264	15.4	-3.4	7.5	-.03	.66	1.029	.367	2.803	.70	.33
.324	14.9	-3.5	9.3	-.04	.63	1.003	.374	2.679	.69	.31
.384	15.2	-3.6	11.0	-.04	.63	1.011	.382	2.649	.70	.31
.457	14.8	-3.7	13.1	-.05	.60	.987	.389	2.539	.69	.30
.508	14.7	-3.8	14.5	-.06	.58	.980	.396	2.476	.69	.29
.550	14.4	-3.8	15.7	-.06	.56	.960	.396	2.425	.68	.28

RATE OF STRAIN - .020

Figure B2. (Continued)

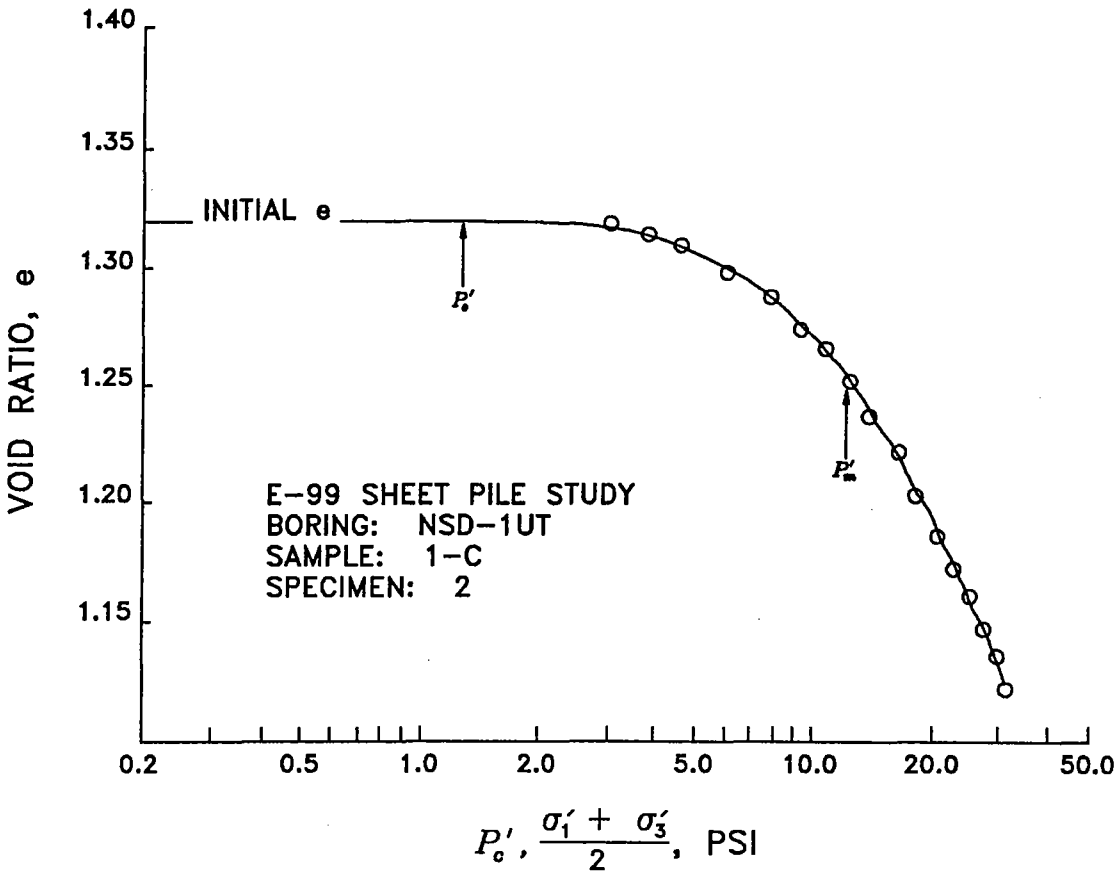

Figure B2. (Concluded)

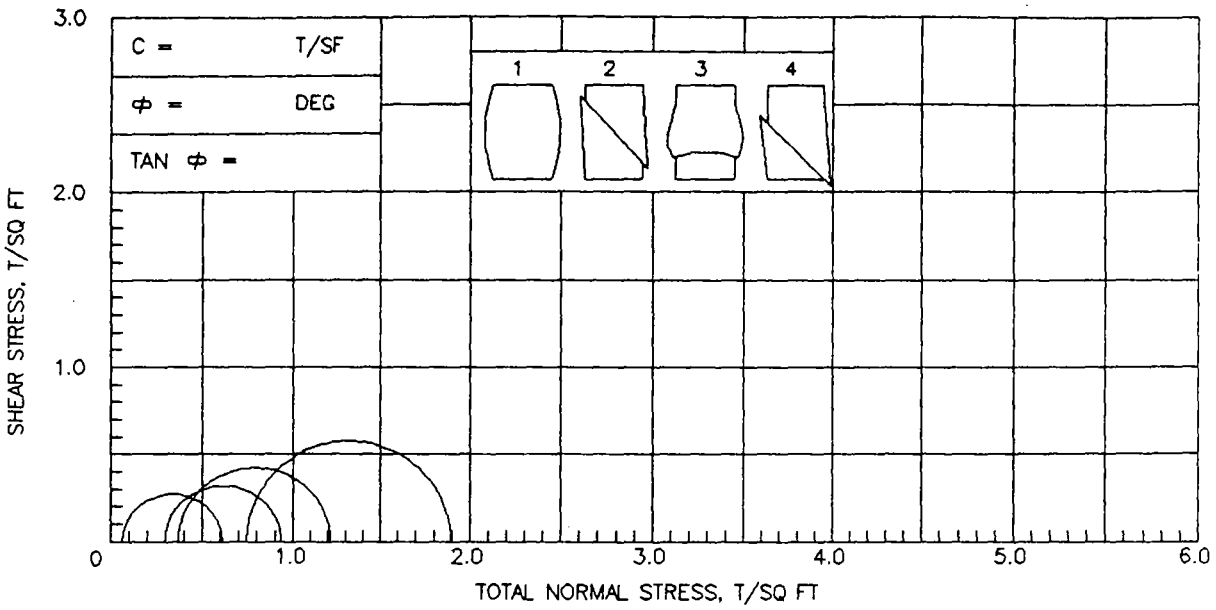

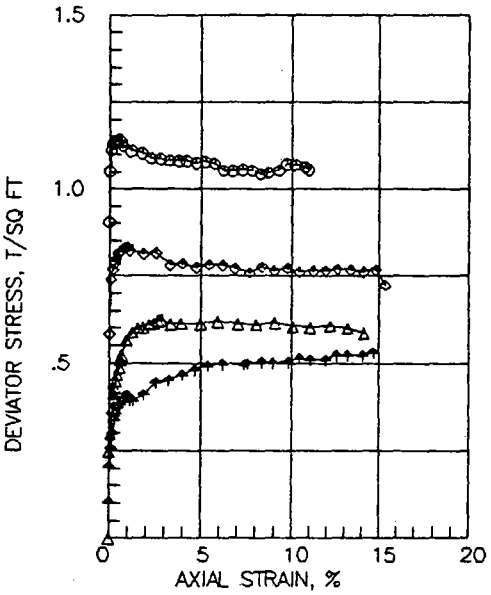

SPECIMEN NO.		○ 1	△ 2	◇ 3	☆ 4
INITIAL	WATER CONTENT, %	33.0	32.3	32.3	33.2
	DRY DENSITY, PCF	87.0	85.8	86.2	86.6
	SATURATION, %	95.0	90.4	91.2	94.8
	VOID RATIO	.938	.964	.956	.946
BEFORE SHEAR	WATER CONTENT, %	30.5	32.1	32.1	33.6
	DRY DENSITY, PCF	89.7	85.9	88.5	88.0
	SATURATION, %	93.8	90.0	95.9	99.1
	VOID RATIO	.878	.963	.904	.915
	BACK PRESS., TSF	.72	.45	3.60	2.16
MIN PRIN. STRESS, TSF		.75	.30	.37	.07
MAX. DEV. STRESS, TSF		1.14	.63	.84	.53
TIME TO FAILURE, MIN.		27	151	51	743
RATE OF STRAIN, %/MIN		.019	.019	.020	.020
INITIAL DIAMETER, IN.		1.37	1.37	1.38	1.38
INITIAL HEIGHT, IN.		3.50	3.50	3.50	3.50

CONTROLLED-STRAIN TEST

DESCRIPTION OF SPECIMENS:

LL	PL	PI	GS 2.70 (ESTIMATED)	UNDISTURBED SPECIMEN	$\bar{R}$ TEST

REMARKS:	PROJECT E-99 SHEETPILE TEST	
	BORING NO. NSD-1UT	SAMPLE NO. 4C
	DEPTH/ELEV 13.0	TECH. LRC
	LABORATORY USAE WES	DATE 13 SEPT 88
	$\bar{R}$-TRIAXIAL COMPRESSION TEST REPORT	

Figure B3. Data packet for sample 4-C

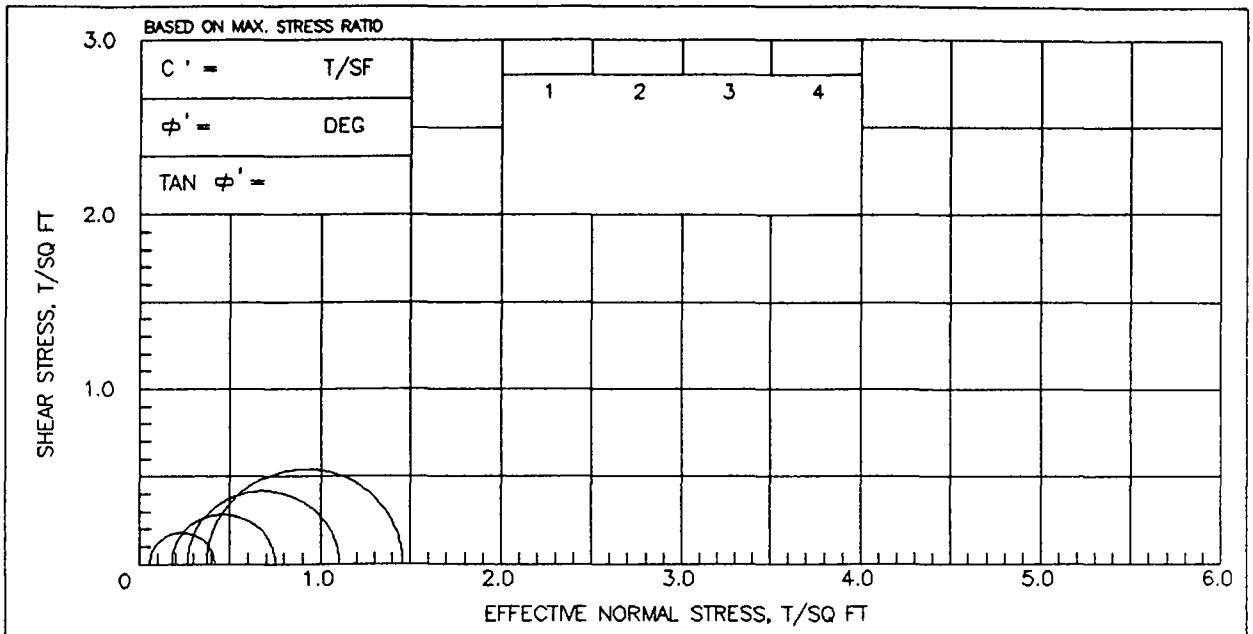

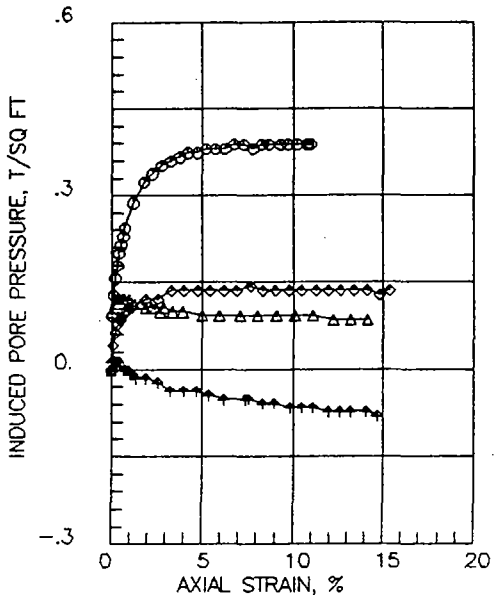

SPECIMEN NO.		○ 1	△ 2	◇ 3	✦ 4
INITIAL	WATER CONTENT, %	33.0	32.3	32.3	33.2
	DRY DENSITY, PCF	87.0	85.8	86.2	86.6
	SATURATION, %	95.0	90.4	91.2	94.8
	VOID RATIO	.938	.964	.956	.946
BEFORE SHEAR	WATER CONTENT, %	30.5	32.1	32.1	33.6
	DRY DENSITY, PCF	89.7	85.9	88.5	88.0
	SATURATION, %	93.8	90.0	95.9	99.1
	VOID RATIO	.878	.963	.904	.915
	BACK PRESS., TSF	.72	.45	3.60	2.16
MIN PRIN. STRESS, TSF		.37	.18	.27	.06
MAX. DEV. STRESS, TSF		1.08	.57	.84	.36
TIME TO FAILURE, MIN.		222	50	51	21
RATE OF STRAIN, %/MIN		.019	.019	.020	.020
INITIAL DIAMETER, IN.		1.37	1.37	1.38	1.38
INITIAL HEIGHT, IN.		3.50	3.50	3.50	3.50

CONTROLLED−STRAIN TEST

DESCRIPTION OF SPECIMENS:

LL	PL	PI	GS 2.70 (ESTIMATED)	UNDISTURBED SPECIMEN	$\bar{R}$ TEST

REMARKS:	PROJECT E−99 SHEETPILE TEST	
	BORING NO. NSD−1UT	SAMPLE NO. 4C
	DEPTH/ELEV 13.0	TECH. LRC
	LABORATORY USAE WES	DATE 13 SEPT 88
	$\bar{R}$−TRIAXIAL COMPRESSION TEST REPORT	

Figure B3. (Continued)

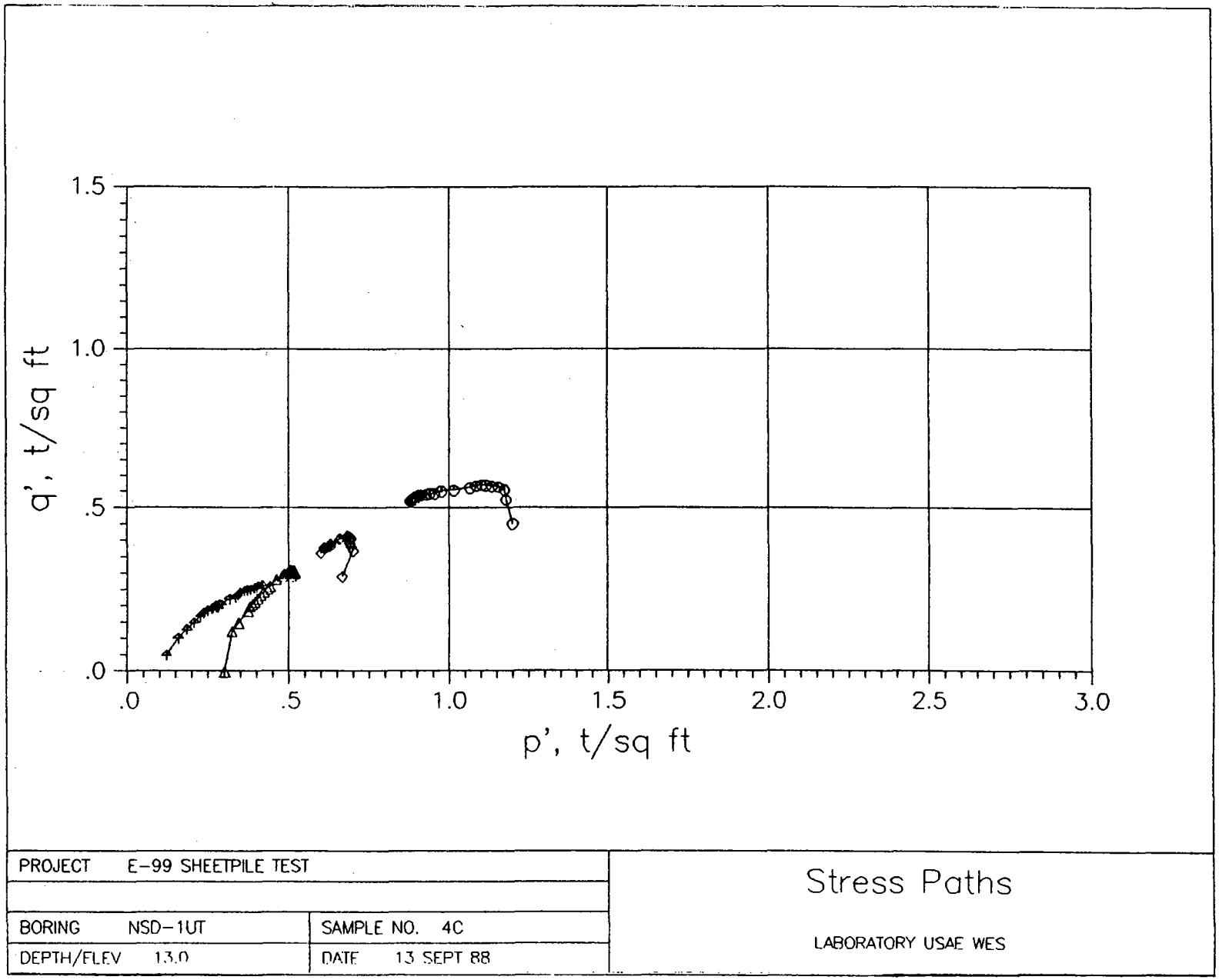

Figure B3. (Continued)

R-BAR TRIAXIAL COMPRESSION TEST REPORT

TLE: E-99 SHEETPILE TEST

BOR: NSD-1UT SAM: 4C DEP: 13.0 DAT: 13 SEPT 88 TEC: LRC
DES:

SAMPLE TYPE - UNDISTURBED
GS: 2.70 (ESTIMATED)
LL: 0 PL: 0 PI: 0

WEIGHT OF SOLIDS - 118.29 I. HEIGHT - 3.500" I. DIAMETER - 1.373"

HEIGHT CHANGES: PRE-CONS. - .00900" DURING CONS. - .09300"

VOLUME CHANGE DURING CONS. - 2.0 CC TIME OF TEST - 563 MINS.

BACK PRESSURE - 10.00 PSI (.72 TSF) CHAMBER PRESSURE - 20.40

EFF CONFINING PRESSURE, TSF - .75

	INITIAL	BEFORE SHEAR
WATER CONTENT, %	33.00	30.50
VOID RATIO	.938	.878
SATURATION, %	94.98	93.77
DRY DENSITY, PCF	86.97	89.74

V DEF IN.	AXIAL LOAD LBS	PORE PRESS PSI	STRAIN %	IND POR PRESS TSF	DEVIAT STRESS TSF	EFFECTIVE E1 - TSF -	E3	RATIO E1/ E3	NORML STRES TSF	SHEAR STRES TSF
.000	18.6	10.0	.0	.00	.91	1.655	.749	2.210	1.20	.45
.001	21.6	11.3	.0	.09	1.05	1.707	.655	2.606	1.18	.53
.004	22.9	11.8	.1	.13	1.11	1.733	.619	2.800	1.18	.56
.007	23.3	12.2	.2	.16	1.13	1.723	.590	2.919	1.16	.57
.011	23.4	12.5	.3	.18	1.14	1.705	.569	2.998	1.14	.57
.014	23.5	12.8	.4	.20	1.14	1.687	.547	3.084	1.12	.57
.018	23.6	13.0	.5	.22	1.14	1.676	.533	3.146	1.10	.57
.022	23.5	13.2	.6	.23	1.14	1.656	.518	3.194	1.09	.57
.025	23.3	13.4	.7	.24	1.13	1.631	.504	3.236	1.07	.56
.041	23.1	14.0	1.2	.29	1.11	1.572	.461	3.413	1.02	.56
.061	23.1	14.5	1.8	.32	1.11	1.530	.425	3.602	.98	.55
.077	22.9	14.7	2.3	.34	1.09	1.501	.410	3.657	.96	.55
.094	23.0	14.9	2.8	.35	1.09	1.485	.396	3.751	.94	.54
.111	23.0	15.0	3.3	.36	1.08	1.473	.389	3.788	.93	.54
.128	23.1	15.1	3.8	.37	1.08	1.464	.382	3.838	.92	.54
.143	23.2	15.2	4.2	.37	1.08	1.457	.374	3.892	.92	.54
.160	23.2	15.2	4.7	.37	1.08	1.451	.374	3.877	.91	.54
.177	23.4	15.3	5.2	.38	1.08	1.448	.367	3.943	.91	.54
.194	23.4	15.3	5.7	.38	1.07	1.442	.367	3.927	.90	.54
.211	23.1	15.3	6.2	.38	1.06	1.423	.367	3.874	.89	.53
.228	23.2	15.4	6.7	.39	1.05	1.414	.360	3.929	.89	.53
.246	23.4	15.4	7.2	.39	1.06	1.417	.360	3.937	.89	.53
.264	23.5	15.3	7.8	.38	1.06	1.423	.367	3.876	.90	.53
.281	23.4	15.4	8.3	.39	1.05	1.406	.360	3.905	.88	.52
.295	23.6	15.4	8.7	.39	1.05	1.410	.360	3.916	.88	.52
.316	23.9	15.4	9.3	.39	1.06	1.416	.360	3.934	.89	.53
.330	24.4	15.4	9.7	.39	1.07	1.433	.360	3.981	.90	.54
.347	24.5	15.4	10.2	.39	1.07	1.432	.360	3.977	.90	.54
.366	24.5	15.4	10.8	.39	1.06	1.425	.360	3.958	.89	.53
.373	24.4	15.4	11.0	.39	1.06	1.418	.360	3.940	.89	.53

RATE OF STRAIN - .019

Figure B3. (Continued)

R-BAR TRIAXIAL COMPRESSION TEST REPORT

TLE: E-99 SHEETPILE TEST

BOR: NSD-1UT SAM: 4C DEP: 13.0 DAT: 13 SEPT 88 TEC: LRC
DES:

SAMPLE TYPE - UNDISTURBED
GS: 2.70 (ESTIMATED)
LL: 0 PL: 0 PI: 0

WEIGHT OF SOLIDS - 117.06 I. HEIGHT - 3.500" I. DIAMETER - 1.375"

HEIGHT CHANGES: PRE-CONS. - .00100" DURING CONS. - .00000"

VOLUME CHANGE DURING CONS. - .0 CC TIME OF TEST - 740 MINS.

BACK PRESSURE - 6.20 PSI (.45 TSF) CHAMBER PRESSURE - 10.40

EFF CONFINING PRESSURE, TSF - .30

	INITIAL	BEFORE SHEAR
WATER CONTENT, %	32.30	32.10
VOID RATIO	.964	.963
SATURATION, %	90.45	90.04
DRY DENSITY, PCF	85.82	85.89

V DEF IN.	AXIAL LOAD LBS	PORE PRESS PSI	STRAIN %	IND POR PRESS TSF	DEVIAT STRESS TSF	EFFECTIVE E1 - TSF -	E3	RATIO E1/ E3	NORML STRES TSF	SHEAR STRES TSF
.000	.0	6.2	.0	.00	.00	.302	.302	1.000	.30	.00
.001	5.1	7.6	.0	.10	.25	.449	.202	2.227	.33	.12
.004	6.2	7.7	.1	.11	.30	.495	.194	2.546	.34	.15
.008	7.7	7.8	.2	.12	.37	.560	.187	2.991	.37	.19
.009	8.3	7.9	.3	.12	.40	.582	.180	3.231	.38	.20
.010	8.6	7.9	.3	.12	.42	.596	.180	3.311	.39	.21
.012	8.9	7.9	.3	.12	.43	.610	.180	3.391	.40	.22
.014	9.3	7.9	.4	.12	.45	.629	.180	3.497	.40	.22
.017	9.7	7.9	.5	.12	.47	.648	.180	3.602	.41	.23
.020	10.1	7.9	.6	.12	.49	.667	.180	3.707	.42	.24
.022	10.6	7.9	.6	.12	.51	.691	.180	3.839	.44	.26
.025	10.9	7.9	.7	.12	.53	.705	.180	3.917	.44	.26
.034	11.8	7.9	1.0	.12	.57	.747	.180	4.150	.46	.28
.045	12.3	7.8	1.3	.12	.59	.776	.187	4.147	.48	.29
.055	12.6	7.8	1.6	.12	.60	.789	.187	4.214	.49	.30
.065	12.7	7.7	1.9	.11	.60	.799	.194	4.111	.50	.30
.076	12.9	7.7	2.2	.11	.61	.807	.194	4.149	.50	.31
.086	13.0	7.7	2.5	.11	.62	.810	.194	4.165	.50	.31
.094	13.2	7.6	2.7	.10	.62	.825	.202	4.091	.51	.31
.101	13.3	7.7	2.9	.11	.63	.821	.194	4.223	.51	.31
.118	13.1	7.6	3.4	.10	.61	.816	.202	4.046	.51	.31
.138	13.2	7.6	3.9	.10	.62	.817	.202	4.051	.51	.31
.174	13.3	7.5	5.0	.09	.61	.822	.209	3.937	.52	.31
.208	13.6	7.5	5.9	.09	.62	.829	.209	3.972	.52	.31
.246	13.6	7.5	7.0	.09	.61	.822	.209	3.938	.52	.31
.281	13.7	7.5	8.0	.09	.61	.820	.209	3.928	.51	.31
.318	14.0	7.5	9.1	.09	.62	.826	.209	3.957	.52	.31
.353	13.9	7.5	10.1	.09	.61	.815	.209	3.904	.51	.30
.388	14.0	7.5	11.1	.09	.60	.813	.209	3.892	.51	.30
.426	14.3	7.4	12.2	.09	.61	.825	.216	3.821	.52	.30
.462	14.3	7.4	13.2	.09	.60	.818	.216	3.788	.52	.30
.495	14.1	7.4	14.1	.09	.59	.803	.216	3.719	.51	.29

RATE OF STRAIN - .019

Figure B3: (Continued)

R-BAR TRIAXIAL COMPRESSION TEST REPORT

TLE: E-99 SHEETPILE TEST

BOR: NSD-1UT SAM: 4C DEP: 13.0 DAT: 13 SEPT 88 TEC: LRC
DES:

SAMPLE TYPE - UNDISTURBED
GS: 2.70 (ESTIMATED)
LL: 0 PL: 0 PI: 0

WEIGHT OF SOLIDS - 118.91 I. HEIGHT - 3.500" I. DIAMETER - 1.383"

HEIGHT CHANGES: PRE-CONS. - .02900" DURING CONS. - .00300"

VOLUME CHANGE DURING CONS. - .2 CC TIME OF TEST - 771 MINS.

BACK PRESSURE - 50.00 PSI (3.60 TSF) CHAMBER PRESSURE - 55.20

EFF CONFINING PRESSURE, TSF - .37

	INITIAL	BEFORE SHEAR
WATER CONTENT, %	32.30	32.10
VOID RATIO	.956	.904
SATURATION, %	91.20	95.87
DRY DENSITY, PCF	86.17	88.53

V DEF IN.	AXIAL LOAD LBS	PORE PRESS PSI	STRAIN %	IND POR PRESS TSF	DEVIAT STRESS TSF	EFFECTIVE E1 - TSF -	E3	RATIO E1/ E3	NORML STRES TSF	SHEAR STRES TSF
.000	12.0	50.0	.0	.00	.59	.960	.374	2.564	.67	.29
.004	15.2	50.6	.1	.04	.74	1.072	.331	3.237	.70	.37
.008	15.8	50.9	.2	.06	.77	1.079	.310	3.484	.69	.38
.011	16.2	51.1	.3	.08	.79	1.083	.295	3.669	.69	.39
.015	16.5	51.2	.4	.09	.80	1.090	.288	3.783	.69	.40
.018	16.8	51.2	.5	.09	.82	1.103	.288	3.831	.70	.41
.021	16.9	51.3	.6	.09	.82	1.100	.281	3.919	.69	.41
.025	17.0	51.4	.7	.10	.82	1.097	.274	4.010	.69	.41
.028	17.2	51.4	.8	.10	.83	1.106	.274	4.043	.69	.42
.031	17.2	51.5	.9	.11	.83	1.098	.266	4.122	.68	.42
.035	17.3	51.5	1.0	.11	.84	1.102	.266	4.137	.68	.42
.039	17.1	51.5	1.1	.11	.82	1.091	.266	4.097	.68	.41
.065	17.0	51.7	1.9	.12	.81	1.066	.252	4.230	.66	.41
.089	17.2	51.7	2.6	.12	.82	1.070	.252	4.245	.66	.41
.115	16.6	51.9	3.3	.14	.78	1.021	.238	4.296	.63	.39
.138	16.8	51.9	4.0	.14	.79	1.025	.238	4.313	.63	.39
.165	16.7	51.9	4.8	.14	.78	1.014	.238	4.266	.63	.39
.189	17.0	51.9	5.4	.14	.78	1.022	.238	4.301	.63	.39
.214	17.1	51.9	6.2	.14	.78	1.020	.238	4.295	.63	.39
.238	17.0	51.9	6.9	.14	.77	1.010	.238	4.252	.62	.39
.265	16.9	52.0	7.6	.14	.76	.992	.230	4.306	.61	.38
.289	17.4	51.9	8.3	.14	.78	1.016	.238	4.275	.63	.39
.314	17.3	51.9	9.1	.14	.77	1.005	.238	4.231	.62	.38
.339	17.6	51.9	9.8	.14	.77	1.012	.238	4.261	.62	.39
.363	17.5	51.9	10.5	.14	.76	1.002	.238	4.218	.62	.38
.390	17.7	51.9	11.2	.14	.77	1.004	.238	4.226	.62	.38
.415	17.9	51.9	12.0	.14	.77	1.006	.238	4.236	.62	.38
.437	18.1	51.9	12.6	.14	.77	1.009	.238	4.249	.62	.39
.464	18.2	51.9	13.4	.14	.77	1.007	.238	4.237	.62	.38
.489	18.2	51.9	14.1	.14	.76	1.000	.238	4.211	.62	.38
.513	18.5	51.8	14.8	.13	.77	1.014	.245	4.142	.63	.38
.533	17.6	51.9	15.4	.14	.73	.964	.238	4.059	.60	.36

RATE OF STRAIN - .020

Figure B3. (Continued)

R-BAR TRIAXIAL COMPRESSION TEST REPORT

TLE: E-99 SHEETPILE TEST

BOR: NSD-1UT SAM: 4C DEP: 13.0 DAT: 13 SEPT 88 TEC: LRC
DES:

SAMPLE TYPE - UNDISTURBED
GS: 2.70 (ESTIMATED)
LL: 0 PL: 0 PI: 0

WEIGHT OF SOLIDS - 118.84 I. HEIGHT - 3.500" I. DIAMETER - 1.379"

HEIGHT CHANGES: PRE-CONS. - .01700" DURING CONS. - .00000"

VOLUME CHANGE DURING CONS. - .1 CC TIME OF TEST - 740 MINS.

BACK PRESSURE - 30.00 PSI (2.16 TSF) CHAMBER PRESSURE - 31.00

EFF CONFINING PRESSURE, TSF - .07

	INITIAL	BEFORE SHEAR
WATER CONTENT, %	33.20	33.60
VOID RATIO	.946	.915
SATURATION, %	94.75	99.14
DRY DENSITY, PCF	86.62	88.02

V DEF IN.	AXIAL LOAD LBS	PORE PRESS PSI	STRAIN %	IND POR PRESS TSF	DEVIAT STRESS TSF	EFFECTIVE E1 - TSF -	E3	RATIO E1/ E3	NORML STRES TSF	SHEAR STRES TSF
.000	2.1	30.0	.0	.00	.10	.174	.072	2.422	.12	.05
.001	4.2	30.2	.0	.01	.20	.262	.058	4.554	.16	.10
.005	5.3	30.2	.1	.01	.26	.316	.058	5.479	.19	.13
.008	6.2	30.2	.2	.01	.30	.359	.058	6.235	.21	.15
.011	7.0	30.2	.3	.01	.34	.398	.058	6.906	.23	.17
.015	7.4	30.2	.4	.01	.36	.417	.058	7.236	.24	.18
.018	7.7	30.1	.5	.01	.37	.438	.065	6.763	.25	.19
.022	7.9	30.0	.6	.00	.38	.455	.072	6.315	.26	.19
.026	8.1	30.0	.7	.00	.39	.464	.072	6.443	.27	.20
.029	8.4	30.0	.8	.00	.41	.478	.072	6.640	.28	.20
.033	8.4	30.0	.9	.00	.41	.478	.072	6.634	.27	.20
.036	8.5	29.9	1.0	-.01	.41	.489	.079	6.178	.28	.21
.039	8.2	29.9	1.1	-.01	.40	.474	.079	5.991	.28	.20
.046	8.2	29.8	1.3	-.01	.39	.481	.086	5.566	.28	.20
.065	8.6	29.8	1.9	-.01	.41	.498	.086	5.762	.29	.21
.090	9.4	29.7	2.6	-.02	.45	.540	.094	5.769	.32	.22
.114	9.6	29.5	3.3	-.04	.45	.561	.108	5.191	.33	.23
.140	10.0	29.5	4.0	-.04	.47	.576	.108	5.332	.34	.23
.163	10.4	29.5	4.7	-.04	.48	.591	.108	5.475	.35	.24
.187	10.7	29.4	5.4	-.04	.49	.609	.115	5.285	.36	.25
.215	10.9	29.3	6.2	-.05	.50	.621	.122	5.073	.37	.25
.257	11.0	29.3	7.4	-.05	.50	.619	.122	5.058	.37	.25
.263	11.1	29.3	7.6	-.05	.50	.623	.122	5.087	.37	.25
.291	11.3	29.2	8.4	-.06	.50	.634	.130	4.895	.38	.25
.312	11.3	29.2	9.0	-.06	.50	.631	.130	4.870	.38	.25
.343	11.5	29.1	9.8	-.06	.51	.642	.137	4.695	.39	.25
.364	11.8	29.1	10.5	-.06	.52	.652	.137	4.766	.39	.26
.385	11.8	29.1	11.1	-.06	.51	.648	.137	4.740	.39	.26
.416	11.9	29.0	11.9	-.07	.51	.655	.144	4.547	.40	.26
.438	12.3	29.0	12.6	-.07	.52	.668	.144	4.640	.41	.26
.460	12.4	29.0	13.2	-.07	.52	.669	.144	4.643	.41	.26
.490	12.5	29.0	14.1	-.07	.52	.668	.144	4.636	.41	.26
.511	12.8	28.9	14.7	-.08	.53	.684	.151	4.521	.42	.27

RATE OF STRAIN - .020

Figure B3. (Continued)

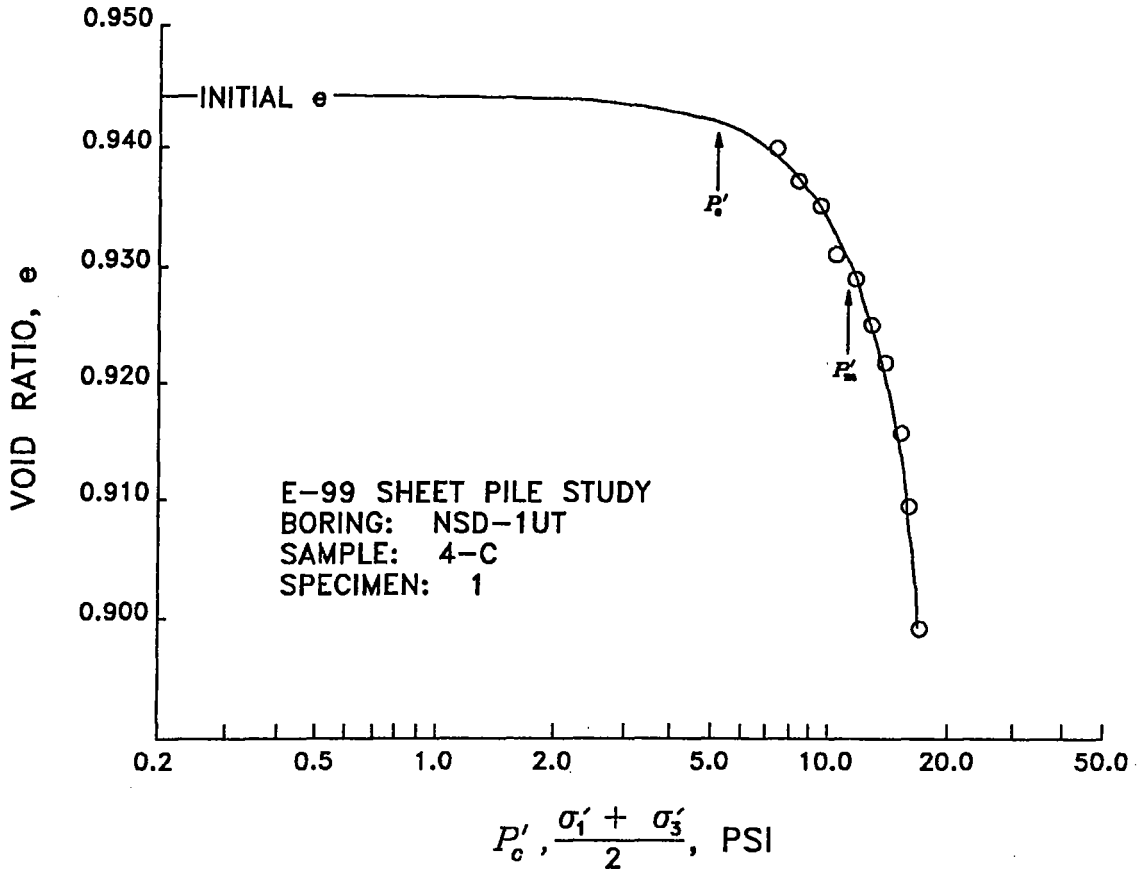

Figure B3. (Concluded)

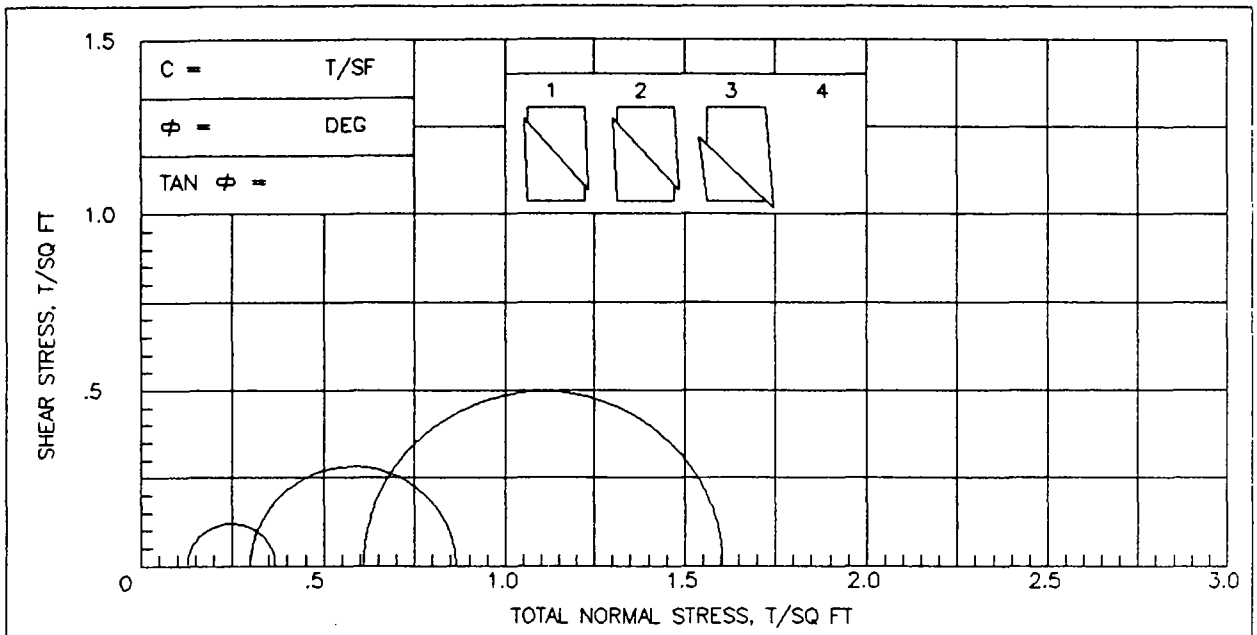

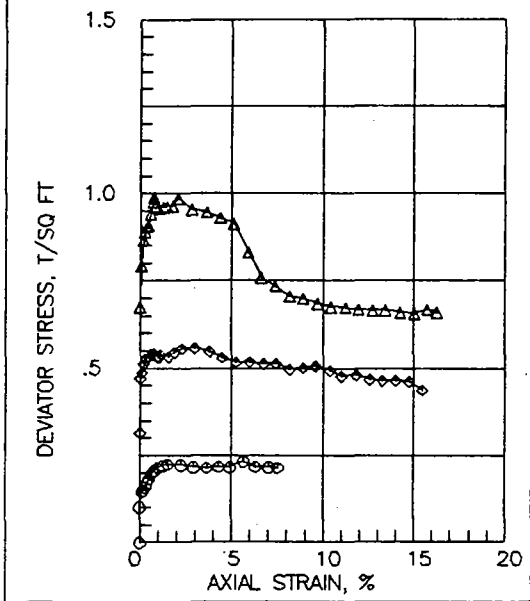

SPECIMEN NO.		⊙ 1	△ 2	◇ 3	4
INITIAL	WATER CONTENT, %	75.0	67.0	68.3	
	DRY DENSITY, PCF	54.0	59.9	59.3	
	SATURATION, %	95.4	99.8	100.0	
	VOID RATIO	2.122	1.812	1.845	
BEFORE SHEAR	WATER CONTENT, %	75.4	60.3	66.1	
	DRY DENSITY, PCF	54.1	64.8	61.4	
	SATURATION, %	96.3	100+	100+	
	VOID RATIO	2.114	1.600	1.746	
	BACK PRESS., TSF	.95	.58	3.46	
MIN PRIN. STRESS, TSF		.13	.61	.30	
MAX. DEV. STRESS, TSF		.23	.99	.56	
TIME TO FAILURE, MIN.		289	39	153	
RATE OF STRAIN, %/MIN		.020	.021	.020	
INITIAL DIAMETER, IN.		1.37	1.37	1.40	
INITIAL HEIGHT, IN.		3.50	3.50	3.50	

CONTROLLED-STRAIN TEST

DESCRIPTION OF SPECIMENS:

LL	PL	PI	GS 2.70 (ESTIMATED)	UNDISTURBED SPECIMEN	$\bar{R}$ TEST

REMARKS:	PROJECT E-99 SHEETPILE TEST	
	BORING NO. NSD-1UT	SAMPLE NO. 6-D
	DEPTH/ELEV 21.6	TECH. LRC
	LABORATORY USAE WES	DATE 21 SEP 88
	$\bar{R}$-TRIAXIAL COMPRESSION TEST REPORT	

Figure B4. Data packet for sample 6-D

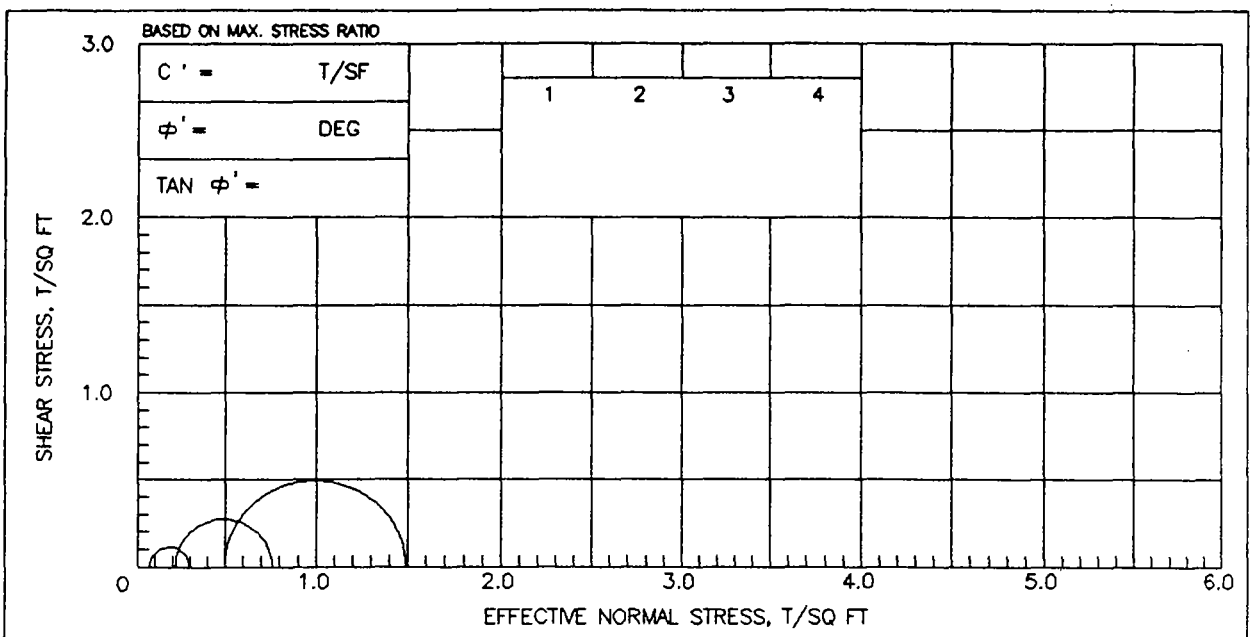

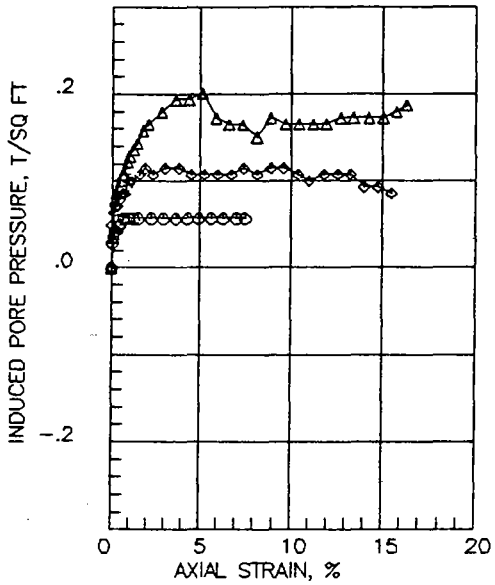

SPECIMEN NO.		○ 1	△ 2	◇ 3	4
INITIAL	WATER CONTENT, %	75.0	67.0	68.3	
	DRY DENSITY, PCF	54.0	59.9	59.3	
	SATURATION, %	95.4	99.8	100.0	
	VOID RATIO	2.122	1.812	1.845	
BEFORE SHEAR	WATER CONTENT, %	75.4	60.3	66.1	
	DRY DENSITY, PCF	54.1	64.8	61.4	
	SATURATION, %	96.3	100+	100+	
	VOID RATIO	2.114	1.600	1.746	
	BACK PRESS., TSF	.95	.58	3.46	
MIN PRIN. STRESS, TSF		.07	.50	.22	
MAX. DEV. STRESS, TSF		.23	.99	.54	
TIME TO FAILURE, MIN.		78	39	32	
RATE OF STRAIN, %/MIN		.020	.021	.020	
INITIAL DIAMETER, IN.		1.37	1.37	1.40	
INITIAL HEIGHT, IN.		3.50	3.50	3.50	

CONTROLLED-STRAIN TEST

DESCRIPTION OF SPECIMENS:

LL	PL	PI	GS 2.70 (ESTIMATED)	UNDISTURBED SPECIMEN	$\bar{R}$ TEST

REMARKS:	PROJECT E-99 SHEETPILE TEST	
	BORING NO. NSD-1UT	SAMPLE NO. 6-D
	DEPTH/ELEV 21.6	TECH. LRC
	LABORATORY USAE WES	DATE 21 SEP 88
	$\bar{R}$-TRIAXIAL COMPRESSION TEST REPORT	

Figure B4. (Continued)

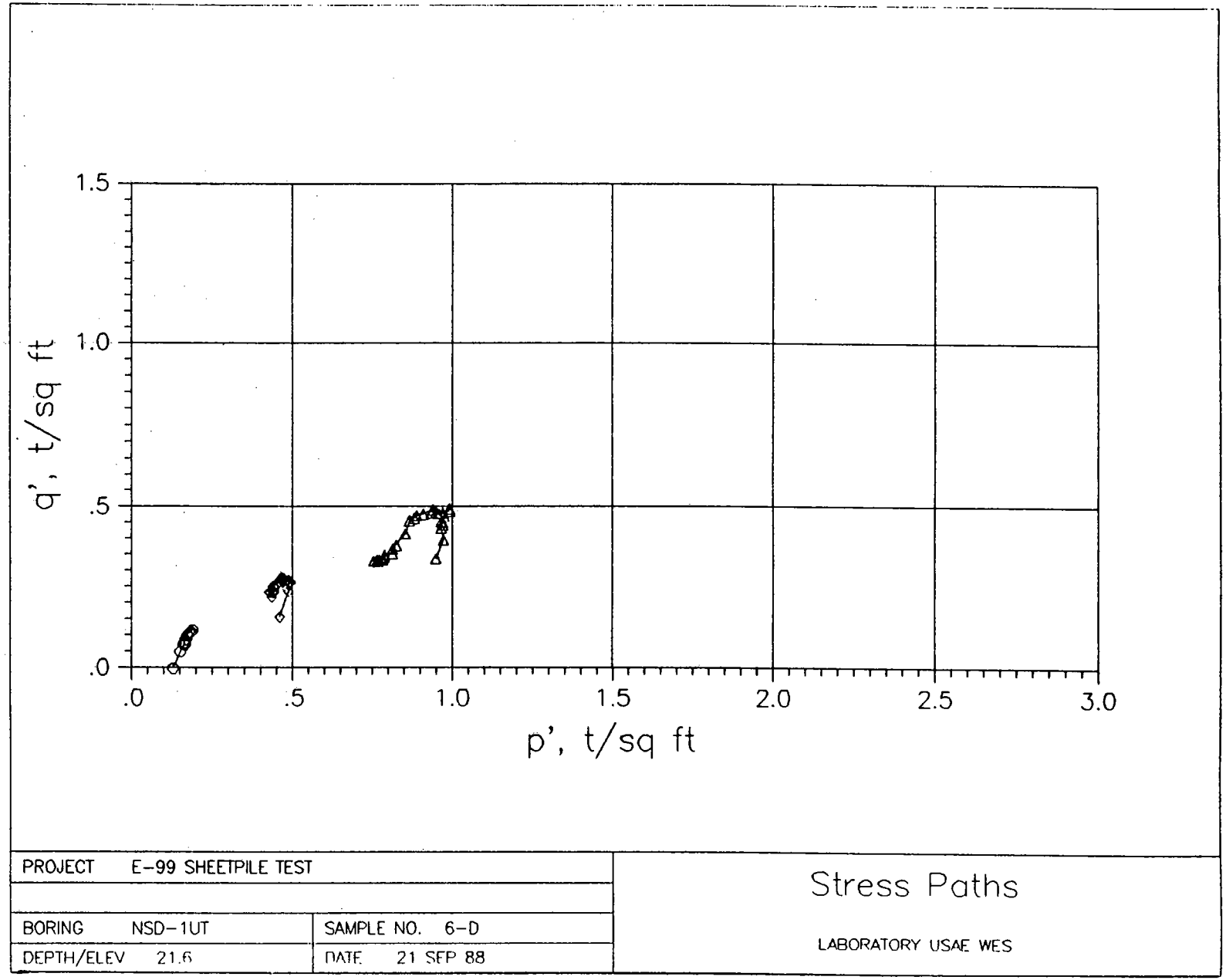

Figure B4. (Continued)

R-BAR TRIAXIAL COMPRESSION TEST REPORT

TLE: E-99 SHEETPILE TEST

BOR: NSD-1UT SAM: 6-D DEP: 21.6 DAT: 21 SEP 88 TEC: LRC
DES:

SAMPLE TYPE - UNDISTURBED
GS: 2.70 (ESTIMATED)
LL: 0 PL: 0 PI: 0

WEIGHT OF SOLIDS - 73.53 I. HEIGHT - 3.500" I. DIAMETER - 1.374"

HEIGHT CHANGES: PRE-CONS. - .00300" DURING CONS. - .00000"

VOLUME CHANGE DURING CONS. - .0 CC TIME OF TEST - 384 MINS.

BACK PRESSURE - 13.20 PSI (.95 TSF) CHAMBER PRESSURE - 15.00

EFF CONFINING PRESSURE, TSF - .13

	INITIAL	BEFORE SHEAR
WATER CONTENT, %	75.00	75.40
VOID RATIO	2.122	2.114
SATURATION, %	95.41	96.28
DRY DENSITY, PCF	53.98	54.12

V DEF IN.	AXIAL LOAD LBS	PORE PRESS PSI	STRAIN %	IND POR PRESS TSF	DEVIAT STRESS TSF	EFFECTIVE E1 - TSF -	E3	RATIO E1/ E3	NORML STRES TSF	SHEAR STRES TSF
.000	.0	13.2	.0	.00	.00	.130	.130	1.000	.13	.00
.001	2.1	13.6	.0	.03	.10	.203	.101	2.013	.15	.05
.004	3.0	13.7	.1	.04	.15	.239	.094	2.557	.17	.07
.008	3.1	13.8	.2	.04	.15	.237	.086	2.741	.16	.08
.011	3.3	13.8	.3	.04	.16	.246	.086	2.852	.17	.08
.015	3.6	13.9	.4	.05	.17	.254	.079	3.202	.17	.09
.019	3.8	13.9	.5	.05	.18	.263	.079	3.321	.17	.09
.022	4.1	14.0	.6	.06	.20	.270	.072	3.752	.17	.10
.025	4.2	14.0	.7	.06	.20	.275	.072	3.817	.17	.10
.029	4.3	14.0	.8	.06	.21	.279	.072	3.881	.18	.10
.035	4.5	14.0	1.0	.06	.22	.289	.072	4.010	.18	.11
.044	4.6	14.0	1.3	.06	.22	.293	.072	4.069	.18	.11
.054	4.7	14.0	1.5	.06	.23	.297	.072	4.126	.18	.11
.079	4.7	14.0	2.3	.06	.22	.295	.072	4.104	.18	.11
.103	4.6	14.0	2.9	.06	.22	.289	.072	4.016	.18	.11
.128	4.6	14.0	3.7	.06	.22	.288	.072	3.994	.18	.11
.151	4.7	14.0	4.3	.06	.22	.291	.072	4.038	.18	.11
.173	4.7	14.0	4.9	.06	.22	.289	.072	4.018	.18	.11
.198	5.1	14.0	5.7	.06	.23	.306	.072	4.250	.19	.12
.221	4.8	14.0	6.3	.06	.22	.291	.072	4.038	.18	.11
.246	4.8	14.0	7.0	.06	.22	.289	.072	4.015	.18	.11
.263	4.8	14.0	7.5	.06	.22	.288	.072	3.999	.18	.11

RATE OF STRAIN - .020

Figure B4: (Continued)

R-BAR TRIAXIAL COMPRESSION TEST REPORT

TLE: E-99 SHEETPILE TEST

BOR: NSD-1UT SAM: 6-D DEP: 21.6 DAT: 21 SEP 88 TEC: LRC
DES:

SAMPLE TYPE = UNDISTURBED
GS: 2.70 (ESTIMATED)
LL: 0 PL: 0 PI: 0

WEIGHT OF SOLIDS = 81.65 I. HEIGHT = 3.500" I. DIAMETER = 1.374"

HEIGHT CHANGES: PRE-CONS. = .00000" DURING CONS. = .20700"

VOLUME CHANGE DURING CONS. = 6.4 CC TIME OF TEST = 768 MINS.

BACK PRESSURE = 8.00 PSI (.58 TSF) CHAMBER PRESSURE = 16.50

EFF CONFINING PRESSURE, TSF = .61

	INITIAL	BEFORE SHEAR
WATER CONTENT, %	67.00	60.30
VOID RATIO	1.812	1.600
SATURATION, %	99.84	101.73
DRY DENSITY, PCF	59.94	64.82

V DEF IN.	AXIAL LOAD LBS	PORE PRESS PSI	STRAIN %	IND POR PRESS TSF	DEVIAT STRESS TSF	EFFECTIVE E1 - TSF -	E3	RATIO E1/ E3	NORML STRES TSF	SHEAR STRES TSF
.000	13.7	8.0	.0	.00	.68	1.289	.612	2.106	.95	.34
.003	16.1	8.5	.1	.04	.79	1.371	.576	2.380	.97	.40
.006	17.6	9.1	.2	.08	.87	1.401	.533	2.629	.97	.43
.009	18.1	9.2	.3	.09	.89	1.417	.526	2.697	.97	.45
.013	18.4	9.3	.4	.09	.91	1.424	.518	2.747	.97	.45
.016	18.5	9.4	.5	.10	.91	1.421	.511	2.779	.97	.45
.020	19.2	9.5	.6	.11	.94	1.447	.504	2.871	.98	.47
.023	19.9	9.5	.7	.11	.98	1.480	.504	2.937	.99	.49
.026	20.2	9.6	.8	.12	.99	1.487	.497	2.993	.99	.50
.030	19.7	9.7	.9	.12	.96	1.454	.490	2.970	.97	.48
.034	19.6	9.8	1.0	.13	.96	1.441	.482	2.987	.96	.48
.041	19.7	9.9	1.2	.14	.96	1.436	.475	3.023	.96	.48
.048	19.8	10.0	1.5	.14	.96	1.432	.468	3.060	.95	.48
.059	19.9	10.2	1.8	.16	.97	1.419	.454	3.129	.94	.48
.069	20.4	10.3	2.1	.17	.99	1.433	.446	3.210	.94	.49
.093	19.9	10.5	2.8	.18	.96	1.387	.432	3.212	.91	.48
.120	19.9	10.7	3.6	.19	.95	1.365	.418	3.268	.89	.47
.144	19.7	10.7	4.4	.19	.93	1.348	.418	3.229	.88	.47
.169	19.5	10.8	5.1	.20	.91	1.324	.410	3.227	.87	.46
.194	17.9	10.4	5.9	.17	.83	1.271	.439	2.895	.86	.42
.218	16.5	10.3	6.6	.17	.76	1.208	.446	2.705	.83	.38
.243	16.1	10.3	7.4	.17	.74	1.183	.446	2.650	.81	.37
.268	15.6	10.1	8.1	.15	.71	1.169	.461	2.536	.81	.35
.294	15.6	10.4	8.9	.17	.70	1.141	.439	2.598	.79	.35
.319	15.4	10.3	9.7	.17	.69	1.133	.446	2.539	.79	.34
.345	15.3	10.3	10.5	.17	.68	1.123	.446	2.516	.78	.34
.370	15.4	10.3	11.2	.17	.68	1.122	.446	2.513	.78	.34
.394	15.4	10.3	12.0	.17	.67	1.116	.446	2.500	.78	.33
.419	15.5	10.4	12.7	.17	.67	1.107	.439	2.522	.77	.33
.443	15.6	10.4	13.5	.17	.67	1.106	.439	2.519	.77	.33
.470	15.6	10.4	14.3	.17	.66	1.100	.439	2.504	.77	.33
.495	15.7	10.4	15.0	.17	.66	1.098	.439	2.501	.77	.33
.519	16.1	10.5	15.8	.18	.67	1.102	.432	2.551	.77	.33
.536	16.0	10.6	16.3	.19	.66	1.087	.425	2.558	.76	.33

RATE OF STRAIN = .021

Figure B4. (Continued)

R-BAR TRIAXIAL COMPRESSION TEST REPORT

TLE: E-99 SHEETPILE TEST

BOR: NSD-1UT SAM: 6-D DEP: 21.6 DAT: 21 SEP 88 TEC: LRC
DES:

SAMPLE TYPE - UNDISTURBED
GS: 2.70 (ESTIMATED)
LL: 0 PL: 0 PI: 0

WEIGHT OF SOLIDS - 84.03 I. HEIGHT - 3.500" I. DIAMETER - 1.402"

HEIGHT CHANGES: PRE-CONS. - .00700" DURING CONS. - .07300"

VOLUME CHANGE DURING CONS. - 2.5 CC TIME OF TEST - 768 MINS.

BACK PRESSURE - 48.00 PSI (3.46 TSF) CHAMBER PRESSURE - 52.20

EFF CONFINING PRESSURE, TSF - .30

	INITIAL	BEFORE SHEAR
WATER CONTENT, %	68.30	66.10
VOID RATIO	1.845	1.746
SATURATION, %	99.96	102.21
DRY DENSITY, PCF	59.25	61.38

V DEF IN.	AXIAL LOAD LBS	PORE PRESS PSI	STRAIN %	IND POR PRESS TSF	DEVIAT STRESS TSF	EFFECTIVE E1 - TSF -	E3	RATIO E1/ E3	NORML STRES TSF	SHEAR STRES TSF
.000	6.7	48.0	.0	.00	.32	.619	.302	2.046	.46	.16
.001	10.0	48.7	.0	.05	.47	.724	.252	2.873	.49	.24
.004	10.4	48.9	.1	.06	.49	.728	.238	3.064	.48	.25
.008	10.9	49.0	.2	.07	.51	.744	.230	3.228	.49	.26
.012	11.2	49.0	.4	.07	.53	.757	.230	3.287	.49	.26
.015	11.4	49.1	.4	.08	.54	.759	.223	3.401	.49	.27
.019	11.5	49.2	.6	.09	.54	.756	.216	3.500	.49	.27
.022	11.6	49.2	.6	.09	.54	.760	.216	3.519	.49	.27
.026	11.5	49.2	.8	.09	.54	.755	.216	3.494	.49	.27
.029	11.6	49.3	.8	.09	.54	.752	.209	3.601	.48	.27
.033	11.4	49.4	1.0	.10	.53	.735	.202	3.644	.47	.27
.036	11.4	49.4	1.1	.10	.53	.734	.202	3.641	.47	.27
.040	11.6	49.4	1.2	.10	.54	.743	.202	3.685	.47	.27
.053	11.5	49.5	1.5	.11	.53	.729	.194	3.749	.46	.27
.064	11.8	49.6	1.9	.12	.55	.734	.187	3.920	.46	.27
.080	12.1	49.5	2.3	.11	.56	.752	.194	3.870	.47	.28
.103	12.2	49.6	3.0	.12	.56	.746	.187	3.984	.47	.28
.130	12.1	49.6	3.8	.12	.55	.737	.187	3.935	.46	.27
.154	11.8	49.5	4.5	.11	.53	.726	.194	3.737	.46	.27
.179	11.6	49.5	5.2	.11	.52	.713	.194	3.670	.45	.26
.204	11.7	49.5	6.0	.11	.52	.714	.194	3.672	.45	.26
.230	11.7	49.5	6.7	.11	.52	.710	.194	3.650	.45	.26
.254	11.8	49.6	7.4	.12	.52	.703	.187	3.755	.45	.26
.279	11.5	49.5	8.2	.11	.50	.693	.194	3.565	.44	.25
.304	11.7	49.6	8.9	.12	.50	.690	.187	3.688	.44	.25
.328	11.9	49.6	9.6	.12	.51	.695	.187	3.713	.44	.25
.356	11.7	49.5	10.4	.11	.49	.689	.194	3.546	.44	.25
.377	11.4	49.4	11.0	.10	.48	.680	.202	3.375	.44	.24
.405	11.6	49.5	11.8	.11	.48	.677	.194	3.483	.44	.24
.429	11.4	49.5	12.5	.11	.47	.665	.194	3.421	.43	.24
.454	11.4	49.5	13.3	.11	.47	.661	.194	3.401	.43	.23
.479	11.5	49.3	14.0	.09	.47	.676	.209	3.236	.44	.23
.504	11.5	49.3	14.7	.09	.46	.672	.209	3.217	.44	.23
.529	11.0	49.2	15.5	.09	.44	.655	.216	3.032	.44	.22

RATE OF STRAIN - .020

Figure B4: (Continued)

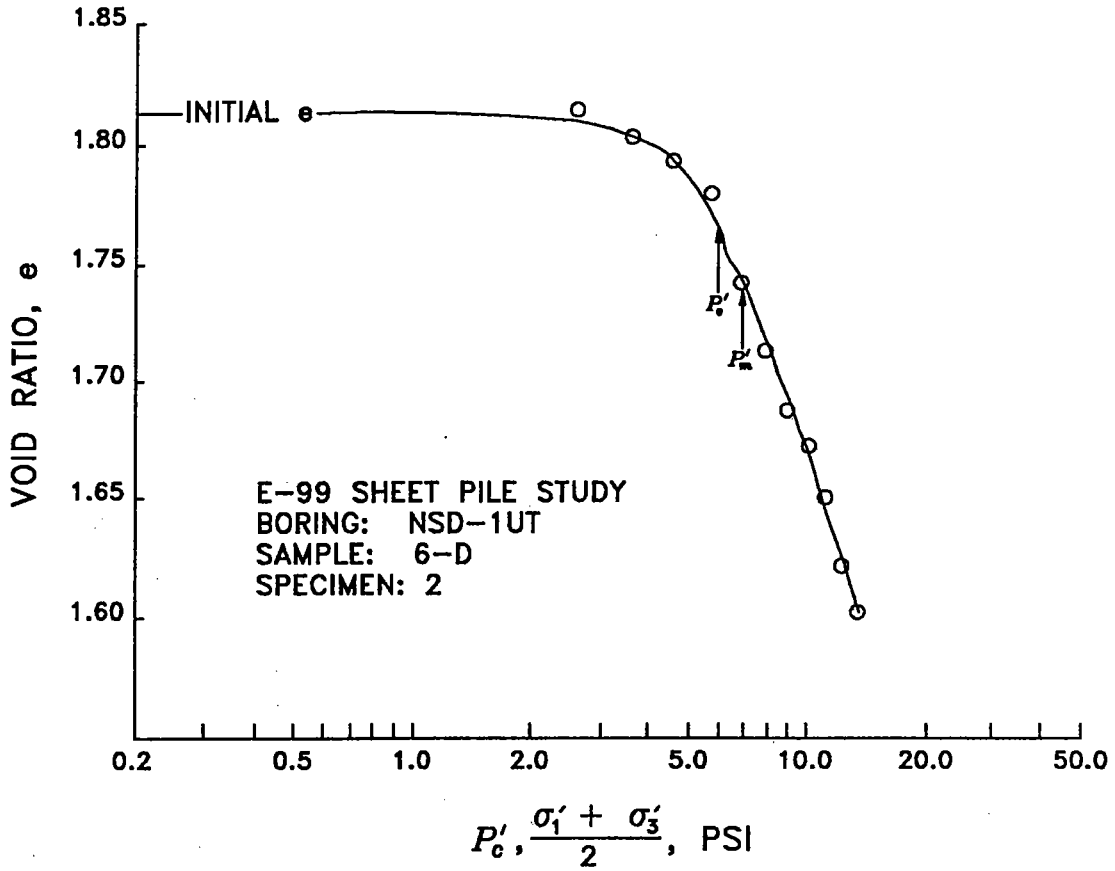

Figure B4. (Concluded)

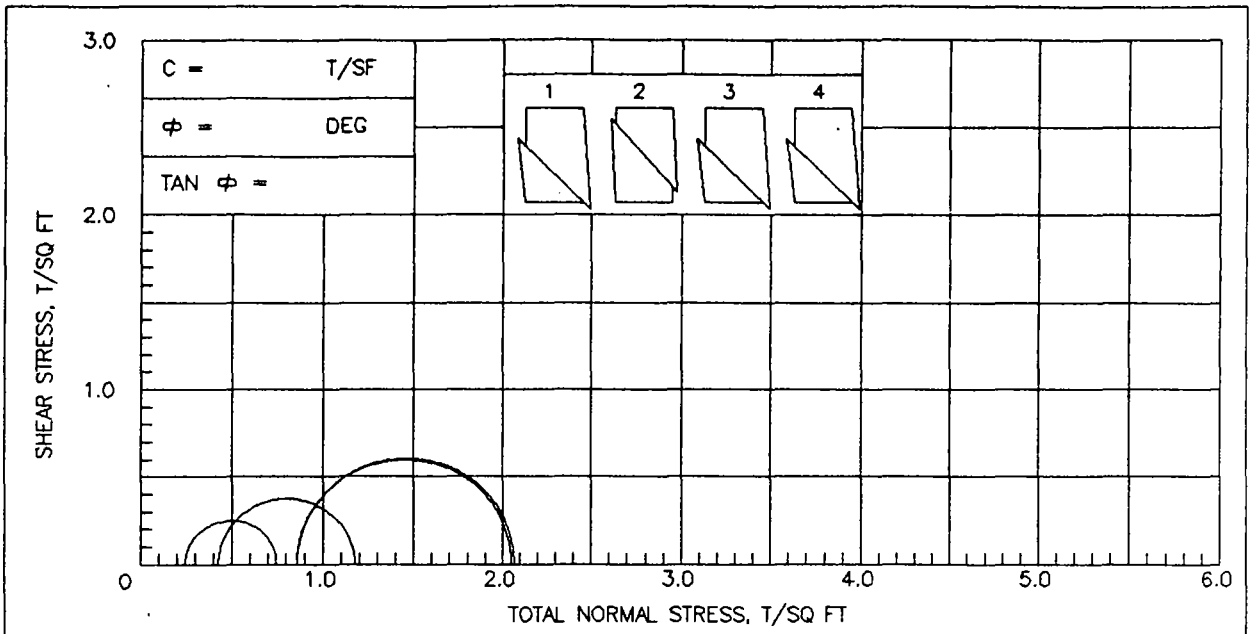

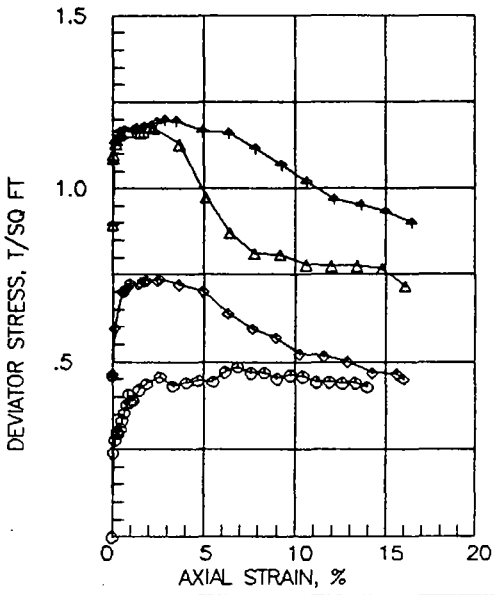

SPECIMEN NO.		◇ 1	△ 2	◇ 3	+ 4
INITIAL	WATER CONTENT, %	58.8	59.5	77.4	74.8
	DRY DENSITY, PCF	65.2	64.8	52.9	54.9
	SATURATION, %	100+	100+	95.6	97.6
	VOID RATIO	1.584	1.603	2.186	2.068
BEFORE SHEAR	WATER CONTENT, %	59.0	52.5	76.3	64.4
	DRY DENSITY, PCF	65.7	70.7	55.1	61.8
	SATURATION, %	100+	100+	100+	100+
	VOID RATIO	1.564	1.385	2.058	1.729
	BACK PRESS., TSF	.61	.94	2.59	1.73
MIN PRIN. STRESS, TSF		.25	.86	.43	.86
MAX. DEV. STRESS, TSF		.49	1.18	.74	1.20
TIME TO FAILURE, MIN.		347	110	131	147
RATE OF STRAIN, %/MIN		.020	.021	.020	.022
INITIAL DIAMETER, IN.		1.40	1.40	1.41	1.40
INITIAL HEIGHT, IN.		3.50	3.50	3.50	3.50

CONTROLLED-STRAIN TEST

DESCRIPTION OF SPECIMENS:

LL	PL	PI	GS 2.70 (ESTIMATED)	UNDISTURBED SPECIMEN	$\bar{R}$ TEST

REMARKS:	PROJECT E-99 SHEETPILE TEST	
	BORING NO. NSD-1UT	SAMPLE NO. 9D
	DEPTH/ELEV 33.9	TECH. LRC
	LABORATORY USAE WES	DATE 06 OCT 88
	$\bar{\bar{R}}$-TRIAXIAL COMPRESSION TEST REPORT	

Figure B5. Data packet for sample 9-D

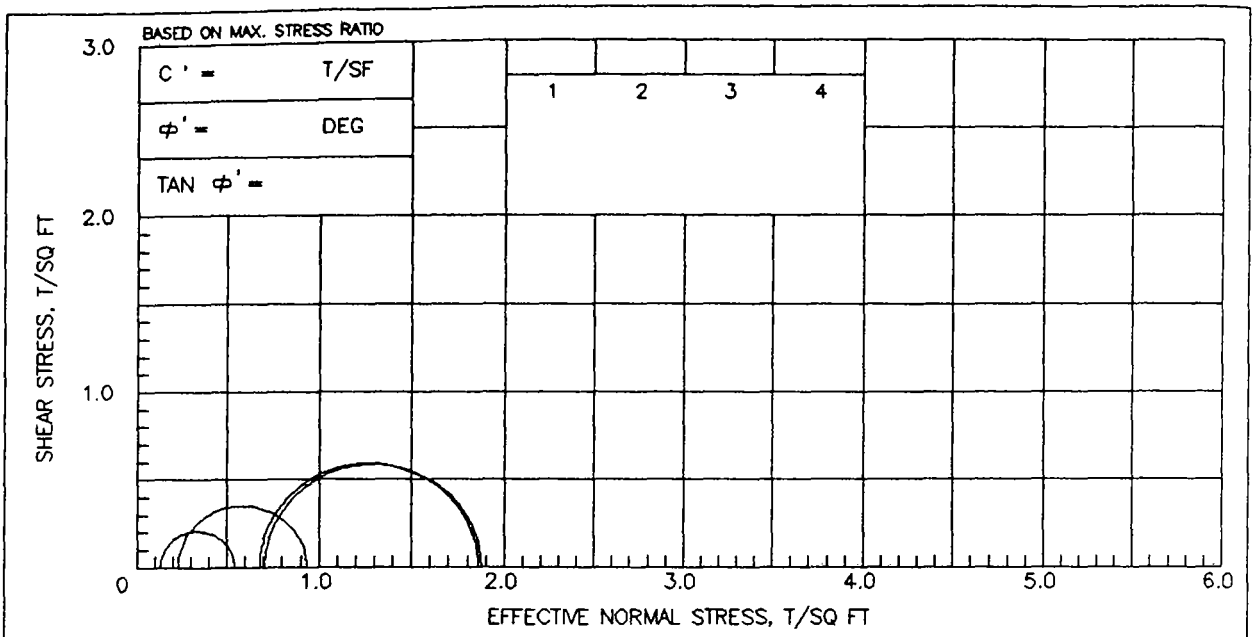

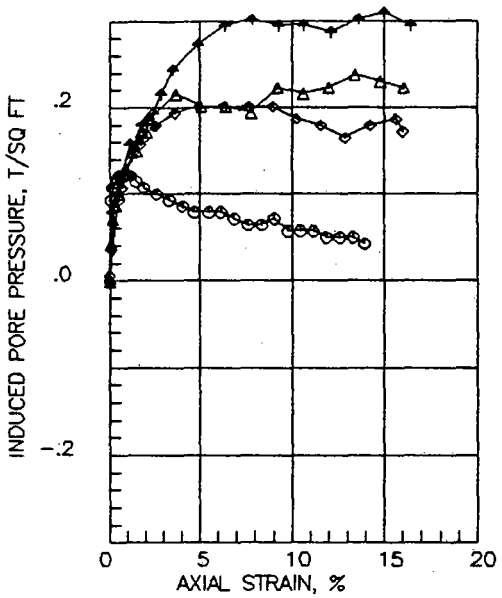

SPECIMEN NO.		◇ 1	△ 2	○ 3	+ 4
INITIAL	WATER CONTENT, %	58.8	59.5	77.4	74.8
	DRY DENSITY, PCF	65.2	64.8	52.9	54.9
	SATURATION, %	100+	100+	95.6	97.6
	VOID RATIO	1.584	1.603	2.186	2.068
BEFORE SHEAR	WATER CONTENT, %	59.0	52.5	76.3	64.4
	DRY DENSITY, PCF	65.7	70.7	55.1	61.8
	SATURATION, %	100+	100+	100+	100+
	VOID RATIO	1.564	1.385	2.058	1.729
	BACK PRESS., TSF	.61	.94	2.59	1.73
MIN PRIN. STRESS, TSF		.13	.68	.23	.71
MAX. DEV. STRESS, TSF		.41	1.18	.70	1.17
TIME TO FAILURE, MIN.		43	110	250	58
RATE OF STRAIN, %/MIN		.020	.021	.020	.022
INITIAL DIAMETER, IN.		1.40	1.40	1.41	1.40
INITIAL HEIGHT, IN.		3.50	3.50	3.50	3.50

CONTROLLED-STRAIN TEST

DESCRIPTION OF SPECIMENS:

LL	PL	PI	GS 2.70 (ESTIMATED)	UNDISTURBED SPECIMEN	$\bar{R}$ TEST

REMARKS:	PROJECT E-99 SHEETPILE TEST	
	BORING NO. NSD-1UT	SAMPLE NO. 9D
	DEPTH/ELEV 33.9	TECH. LRC
	LABORATORY USAE WES	DATE 06 OCT 88
	$\bar{R}$-TRIAXIAL COMPRESSION TEST REPORT	

Figure B5. (Continued)

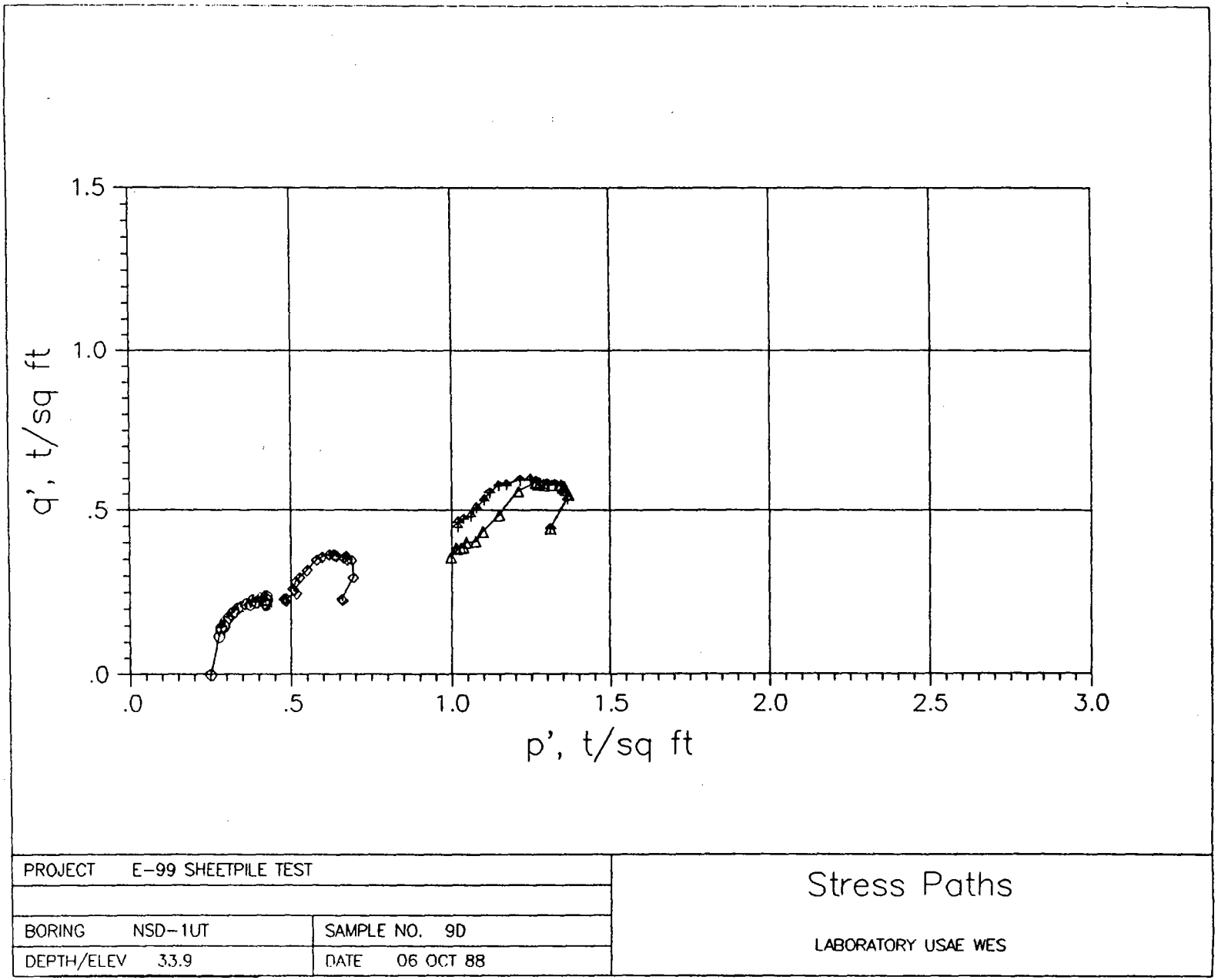

Figure B5. (Continued)

R-BAR TRIAXIAL COMPRESSION TEST REPORT

TLE: E-99 SHEETPILE TEST

BOR: NSD-1UT SAM: 9D DEP: 33.9 DAT: 06 OCT 88 TEC: LRC
DES:

SAMPLE TYPE - UNDISTURBED
GS: 2.70 (ESTIMATED)
LL: 0 PL: 0 PI: 0

WEIGHT OF SOLIDS - 91.97 I. HEIGHT - 3.500" I. DIAMETER - 1.398"

HEIGHT CHANGES: PRE-CONS. - .00900" DURING CONS. - .00000"

VOLUME CHANGE DURING CONS. - .0 CC TIME OF TEST - 703 MINS.

BACK PRESSURE - 8.50 PSI (.61 TSF) CHAMBER PRESSURE - 12.00

EFF CONFINING PRESSURE, TSF - .25

	INITIAL	BEFORE SHEAR
WATER CONTENT, %	58.80	59.00
VOID RATIO	1.584	1.564
SATURATION, %	100.20	101.82
DRY DENSITY, PCF	65.22	65.73

V DEF IN.	AXIAL LOAD LBS	PORE PRESS PSI	STRAIN %	IND POR PRESS TSF	DEVIAT STRESS TSF	EFFECTIVE E1 - TSF -	E3	RATIO E1/ E3	NORML STRES TSF	SHEAR STRES TSF
.000	.0	8.5	.0	.00	.00	.252	.252	1.000	.25	.00
.002	5.1	9.8	.1	.09	.24	.399	.158	2.517	.28	.12
.005	5.9	10.0	.1	.11	.28	.422	.144	2.929	.28	.14
.009	6.4	10.0	.3	.11	.30	.445	.144	3.090	.29	.15
.012	6.3	10.1	.3	.12	.30	.433	.137	3.164	.28	.15
.016	6.6	10.1	.5	.12	.31	.447	.137	3.264	.29	.15
.019	7.1	10.2	.5	.12	.33	.462	.130	3.569	.30	.17
.023	7.6	10.2	.7	.12	.36	.486	.130	3.747	.31	.18
.026	8.1	10.2	.7	.12	.38	.509	.130	3.925	.32	.19
.030	8.8	10.2	.9	.12	.41	.541	.130	4.174	.34	.21
.034	8.3	10.2	1.0	.12	.39	.517	.130	3.990	.32	.19
.037	8.4	10.2	1.1	.12	.39	.521	.130	4.024	.33	.20
.040	8.4	10.2	1.1	.12	.39	.521	.130	4.021	.33	.20
.051	9.1	10.1	1.5	.12	.42	.560	.137	4.091	.35	.21
.065	9.5	10.0	1.9	.11	.44	.584	.144	4.053	.36	.22
.091	10.0	9.9	2.6	.10	.46	.610	.151	4.037	.38	.23
.115	9.5	9.8	3.3	.09	.43	.592	.158	3.735	.37	.22
.141	9.8	9.7	4.0	.09	.44	.609	.166	3.677	.39	.22
.164	10.0	9.6	4.7	.08	.45	.622	.173	3.600	.40	.22
.192	10.0	9.6	5.5	.08	.45	.618	.173	3.578	.40	.22
.215	10.7	9.6	6.2	.08	.47	.646	.173	3.740	.41	.24
.240	11.1	9.5	6.9	.07	.49	.667	.180	3.708	.42	.24
.265	10.8	9.4	7.6	.06	.47	.658	.187	3.514	.42	.24
.291	10.9	9.4	8.3	.06	.47	.658	.187	3.516	.42	.24
.316	10.6	9.5	9.1	.07	.45	.634	.180	3.525	.41	.23
.341	10.9	9.3	9.8	.06	.46	.658	.194	3.385	.43	.23
.365	10.9	9.3	10.5	.06	.46	.655	.194	3.367	.42	.23
.390	10.6	9.3	11.2	.06	.44	.638	.194	3.284	.42	.22
.414	10.7	9.2	11.9	.05	.44	.646	.202	3.206	.42	.22
.439	10.7	9.2	12.6	.05	.44	.643	.202	3.188	.42	.22
.464	10.8	9.2	13.3	.05	.44	.643	.202	3.190	.42	.22
.487	10.6	9.1	14.0	.04	.43	.639	.209	3.060	.42	.22

RATE OF STRAIN - .020

Figure B5. (Continued)

R-BAR TRIAXIAL COMPRESSION TEST REPORT

TLE: E-99 SHEETPILE TEST

BOR: NSD-1UT SAM: 9D DEP: 33.9 DAT: 06 OCT 88 TEC: LRC
DES:

SAMPLE TYPE - UNDISTURBED
GS: 2.70 (ESTIMATED)
LL: 0 PL: 0 PI: 0

WEIGHT OF SOLIDS - 91.84 I. HEIGHT - 3.500" I. DIAMETER - 1.402"

HEIGHT CHANGES: PRE-CONS. - .00000" DURING CONS. - .25500"

VOLUME CHANGE DURING CONS. - 7.4 CC TIME OF TEST - 765 MINS.

BACK PRESSURE - 13.00 PSI (.94 TSF) CHAMBER PRESSURE - 25.00

EFF CONFINING PRESSURE, TSF - .86

	INITIAL	BEFORE SHEAR
WATER CONTENT, %	59.50	52.50
VOID RATIO	1.603	1.385
SATURATION, %	100.23	102.34
DRY DENSITY, PCF	64.76	70.67

V DEF IN.	AXIAL LOAD LBS	PORE PRESS PSI	STRAIN %	IND POR PRESS TSF	DEVIAT STRESS TSF	EFFECTIVE E1 - TSF -	E3	RATIO E1/ E3	NORML STRES TSF	SHEAR STRES TSF
.000	19.0	13.0	.0	.00	.90	1.760	.864	2.038	1.31	.45
.003	23.3	13.6	.1	.04	1.10	1.919	.821	2.338	1.37	.55
.006	24.0	14.0	.2	.07	1.13	1.922	.792	2.427	1.36	.57
.009	24.3	14.2	.3	.09	1.14	1.921	.778	2.471	1.35	.57
.013	24.6	14.2	.4	.09	1.16	1.934	.778	2.487	1.36	.58
.016	24.7	14.4	.5	.10	1.16	1.923	.763	2.520	1.34	.58
.019	24.8	14.4	.6	.10	1.16	1.926	.763	2.524	1.34	.58
.029	24.9	14.8	.9	.13	1.16	1.899	.734	2.586	1.32	.58
.050	25.0	15.1	1.5	.15	1.16	1.874	.713	2.630	1.29	.58
.056	25.1	15.4	1.7	.17	1.16	1.855	.691	2.684	1.27	.58
.060	25.4	15.4	1.8	.17	1.18	1.867	.691	2.702	1.28	.59
.067	25.5	15.4	2.1	.17	1.18	1.870	.691	2.705	1.28	.59
.070	25.6	15.6	2.2	.19	1.18	1.859	.677	2.746	1.27	.59
.074	25.5	15.6	2.3	.19	1.18	1.853	.677	2.737	1.26	.59
.120	24.8	16.0	3.7	.22	1.13	1.775	.648	2.739	1.21	.56
.165	21.8	15.8	5.1	.20	.98	1.639	.662	2.474	1.15	.49
.208	19.8	15.8	6.4	.20	.87	1.537	.662	2.320	1.10	.44
.253	18.7	15.7	7.8	.19	.81	1.483	.670	2.215	1.08	.41
.299	18.9	16.1	9.2	.22	.81	1.450	.641	2.264	1.05	.40
.345	18.5	16.0	10.6	.22	.78	1.428	.648	2.204	1.04	.39
.390	18.7	16.1	12.0	.22	.78	1.417	.641	2.212	1.03	.39
.435	19.0	16.3	13.4	.24	.78	1.403	.626	2.239	1.01	.39
.480	19.1	16.2	14.8	.23	.77	1.401	.634	2.212	1.02	.38
.521	18.1	16.1	16.1	.22	.72	1.358	.641	2.119	1.00	.36

RATE OF STRAIN - .021

Figure B5. (Continued)

R-BAR TRIAXIAL COMPRESSION TEST REPORT

TLE: E-99 SHEETPILE TEST

BOR: NSD-1UT SAM: 9D DEP: 33.9 DAT: 06 OCT 88 TEC: LRC
DES:

SAMPLE TYPE - UNDISTURBED
GS: 2.70 (ESTIMATED)
LL: 0 PL: 0 PI: 0

WEIGHT OF SOLIDS - 75.47 I. HEIGHT - 3.500" I. DIAMETER - 1.406"

HEIGHT CHANGES: PRE-CONS. - .00000" DURING CONS. - .11100"

VOLUME CHANGE DURING CONS. - 3.6 CC TIME OF TEST - 780 MINS.

BACK PRESSURE - 36.00 PSI (2.59 TSF) CHAMBER PRESSURE - 42.00

EFF CONFINING PRESSURE, TSF - .43

	INITIAL	BEFORE SHEAR
WATER CONTENT, %	77.40	76.30
VOID RATIO	2.186	2.058
SATURATION, %	95.62	100.13
DRY DENSITY, PCF	52.91	55.13

V DEF IN.	AXIAL LOAD LBS	PORE PRESS PSI	STRAIN %	IND POR PRESS TSF	DEVIAT STRESS TSF	EFFECTIVE E1 - TSF -	E3	RATIO E1/ E3	NORML STRES TSF	SHEAR STRES TSF
.000	9.8	36.0	.0	.00	.46	.890	.432	2.061	.66	.23
.001	10.0	36.1	.0	.01	.47	.892	.425	2.101	.66	.23
.004	12.8	36.5	.1	.04	.60	.994	.396	2.510	.70	.30
.018	15.1	37.3	.5	.09	.70	1.041	.338	3.076	.69	.35
.022	15.1	37.5	.6	.11	.70	1.026	.324	3.166	.67	.35
.025	15.2	37.5	.7	.11	.71	1.030	.324	3.179	.68	.35
.028	15.4	37.7	.8	.12	.71	1.024	.310	3.308	.67	.36
.032	15.7	37.7	.9	.12	.73	1.037	.310	3.350	.67	.36
.048	15.7	38.1	1.4	.15	.72	1.005	.281	3.579	.64	.36
.051	15.8	38.2	1.5	.16	.73	1.002	.274	3.661	.64	.36
.057	15.9	38.2	1.7	.16	.73	1.005	.274	3.673	.64	.37
.064	16.0	38.3	1.9	.17	.73	1.001	.266	3.757	.63	.37
.082	16.1	38.5	2.4	.18	.73	.987	.252	3.917	.62	.37
.088	16.2	38.5	2.6	.18	.74	.990	.252	3.929	.62	.37
.123	16.0	38.7	3.6	.19	.72	.959	.238	4.036	.60	.36
.168	15.8	38.8	5.0	.20	.70	.933	.230	4.049	.58	.35
.213	14.6	38.8	6.3	.20	.64	.870	.230	3.778	.55	.32
.259	13.8	38.8	7.6	.20	.60	.827	.230	3.588	.53	.30
.304	13.4	38.8	9.0	.20	.57	.801	.230	3.477	.52	.29
.347	12.5	38.6	10.2	.19	.52	.770	.245	3.144	.51	.26
.392	12.5	38.5	11.6	.18	.52	.769	.252	3.052	.51	.26
.437	12.3	38.3	12.9	.17	.50	.768	.266	2.882	.52	.25
.483	11.7	38.5	14.3	.18	.47	.721	.252	2.863	.49	.23
.529	11.8	38.6	15.6	.19	.47	.711	.245	2.903	.48	.23
.541	11.5	38.4	16.0	.17	.45	.711	.259	2.744	.49	.23

RATE OF STRAIN - .020

Figure B5. (Continued)

R-BAR TRIAXIAL COMPRESSION TEST REPORT

TLE: E-99 SHEETPILE TEST

BOR: NSD-1UT SAM: 9D DEP: 33.9 DAT: 06 OCT 88 TEC: LRC
DES:

SAMPLE TYPE - UNDISTURBED
GS: 2.70 (ESTIMATED)
LL: 0 PL: 0 PI: 0

WEIGHT OF SOLIDS - 77.91 I. HEIGHT - 3.500" I. DIAMETER - 1.402"

HEIGHT CHANGES: PRE-CONS. - .00000" DURING CONS. - .36600"

VOLUME CHANGE DURING CONS. - 9.8 CC TIME OF TEST - 747 MINS.

BACK PRESSURE - 24.00 PSI (1.73 TSF) CHAMBER PRESSURE - 36.00

EFF CONFINING PRESSURE, TSF - .86

	INITIAL	BEFORE SHEAR
WATER CONTENT, %	74.80	64.40
VOID RATIO	2.068	1.729
SATURATION, %	97.65	100.56
DRY DENSITY, PCF	54.94	61.76

V DEF IN.	AXIAL LOAD LBS	PORE PRESS PSI	STRAIN %	IND POR PRESS TSF	DEVIAT STRESS TSF	EFFECTIVE E1 - TSF -	E3	RATIO E1/ E3	NORML STRES TSF	SHEAR STRES TSF
.000	19.1	24.0	.0	.00	.90	1.761	.864	2.038	1.31	.45
.002	22.9	24.5	.1	.04	1.07	1.902	.828	2.298	1.37	.54
.005	24.2	25.1	.2	.08	1.13	1.919	.785	2.445	1.35	.57
.008	24.7	25.3	.3	.09	1.16	1.927	.770	2.501	1.35	.58
.012	24.9	25.4	.4	.10	1.16	1.928	.763	2.526	1.35	.58
.019	25.0	25.6	.6	.12	1.17	1.915	.749	2.558	1.33	.58
.022	25.1	25.7	.7	.12	1.17	1.912	.742	2.578	1.33	.59
.036	25.2	26.2	1.1	.16	1.17	1.875	.706	2.658	1.29	.58
.039	25.3	26.0	1.2	.14	1.17	1.893	.720	2.629	1.31	.59
.042	25.4	26.1	1.3	.15	1.18	1.889	.713	2.651	1.30	.59
.056	25.6	26.5	1.8	.18	1.18	1.864	.684	2.726	1.27	.59
.066	25.7	26.6	2.1	.19	1.18	1.858	.677	2.745	1.27	.59
.077	26.0	26.7	2.5	.19	1.19	1.860	.670	2.778	1.26	.60
.091	26.3	27.0	2.9	.22	1.20	1.847	.648	2.850	1.25	.60
.110	26.4	27.4	3.5	.24	1.20	1.815	.619	2.932	1.22	.60
.154	26.1	27.8	4.9	.27	1.17	1.755	.590	2.974	1.17	.58
.199	26.4	28.1	6.3	.30	1.16	1.729	.569	3.041	1.15	.58
.245	25.8	28.2	7.8	.30	1.12	1.678	.562	2.988	1.12	.56
.291	25.1	28.1	9.3	.30	1.07	1.638	.569	2.880	1.10	.53
.333	24.3	28.1	10.6	.30	1.02	1.588	.569	2.793	1.08	.51
.380	23.5	28.0	12.1	.29	.97	1.545	.576	2.683	1.06	.48
.426	23.5	28.2	13.6	.30	.95	1.515	.562	2.698	1.04	.48
.469	23.4	28.3	15.0	.31	.93	1.489	.554	2.685	1.02	.47
.515	23.0	28.1	16.4	.30	.90	1.471	.569	2.587	1.02	.45

RATE OF STRAIN - .022

Figure B5. (Continued)

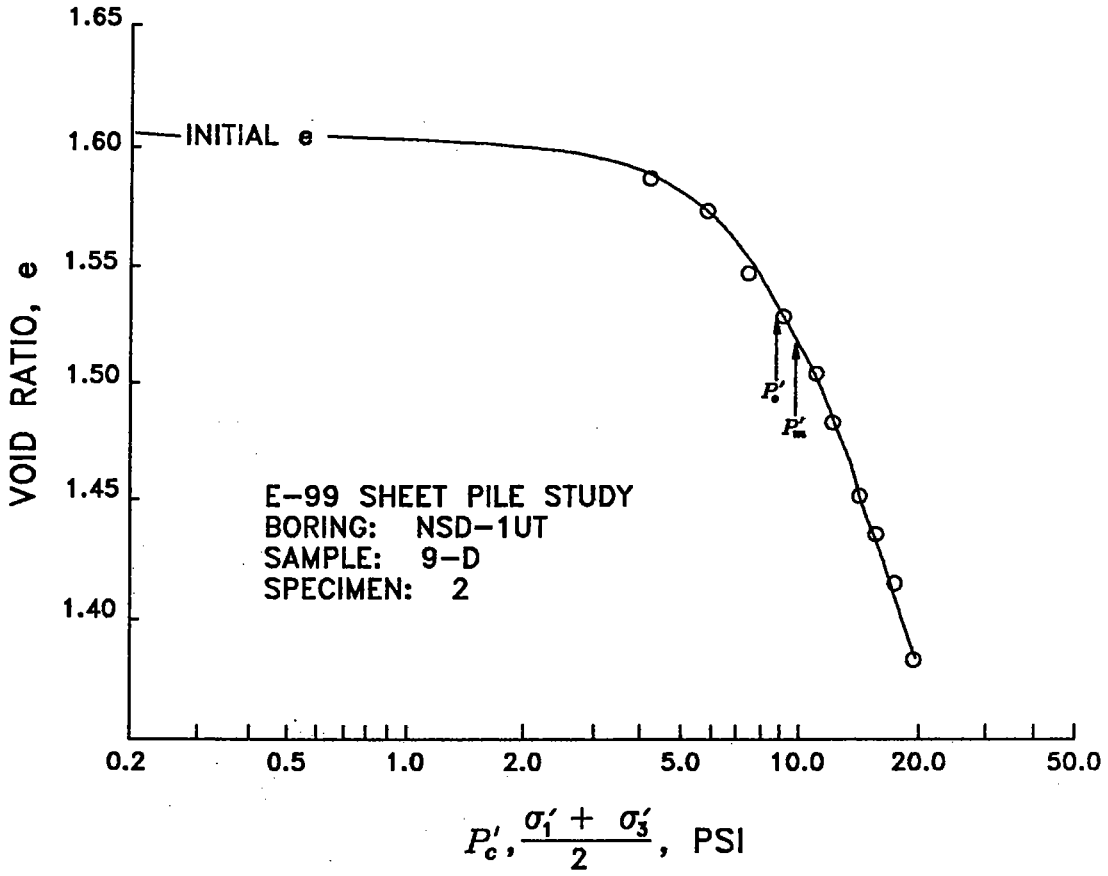

Figure B5. (Concluded)

APPENDIX C: **NOTATION**

Symbol	Definition	Reference
b	Width of beam, ft	fig 2
c	Cohesion of soil, psf	par 14
D	Length of pile for factor of safety of 1.0, ft	par 61
D_i	Embedment depth computed by CANWAL for factor of safety of 1.0, ft	par 61
D_d	Embedment depth computed by CANWAL for design factor of safety, ft	par 61
d	Lateral displacement at tip of pile for factor of safety of 1.0, in	par 61
E	Modulus of elasticity of steel, psf	par 18
E_e	Effective modulus of elasticity for sheet pile finite element, psf	par 18
E_i	Initial tangent modulus of soil, psf	par 11
e	Void ratio	Append B
h	Depth of beam, ft	fig 2
I	Moment of inertia of pile or beam, ft^4	par 18
I_e	Effective moment of inertia for sheet pile finite element, ft^4	par 18
K	Ratio of soil modulus to undrained shear strength E_i/S_u	par 12
K_m	Stiffness of soil, when $\sigma_3' = p_a$	par 12
L	Length of beam, ft	fig 2
l	Distance along beam, ft	fig 2
M	Moment, ft-lb	par 20
n	Parameter that relates initial soil stiffness (E_i) to σ_3'	par 12
P	Applied load at end of beam,lb	fig 2
p_a	Atmospheric pressure, psf	par 12
p_c'	Effective consolidation pressure, psf	par 14
p_m'	Maximum past effective consolidation pressure, psf	Table B2
p_o'	Insitu effective consolidation pressure, psf	Table B2
p_u	Pore water pressure, psf	Table B1
R_f	Ratio of undrained shear strength to hyperbolic strength (S_u/S_f)	par 11
r_c	Radius of curvature for bending, ft	fig 1
S_f	Hyperbolic strength, psf	par 11

Symbol	Definition	Reference
S_u	Undrained shear strength, psf	par 11
u	Lateral displacement, ft	par 20
v_{max}	Maximum vertical deflection of beam, in	fig 2
w	Water content, %	Table B1
X_o	Centerline of levee, ft	fig 15
x	Distance along beam, ft	par 20
Y_o	Elevation (NGVD), ft	fig 15
Y_4	Water elevation, ft	fig 15
Δ	Slope of pile relative to vertical	fig 21
ϵ_a	Axial strain in pile	par 12
ϵ_b	Bending strain in pile	par 21
ϵ_l, ϵ_r	Outer fiber strain in pile	par 21
γ_t	Total unit weight, pcf	Table B1
ν	Poisson's ratio	par 13
ν_i	Poisson's ratio for initial loading	par 13
σ'_h	Horizontal effective stress, psf	par 14
σ_v	Vertical stress, psf	Table B1
σ'_v	Vertical effective stress, psf	par 14
σ'_1	Maximum principal effective stress, psf	Append B
σ'_3	Minimum principal effective stress, psf	par 12
ϕ	Friction angle of soil, deg	par 14